Universidad de Málaga
Dpto. Biología Celular, Genética y Fisiología
Área de Genética

A multidisciplinary approach to investigate plant-pathogen interactions

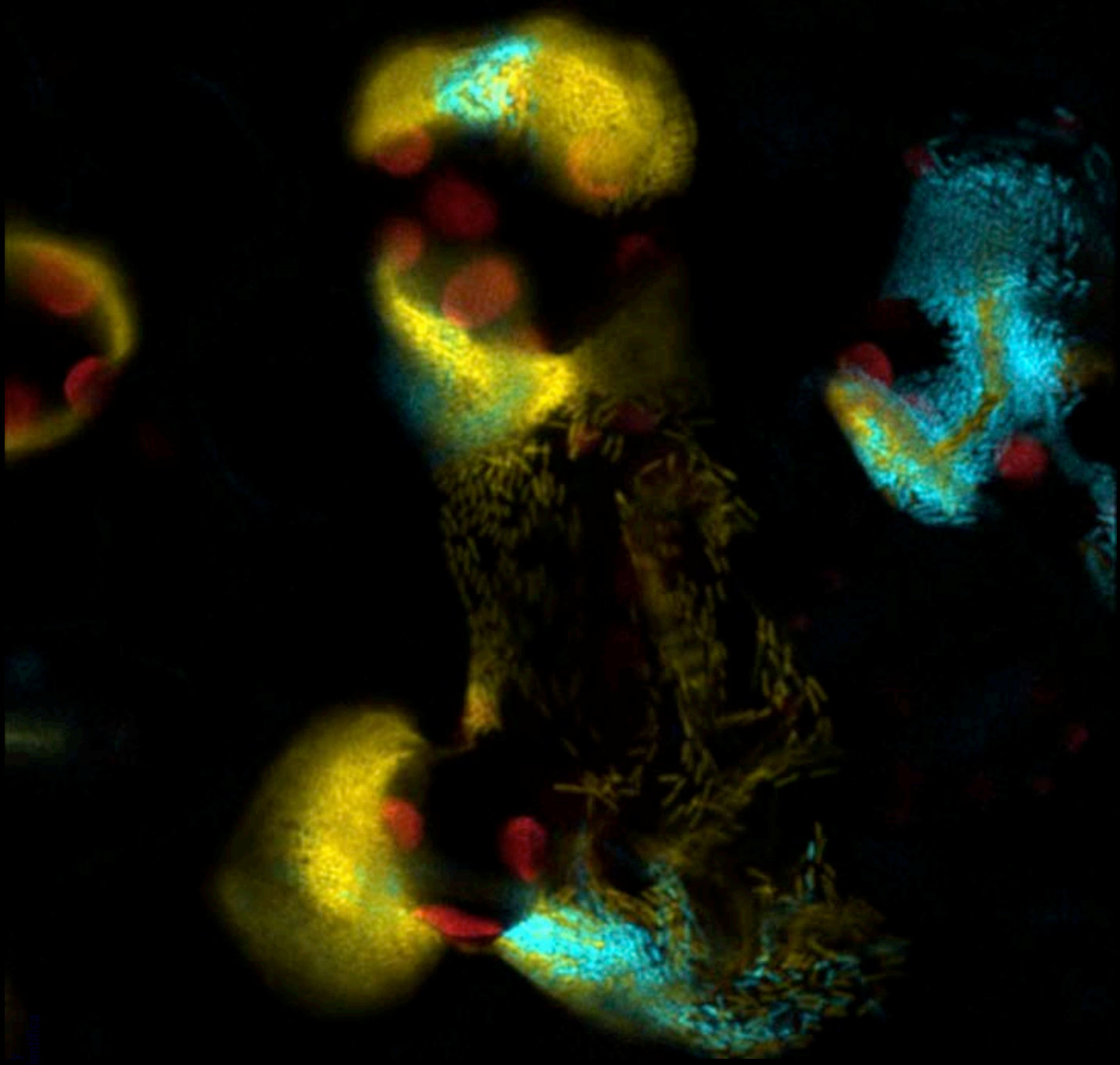

José Sebastián Rufián Plaza

TESIS DOCTORAL

2015

UNIVERSIDAD DE MÁLAGA

Departamento de Biología Celular, Genética y Fisiología

TESIS DOCTORIAL

A multidisciplinary approach to investigate plant-pathogen interactions

Autor: José Sebastián Rufián Plaza

Directores: Carmen R. Beuzón y Eduardo Rodriguez Bejarano

Málaga, 2015

Publicaciones y Divulgación Científica
UNIVERSIDAD DE MÁLAGA

AUTOR: Jose Sebastián Rufián Plaza
http://orcid.org/0000-0002-3871-3706

EDITA: Publicaciones y Divulgación Científica. Universidad de Málaga

UNIVERSIDAD
DE MÁLAGA
Área de Genética
Departamento de Bilogía Celular,
Genética y Fisiología

Dra. Carmen R. Beuzón, Profesora titular del Área de Genética del Departamento de Biología Celular, Genética y Fisiología de la Universidad de Málaga, y

Dr. Eduardo Rodriguez Bejarano, Catedrático del Área de Genética del Departamento de Biología Celular, Genética y Fisiología de la Universidad de Málaga,

CERTIFICAN:

Que Don José S. Rufián Plaza ha realizado bajo su dirección y supervision en la Unversidad de Málaga el trabajo titulado “A multidisciplinary approach to investigate plant-pathogen interactions”, presente en esta memoria, que constituye su tesis doctoral.

Y para que así conste y tenga los efectos que corresponden, en cumplimiento con la legislación vigente, extienden el presente informe.

En Málaga, a 6 de noviembre de 2015.

Carmen R. Beuzón

Eduardo R. Bejarano

PROPUESTA DE TRIBUNAL

Presidente
Dr. Miguel Ángel Botella Mesa
Departamento de Biología Molecular y Bioquímica
Universidad de Málaga

Secretario
Dr. Pablo Tornero Feliciano
Instituto de Biología Molecular y Celular de Plantas
Universidad Politécnica de Valencia-CSIC

Vocales
Dr. Francisco Ramos Morales
Departamento de Genética
Universidad de Sevilla

Dra. Natalia Requena Sánchez
Department of Molecular Phytopathology
Karlsruhe Institute of Technology

Dra. Marta Martín Basanta
Departamento de Biología
Universidad Autónoma de Madrid

Suplentes
Dr. David Posé Padilla
Departamento de Biología Molecular y Bioquímica
Universidad de Málaga

Dr. Francisco Manuel Cazorla López
Departamento de Microbiología
Universidad de Málaga

"When you make the finding yourself – even if you're the last person on Earth to see the light – you'll never forget it"

Carl Sagan

A mi familia

Ha llegado el momento de echar la vista atrás y agradecer a todas las personas que, de una u otra forma, han contribuido, a nivel personal y profesional, en el desarrollo de este trabajo.

En primer lugar debo agradecer a las mariposas. Un problema sobre el sistema de determinación del sexo de estos lepidópteros hizo que entrara en contacto con Carmen en 2006. Cuando salí de aquella revisión de exámen, supe que ella era especial, no era una profesora cualquera. Un año después, cuando buscaba alumnos internos, no dudé en presentarme. Aquel problema de las mariposas seguía presente durante la entrevista-charla que tuvimos, y, seguramente, influyó en que confiara en mi para trabajar en el laboratorio.

Carmen, probablemente necesitaría otro volumen de tesis para agradecerte todo lo que has hecho por mi durante todos estos años. Gracias por confiar en mi y conseguirme financiación desde el principio, por enseñarme tanto y tan bien, por entenderme en momentos difíciles, por hacer que reuniones eternas resulten en motivación, por tener paciencia cada día cuando te interrumpía en el despacho para contarte los últimos resultados, aunque no fueran relevantes. Gracias por haber sido la mejor directora que se pueda tener.A Javi, porque desde el principio has estado involucrado en mi trabajo y porque gracias a tus grandes ideas hemos conseguido grandes resultados. Por esas charlas en el laboratorio en las que, a base de darle vueltas a todo, encontrábamos puntos fuertes y débiles al trabajo. A Eduardo, por darme su confianza y ayudarme en absolutamente todo lo que he necesitado durante este tiempo. Al resto de profesores del área de genética, Araceli, Cayo, Enrique, Ana y Julia, por siempre estar ahí cuando los he necesitado.

A mis compañeros (o mejor dicho, amigos) del laboratorio, por hacer que me costara menos levantarme para ir a trabajar. A Alberto, por ser el que me introdujo en el laboratorio, por tener una paciencia eterna y aguantar como nadie todas las preguntas. Por ayudarme a hacer contactos fuera de nuestras fronteras. Por seguir confiando en mí. A Adela, por sus grandes dotes para enseñar (bajo amenaza de cortar manitas), por nuestras charlas eternas que nos subían los ánimos día a día. A Inma, por su dulzura y su buen carácter. Porque siempre estuvo dispuesta a ayudar. A Ainhoa, porque con ella era imposible no estar de buen humor. Por hacer los experimentos interminables (SAR) más llevaderos. A Spyridoula, porque desde el principio fue una más en el laboratorio, sin barrera idiomática que se interpusiera. Por ser de gran ayuda en mis principios con las proteínas. A Diego, por su serenidad y su aguante cuando me pasaba el día quejándome. Por sus buenos consejos experimentales y por demostrar que no hace falta llevar muchos años trabajando en esto para ser un gran científico (demostrando que pasarse el día leyendo sirve para algo). A Juanjo y Natasa, porque durante mucho tiempo fuisteis un gran apoyo. A las últimas incorporaciones, Javi “chico” y Nieves, porque ya se echaba en falta el entusiasmo y las ganas del principio.

A mis compañeros del departamento. A Pilar, por ser una gran amiga. Por todas esas noches en las que nos esperábamos mutuamente (vale, más tú a mí que yo a tí) para luego irnos de cerves. Porque incluso en la distancia conseguimos no perder el contacto y sacar hueco para ponernos al día. Y espero que siga así. A Isa Aragón e Isa P., por todos los buenos momentos que hemos pasado, tanto dentro como fuera del laboratorio. A Eloy ya Nacho, por masculinizar el departamento y contribuir a que dejáramos de hablar de partos y flujos durante la comida. A Luis, por sus divertidas ocurrencias. Por todos los momentos de risas por cualquier frikada. A Laura, por su carácter complaciente. Por ser una más desde el principio. A Blanca y Bego, mis primeras alumnas internas que ya se han hecho mayores. Gracias por demostrarme vuestras ganas

de aprender. Al resto de compañeros del área, Álvaro, Miguel, Pepe, Adri y Alba. A los compañeros históricos, aquellos que eran “los mayores” cuando yo empecé. A Rosa, por su sentido del humor. Por esa complicidad que siempre hemos tenido. A Ana, por estar siempre dispuesta a ayudar en lo que haga falta. A Manolo, porque ser la persona a quien recurrir, el que todo lo sabe. A Tábata, porque tu buen carácter y tu sentido del humor siempre me hacían sentir bien.

A los profesores y compañeros de los lab meeting de los lunes (o miércoles). Gracias a Miguel Ángel y Victoriano por sus buenos consejos, a Vitor por nuestros intercambios de experiencias con las CoIPs, y al resto de compañeros bioquímicos por estar ahí siempre que los he necesitado. A los técnicos que durante este tiempo nos han hecho la vida más fácil. A Mayte y Silvia, por enseñarme durante los primeros años. A Pablo, por hacerlo todo tan bien y siempre con una sonrisa. A Lucía, por haberme ayudado siempre que la he necesitado.

La vida fuera del laboratorio ha sido muy importante durante este tiempo, para poder desconectar y recargar las pilas. A Laura, porque fuiste una de las primeras personas que conocí en la carrera (creo que te conocí en mi primer día, aunque por aquella época no hablabas), y un gran apoyo durante todos estos años. Además, fuiste la excusa que me llevó a California, y me hizo querer volver allí. A Patri, mi compañera de viaje (y de viajes). Porque contigo no hace falta tomar triptófano para estar feliz. A Agustina, por ser una gran amiga desde el principio (cuando nos conocimos estudiando química). Por tu cercanía y dulzura. A Carlos, porque siempre nos reímos juntos, especialmente si es viernes noche y hay una peli de zombies. A Marco y Ana, porque transmitís algo especial, por hacerme sentir bien cuando estoy con vosotros. A Ana Ortega y Jose, porque aunque no fueron más de dos años los que coincidimos, la amistad que se creó aún perdura. A Charly, por sus locuras contagiosas. A los allegados, Juanje y Miguel, por aguantarnos todas las conversaciones sobre la facultad. A todos, gracias por los Filos, zombies y barbacoas que quedan (con permiso de Laura). A los compañeros que hicieron del máster algo más llevadero. Especialmente a Candelas, gran amiga con la que he compartido tantos momentos, y a Marina y Ana. Gracias por aquel verano insuperable.

I would like to thank all the people that made my life abroad easier. Thanks to Dawn Arnold, because you accepted me in your lab at the very beginning of my PhD. Thanks to David Corry for introducing me to the confocal microscope. Thanks to Bharani, Helen and Alison for help me in the lab.

I am very grateful to Gitta Coaker for all the knowledge you transmit during the seven months y stayed in your lab, which were very beneficial for my scientific training. I would also thank all the people from the Coaker lab for making me feel at home.

No me puedo olvidar de mi pequeña familia americana, a Honza, Barbora y Martin, gracias por acogerme en su casa. A los trotamundos, Inma, Vicent, Ainara, Lucía, María y Ana. Gracias por tantos buenos momentos durante todos los kilómetros que hicimos recorriendo California de punta a punta.

Por último, gracias a mi familia por haberme apoyado durante todo este tiempo. A mis padres, por darme la educación que me han dado y por los esfuerzos que han hecho para que llegue hasta aquí. Porque, a pesar de no entender nada de lo que hago, me hacen sentir su admiración y orgullo. A mis hermanas, gracias por haberme apoyado y cuidado durante toda mi vida. Porque estar con vosotras es sentirme bien . A mis sobrinos, por llenarme de felicidad cada vez que los veo.

Este trabajo ha sido financiado por los proyectos AGL2010-22287-C02-02, concedido a Eduardo R. Bejarano y BIO2012-35641, concedido a Carmen R. Beuzón, así como por una beca para la Formación de Personal Investigador (FPI 2011)

INDEX

Abbreviations

CDPK: Calcium-Dependent Protein Kinase.
CFP: Cyan Fluorescent Protein.
Cfu: Colony-formin units.
CI: Competitive Index.
COI: Cancelled-Out Index.
Col-0: *Arabidopsis thaliana* cultivar Columbia.
DC3000: *Pseudomonas syringae* pv. tomato DC3000.
DEX: Dexamethasone.
Dpi: Days Post Inoculation.
ETI: Effector-Triggered Immunity.
GFP: Green Fluorescent Protein.
HGT: Horizontal Gene Transfer.
Hop: Hrp-outer protein.
HR: Hypersensitive Response.
JA: Jasmonic Acid.
MAPK: Mitogen-Activated Protein Kinase.
NLR: Nucleotide binding Leucin Rich repeat.
PAMP: Pathogen-Asociated Molecular Pattern.
Pf55: *Pseudomonas fluorescens* 55.
Pph: *Pseudomonas syringae* pv. phaseolicola.
PR1: Pathogenesis-Related 1.
PRR: Pattern-Recognition Receptor.
Psy: *Pseudomonas syringae* pv. syringae.
PTI: Pattern-Triggered Immunity.
Pto: *Pseudomonas syringae* pv. tomato.
Pv: Pathovar.
RLCK: Receptor-Like Cytoplasmic Kinase.
RLK: Receptor-Like Kinase.
ROS: Reactive Oxygen Species.
SA: Salycilic Acid.
SAR: Systemic Acquired Resistance.
T3E: Type Three Effectors.
T3SS: Type Three Secretion System.
YFP: Yellow Fluorescent Protein.
ZAR1: HopZ1a-Activated Resistance.
ZED1: HopZ1a-ETI-Deficient.

General introduction

The estimation of human global population from the United Nations indicates that the world total population could rich 9.15 billion in 2050 (Nikos Alexandratos and Bruinsma, 2012). This increase on the world population must be accompanied by an increase on food production. A major restriction to food production is crop losses due to plant diseases. Plant pathogens, including fungi, oomycetes, bacteria and viruses, are a major constraint to production with a strong economic impact. Understanding plant-pathogen interactions is therefore paramount for the development of robust and sustainable strategies to control disease and improve crop production.

This thesis focuses on the interaction between the plant-pathogenic bacteria *Pseudomonas syringae* and its hosts. It includes molecular and cellular studies at both sides of this interaction, canvasing from the bacterial virulence mechanisms to the plant defense response pathways.

Pseudomonas syringae: an archetypal plant pathogen

Pseudomonas syringae is a bacterial plant pathogen that has been extensively researched from the 1980s. *P. syringae* strains have been ranked as number 1 of plant-pathogenic bacteria based on its scientific and economic importance (Mansfield et al., 2012). *P. syringae* is a gram-negative bacterial pathogen that colonizes the aerial part of the plant, including leaves and fruits. It has a dual lifestyle, with an initial epiphytic phase on the surface of the plant, and an endophytic phase inside the plant apoplast, where the bacterial population survives and proliferates establishing a hemibiotrophic interaction with the host plant. The apoplast (the intercellular space between the cells of the parenchima) is the environment where the bacterial population grows better and this growth does not require killing of the plant cells for nutrients, as necrotrophs do. However, the interaction cannot be classified as fully biotrophic since it involves host cell death at later stages of the infection process, either due to the virulence action of the bacteria or to the defenses triggered by the plant in response to the attack.

1. Pseudomonas syringae classification

Pseudomonas syringae is a complex of strains that possess a wide host range, including many economically important crops, woody plants and weeds, such as the model plant *Arabidopsis thaliana*. Plants are generally resistant to most strains, and the

ability of a given strain to cause disease in a given host is considered the exception rather than the rule. On the basis of this more limited host range of the different isolates, the *P. syringae* complex is divided into more than 50 pathovars (Young, 2010). Furthermore, strains belonging to the same pathovar can still differ on their interactions with different cultivars or ecotypes of the same plant species, giving raise to an additional subdivision into races. The sequencing annotation of the whole genomes three model strains belonging to different pathovars of the *P. syringae* complex: pathovar tomato, Pto DC3000 (Buell et al., 2003), pv. phaseolicola, Pph 1448A (Joardar et al., 2005), and pv. syringae, Psy B728a (Feil et al., 2005) provided a large amount of information and tools and determined an qualitative leap for the field.

2. *Pseudomonas syringae* pv. tomato, phaseolicola and syringae

Pseudomonas syringae pv. tomato is the causal agent of bacterial speck in tomato plants. In (1986)**, Cuppels** generated the strain DC3000, a rifampicin resistant derivative of a wild-type strain, which was used for auxotrophy and pathogenicity studies. Some years later, Whalen et al. (1991) showed the ability of DC3000 to produce disease in the model plant *Arabidopsis thaliana*. The ability of DC3000 to infect both tomato and *Arabidopsis* plants made this strain of great interest for the plant pathogen interactions field. DC3000 is a weak epiphyte (Boller and Felix, 2009) compared with other strains such as B728a; while B728a can maintain a high epiphytic population for several days, most of the epyphitic population of DC3000 dies in less than 48h. Thus, DC3000 needs to enter into the apoplast in order to survive. One of the mechanisms that DC3000 uses to effectively enter into the host tissue is mediated by the production of a polyketide toxin called coronatine, a molecular mimic of the plant-hormone methyl-jasomate (Weiler et al., 1994). Upon perception of bacteria entering the plant apoplast, the plant induces closure of stomata in order to prevent further bacterial entry. Coronatine activates cellular pathways that result in the reopening of stomata, thus allowing high numbers of bacteria to invade the apoplast (Melotto et al., 2008).

Pseudomonas syringae pv. phaseolicola is the etiological agent of halo blight disease in common bean (*Phaseolus vulgaris*). This disease is characterized by the appearance of water-soaked lesions in leaves and pods, often surrounded by a chlorotic halo (W.H., 1926), and it is prevalent worldwide. Since bacteria can colonize and

survive into the dry seeds, fields infected by *P. syringae* pv. phaseolicola are usually destroyed to prevent dissemination. One of the control strategies to prevent halo blight is the rotation of resistant cultivars. Based on the resistance/susceptibility interactions between eight bean cultivars and 175 different strains of *P. syringae* pv. phaseolicola, the pathovar was divided in nine races (Taylor et al., 1996). The strains belonging the race 6, including 1448A, are able to produce disease in all cultivars tested.

Pseudomonas syringae pv. syringae is the most heterogeneous group among the *P. syringae* pathovars. It includes strains that produce from brown spot in bean, to blossom blight in pear, or apical necrosis in mango trees, among other diseases. One of the characteristics of many of the strains of this group, including B728a, is the production of the phytotoxin Syringolin A (Ramel et al., 2009). This toxin acts inside the plant cell as a proteasome inhibitor, suppressing defense responses and promoting bacterial proliferation (Schellenberg et al., 2010). Furthermore, Syringolin A allows bacteria to move from the primary infection site through the xylem (Misas-Villamil et al., 2011).

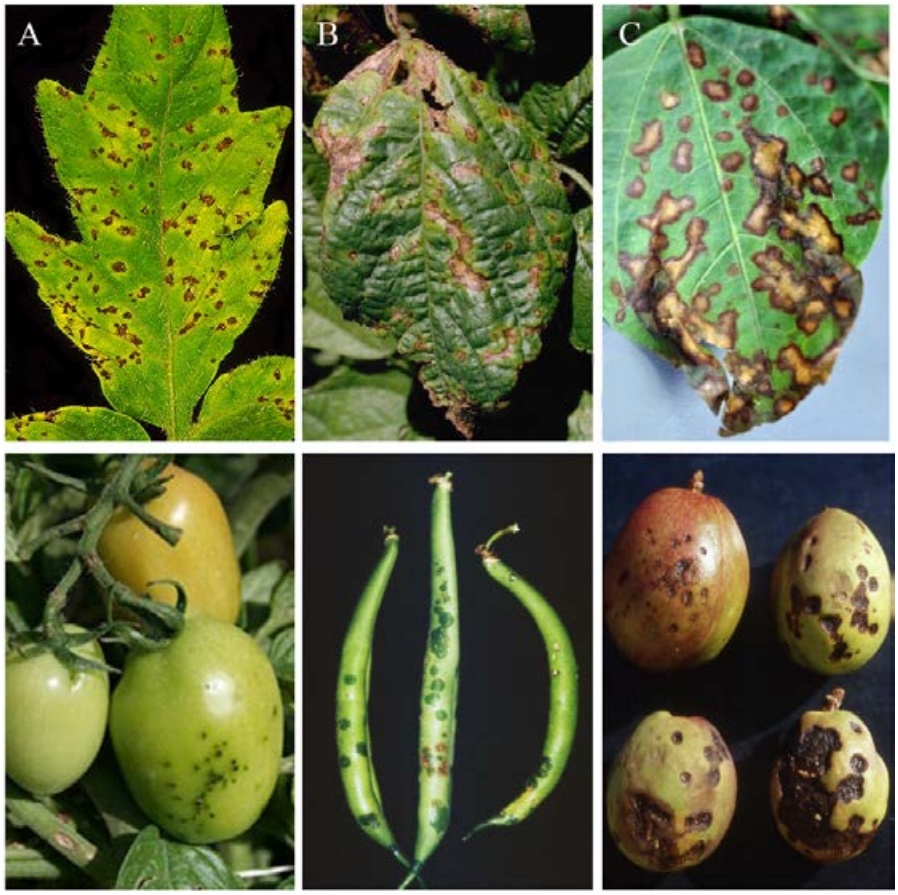

Figure 1. **Diseases caused by different *P. syringae* strains**. (**A**) Bacterial speck of tomato produced by *P. syringae* pv. tomato. (**B**) Halo blight of bean produced by *P. syringae* pv. phaseolicola. (**C**) Bacterial brown spot of lima (top panel) and apical necrosis of mango, produced by *P. syringae* pv. syringae. Fotograph authorship: A, Top panel: A. Collmer. Lower panel: C. Smart. B, Top panel: H. Schwartz. C, Top panel: R. Mulrooney.

The Type III Secretion System: a molecular weapon of gram-negative bacteria.

1. Structural and regulatory components of the T3SS

Many *P. syringae* strains possess toxins that contribute to bacterial virulence. However, all strains require a Type Three Secretion System (T3SS) to be pathogenic. The T3SS is a complex nanomachine that exports proteins across the bacterial inner and outer membrane into the host cell cytosol. The components of the T3SS are very conserved among gram-negative bacteria. The genes encoding such conserved proteins are named as *hrc* (hrp conserved). The *hrp/hrc* genes are clustered in pathogenicity islands located in the chromosome within a single gene cluster called the *hrp* locus (hypersensitive response and pathogenicity). The T3SS is not constitutively expressed in the bacteria, but induced under certain conditions, such as in some minimal-laboratory medium, or the plant apoplast. The central regulatory element of the *hrp/hrc* genes is HrpL, a member of the ECF family of alternative sigma factors that activates the expression of genes containing a consensus sequence, the *hrp* box, within their promoters (Xiao and Hutcheson, 1994; Fouts et al., 2002).

The expression and assembly of the T3SS is an intricate process regulated by positive and negative feedbacks (Ortiz-Martin et al., 2010a; Ortiz-Martin et al., 2010b) in which structural proteins can also play a role in regulation, e.g. HrpA, the main component of the T3SS pillus, which positively regulates expression of *hrpL* (Preston et al., 1998). The structural proteins of the T3SS form a needle composed of an inner-membrane ring, an outer membrane ring and a pillus, through which the proteins are secreted. In addition to regulatory and structural proteins, T3SS also include harpins or helper proteins, chaperones, and effectors. Harpins are secreted but not translocated into the host cell and play an auxiliary role in the penetration of the pillus into the plant cell wall, and in effector delivery (Kvitko et al., 2007). Chaperons are small proteins essential for the appropriated folding of the proteins of the system. These proteins are bound to the corresponding effector within the bacterial cytoplasm, protect them from aggregation or degradation, and may direct them to the needle complex when required. Finally, effectors are the only proteins translocated into the plant cell cytoplasm, where they collectively contribute to virulence by modifying host cellular processes to allow bacterial survival and proliferation

2. Type Three Effectors

Type Three Effectors (T3Es) are the proteins translocated through the T3SS needle complex into the host cell. T3Es are essential for pathogenesis, since bacterial strains carrying a mutation in a T3SS structural gene, such as to be unable to translocate effectors, are non pathogenic (Alfano and Collmer, 1997). Furthermore, strains carrying mutations in one or more effector gene can display virulence attenuation (Cunnac et al., 2004; Macho et al., 2012). More than 60 effector families have been validated in *P. syringae* to date, and this number is still increasing thanks to the complete sequencing of new pathovars (Baltrus et al., 2011; Matas et al., 2014). Historically, effectors were named as virulent (Vir) or avirulent (Avr) proteins based on whether they were identified through their virulence function (Vir) or for triggering the hypersensitive response in a host plant (Avr). However, some of these virulent effectors can be considered avirulent in different plant genotypes and *vice versa*. After identification of the T3SS from *P. syringae*, newly identified effectors started to be named as *hop* (*hrp*-outer protein) followed by a letter and number. In (2005)**, Linderberg and collaborators** proposed unified nomenclature and a set of guidelines to classify a newly identified protein as a T3SS effector. Thus, a new T3E must fulfill the following criteria: (i) a *hrp* box within the promoter of the effector gene, and a N-terminal sequence in the effector protein to target the protein for translocation through the T3SS, (ii) HrpL-dependent expression, and (iii) evidences of expression and translocation into the plant cell. The main function of the effectors is the manipulation of the plant cell in order to promote bacterial proliferation. To do so, T3Es can hijack plant nutrients and metabolites to support bacterial needs, change the hormone balance or modify the physical conditions of the apoplast (Macho, 2015). However, the most common function of T3Es is the suppression of the plant defense responses (Block and Alfano, 2011; Feng and Zhou, 2012; Macho and Zipfel, 2015)

The plant immune system: an unspecialized specific system.

1. PTI: Pattern-Triggered Immunity

Plants, as sessile organisms, are constantly exposed to a variety of biotic and abiotic stresses. Thus, perception of environmental signals is essential to raise alert and trigger a convenient response. Initial alerts are raised through surface-localized Pattern

Recognition Receptors (PRRs). PRRs are proteins with an extracellular receptor domain, and an intracellular domain to activate a signaling cascade. The signals recognized by the PRRs are conserved molecules known as Damage-, Microbe- or Pathogen-Associated Molecular Patterns (DAMPs, MAMPs, or PAMPs, respectively). Examples of MAMPs or PAMPS are bacterial flagellin, the elongation factor Tu, or chitin. Activation of PRRs leads to the onset of a defense response capable of protecting the plant from the attack of non-specialized pathogens, and known as Pattern-Triggered Immunity (PTI) (Henry et al., 2013). The best-characterized PAMP-PRR complex is the flagellin-Flagellin Sensing 2 (FLS2) complex (Gómez-Gómez and Boller, 2000). FLS2 is a Receptor-Like Kinase (RLK) that contains an extracellular Leucine-Rich Repeat (LRR) domain, which recognizes the conserved 22-amino acid flagellin epitope flg22, and an intracellular kinase domain. Upon perception of flagellin, FLS2 forms a heterodimer with its co-receptor BAK1 (BRI1-Associated Kinase 1). BAK1 acts as co-receptor with many others PRRs, activating downstream signals by *trans* phosphorylation (Segonzac and Zipfel, 2011). The FLS2-BAK1 complex phosphorylates BIK1 (Botrytis Induced Kinase 1), a receptor-like cytoplasmic kinase (RLCK) that acts as a substrate for many PRR complexes. BIK1 activation, along with other RLCKs, positively regulates the Calcium influx from the apoplast into the cytosol, and phosphorylates the NADPH oxidase RBOHD, leading to the production of a burst of Reactive Oxygen Species (ROS) and to stomatal closure, restricting bacterial infection (Zhang et al., 2010; Liu et al., 2013). The FLS2-BAK1 complex also activates signal transduction pathways through mitogen-activated protein kinases (MAPK) and calcium-dependent protein kinases (CDPK) cascades, which results in transcriptional activation of defense-related genes. Finally, as a late PTI response, the plant cell wall is reinforced by callose deposition that creates a physical barrier against pathogen invasion.

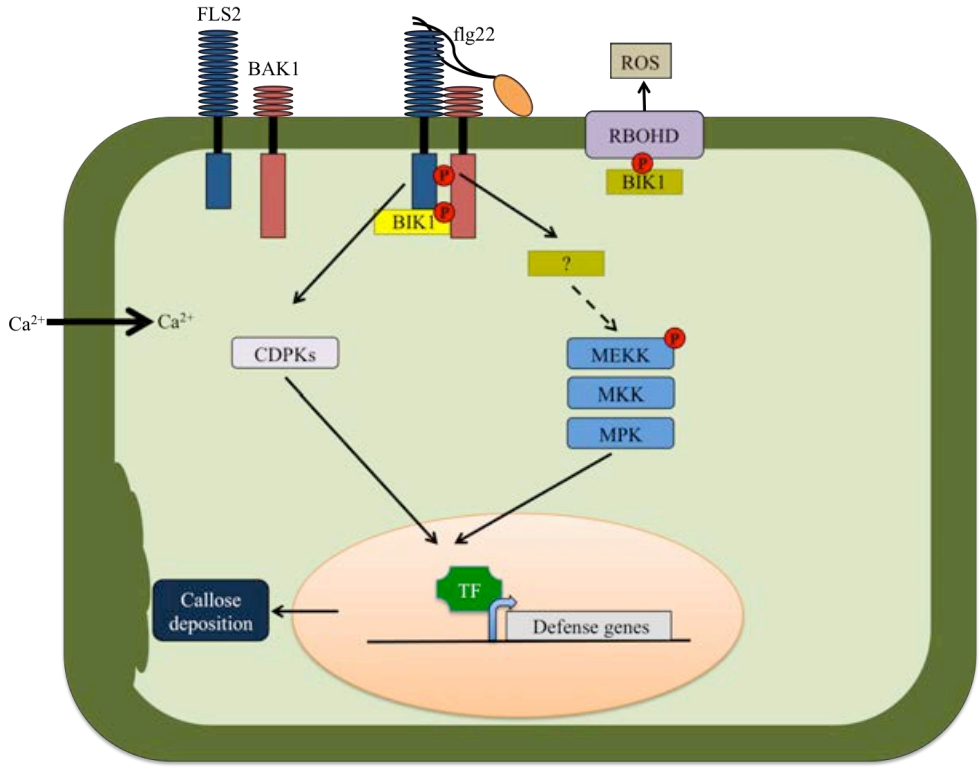

Figure 2. Events occurring during PTI activation by flg22. Adapted from Henry et al., 2013.

2. ETI: Effector-Triggered Immunity

P. syringae can overtake PTI host response and produce infection through T3E-mediated-suppression. However, plants possess a second layer of defense response called effector-triggered immunity (ETI). This response is mediated by resistance or R proteins, intracellular immune receptor proteins also known as NLRs (Nucleotide-binding and Leucine Rich repeat). NLRs are subdivided into two groups based on the structure of their N-terminus, which can be a coiled-coil (CC) domain, or a Toll and Interleukin-1-like receptor domain (TIR). NLRs can recognize effectors directly, or indirectly through the activity of the effector on its target. This indirect recognition model is known as the guard model. A variation on this theme has been found where the effector target being watched by the NLR does not have an actual function on the cell other than mimic the real virulence target protein, in such a case the watched target is known as the decoy. Decoys are thought to have arisen through gene duplications or splice variants of T3E targets. The molecular events upon ETI response are similar to the ones occuring during PTI, and include ROS burst and transcriptional activation of defense genes, but displays major differences in the timing of activation, duration, and

intensity (Thomma et al., 2011). The result of these events is the activation of a programmed cell death process known as the hypersensitive response (HR). The HR is a trademark of ETI.

3. SAR: Systemic Acquired Resistance

Plants do not have a specialized secondary immune system to prevent the infection by incoming pathogens. However, activation of either PTI or ETI induces a faster and stronger defense response in distal leaves than occurs in naïve plants. This is known as systemic acquired resistance or SAR. SAR is a mechanism of induced defense that confers long-lasting resistance against a broad spectrum of microorganisms. This response is characterized by the activation of the expression of the defense-related hormone Salicylic Acid (SA) and the accumulation of Pathogenesis-Related (PR) proteins in distal tissues. Although the nature of the pathogen-induced mobile signal remains unknown, there are a variety of compounds that have been linked to the spread of SAR. SA and Methyl-SA (Mesa et al., 2009) accumulate in distal tissues during activation of SAR, and were thus proposed to act as SAR signal. However, grafting experiments demonstrated that those compounds are dispensable for the spread of the systemic signal (Spoel and Dong, 2012). Another compounds that have been associated to SAR are glycerol-3-phosphate (G3P), azelaic acid (AzA, (Cecchini et al., 2015)), Nitric Oxid (NO) and ROS (El-Shetehy et al., 2015).

The Plant-*P. syringae* interaction: a molecular battle between effectors, their targets and the NLRs proteins.

Plants are capable of detecting bacterial conserved patterns upon contact to trigger PTI. Thus, in order to survive and proliferate within a plant host, bacteria must be able to suppress PTI, and this role is mostly assumed by T3Es in *P. syringae*. Many effectors can suppress PTI at different levels. For example, AvrPtoB ubiquitinates PRRs to promote their degradation by the proteasome (Gohre et al., 2008), AvrPto and HopAO1 block PRR kinase activity and their downstream function (Ding et al., 2007; Macho et al., 2014), HopF2 and HopAI1 modify MAP kinases, inactivating their function (Zhang et al., 2007a; Wang et al., 2010), and several effectors target and modify RIN4, an important regulator of plant immunity (Kim et al., 2005; Shang et al., 2006). However, modification of plant targets may unleash the ETI response. For example, the above-

mentioned inactivation of MPK4 by HopAI1 activates the NLR SUMM2 (Zhang et al., 2012). Similarly, cleavage of RIN 4 by AvrRpt2 switches on the specific NLR RPS2 (Axtell and Staskawicz, 2003). However, activation of other NLRs can follow a more complex pattern, as it is the case for activation of the NLR ZAR1. ZAR1 triggers ETI by detecting acetylation of the pseudokinase ZED1 by the effector HopZ1a (Lewis et al., 2013). In addition, ZAR1 can also activate ETI through detection of uridylylation of another pseudokinase, RKS1, by *Xanthomonas* effector AvrAC (Wang et al., 2015). Interestingly, ZED1 nor RKS1 are necessary for effector virulence activities, therefore, these proteins are believed to act as decoys leading to the activation of ETI. Since the ETI response and the ensuing HR severely restrict pathogen growth, pathogens need to suppress or avoid this defense response in order to survive and proliferate. Avoidance could be achieved by an evolutionary strategy called pathoadaptation (Ma et al., 2006): small changes on the effector protein sequence leading to a loss of recognition by the NLR, and to a new effector that could conserve its virulence function. Suppression could be achieved by the acquisition by the pathogen of another effector(s) capable of suppressing the ETI. This gain can be mediated by horizontal transfer events (Deng et al., 2003). In the latter case, the ETI-suppressing activity of the new effector(s) would allow bacteria to overtake the defense response.

Objectives

1. To characterize the impact and source of diversity within pathogen populations during the interaction with the plant host, using single-cell technology and the model bacterial pathogen *Pseudomonas syringae*.

    1.1 To analyze how strains of *P. syringae* differing in their virulence relate or interfere with each other during colonization of the host.

    1.2 To look for a mechanistic explanation for the phenotypic heterogeneity observed in the development of *P. syringae* populations during colonization of the plant apoplast.

2. To characterize new molecular mechanism of plant defense suppression, through the analysis of how *P. syringae* effector HopZ1a suppresses plant defenses.

    2.1 To evaluate and characterize the role of lysine 289 on HopZ1a function.

    2.2 To evaluate plant MAP Kinase Kinase 7 as putative virulence target of HopZ1a.

Experimental procedures

Bacterial strains and growth conditions

Bacterial strains used in this work are listed in the Table 1 of each chapter**.** All bacterial strains were grown in Lennox Broth (LB, Lennox (1955)), unless otherwise stated. *Escherichia coli* DH5α (Hanahan, 1983) derivatives were grown at 37ºC. *Pseudomonas syringae* strains and *Agrobacterium tumefaciens* C58C1 (Deblaere et al., 1985), derivatives were grown at 28°C. Antibiotics were used at the following concentrations: for *E. coli* DH5a, ampicillin (Amp), 100 mg/ml, kanamycin (Km), 50 mg/ml; gentamycin (Gm), 10 mg/ml and chloramphenicol (Cm), 6 mg/ml. For *P. syringae* and *P. fluorescens* strains, Km 15 mg/ml, Gm 10 mg/ml and nitrofurantoin (Nf), 50 μg/ml. For *A. tumefaciens*, Km 50 mg/ml, tetracycline (Tc) 5 μg/ml and rifampicin (Rf) 50 μg/ml. All plates used to grow plant-extracted bacteria contained cycloheximide (2 μg/ml) to prevent fungal contamination.

Plant material

Phaseolus vulgaris bean cultivar Canadian Wonder plants were grown at 23°C, 95% humidity, with a controlled photoperiod of 16h light/ 8h dark with a light intensity of 200 μmol/m^2/s. *Arabidopsis thaliana* Col-0 and derivatives were grown in soil, or for disease development assays, in jiffy-7 (Jiffy Products Ltd, Norway). In either case, they were grown in temperature-controlled chambers, at 21ºC with a controlled photoperiod of 8h light/ 16h dark with a light intensity of 200 μmol/m^2/s. *Nicotiana benthamiana* was grown in soil in temperature-controlled chambers, at 21ºC with a controlled photoperiod of 16h light/ 8h dark with a light intensity of 200 μmol/m^2/s.

Arabidopsis zar1-1 (Lewis et al., 2010) and DEX-MKK7 (Zhang et al., 2007) plants were crossed to obtain homozygous *zar1-1*/DEX-MKK7 lines.

Bacterial inoculation and recovery from plant leaves

For *P. syringae* inoculum preparation, bacterial lawns were grown on LB plates for 48 h at 28°C, collected and suspended in 2 mL of 10 mM $MgCl_2$. The OD_{600} was adjusted to 0.1, corresponding to 5 x 10^7 colony forming units (cfu/mL) and serial dilutions made to reach the desired inoculum concentration.

Plant inoculation by infiltration to be used for either microscopy, bacterial growth assays, symptoms development on bean leaves, or PR1 accumulation, in either bean

plants or *Arabidopsis* were carried out as follows: one fully expanded leaf from a 10-days old bean plant, or three fully expanded young leaves from 5-week-old *Arabidopsis* plants were pressure infiltrated using a 1-mL syringe without needle. The inoculum concentration for microscopy varied from 5 x 10^7 cfu/mL to 5 x 10^4 cfu/mL, depending on the experiment. For bacterial growth assays, the inoculum dose used was 5 x 10^4 cfu/mL, unless otherwise stated, and for PR1 accumulation experiments 5 x 10^5 cfu/mL.

For standard growth assays, three 10-mm-leaf discs were taken from either the inoculated or outside the inoculated area and ground in 1 mL $MgCl_2$. Serial dilutions were plated and bacteria enumerated.

Dip-inoculation for microscopy or growth assays was carried out by dipping leaves for 30 seconds in a 5 x 10^7 cfu/ml mixed bacterial suspension in 10 mM $MgCl_2$ and 0.02% Silwett L-77 (Crompton Europe Ltd, Evesham, UK).

Infiltration of bean leaves to be analyzed for flow cytometry was carried out after dipping a whole leaf into a 5 x 10^5 cfu/ml bacterial solution in 0.01% Silwett L-77 (Crompton Europe Ltd, Evesham, UK), using a pressure chamber. Four days post inoculation (dpi) bacteria were recovered from the plant by an apoplast fluid extraction. This extraction was carried out by pressure infiltrating a full leaf with 10 ml of a 10 mM $MgCl_2$ solution inside a 20 ml syringe. Following 5 cycles of pressure application, the flow-through was removed and placed into a fresh 50 ml tube, and the leaf retained within the syringe introduced into another. Both tubes were centrifuged at 4ºC for 30 min at low speed (900 *g*). Pellets were resuspended into 1 ml of $MgCl_2$ and analyzed by flow cytometry.

For *Arabidopsis* symptom visualization, 3-week-old plants were sprayed with a bacterial suspension containing 5x10^7 cfu/ml in 10 mM $MgCl_2$ containing 0.02% Silwet-L77 (Crompton Europe Ltd, Evesham, UK). Plants were kept covered for 24h to keep humidity high.

Competitive index and cancelled-out assays

A detailed protocol for Competitive Index (CI) assays is attached as Apendix 1 (Macho et al., 2016). To calculate ^{LB}CIs, 500 µl of a 5x10^4 cfu/ml mixed inoculum, containing equal cfu of wild type and derivate strains, was inoculated into 4.5 ml of LB medium and grown for 24h at 28ºC with aeration. Serial dilutions were then plated onto LB agar

and LB agar with the corresponding antibiotic, to determine the precise ratio between the co-inoculated strains. In plants, competitive index and cancelled-out (COI) assays were performed as previously described (Macho et al., 2007). Using a blunt syringe, 4- to 5-week old plants were inoculated with a $5x10^4$ cfu/ml mixed bacterial suspension, containing equal numbers of wild type and derivative strains. Serial dilutions of the inoculum were plated onto LB agar and LB agar with kanamycin to confirm dose and relative proportion between the strains, which should be close to one. At 4 dpi, three 10-mm-diameter leaf discs were homogenized into 1 ml of 10 mM $MgCl_2$, by mechanical disruption. Bacteria were enumerated by plating serial dilutions onto LB agar with cycloheximide, and LB agar with kanamycin and cycloheximide, to differentiate the strains within the mixed infection. Bacterial enumeration was carried out in the dilution displaying between 50 and 500 colonies per plate. The CI is defined as the mutant-to-wild type ratio within the output sample divided by the mutant-to-wild type ratio within the input (inoculum) (Freter et al., 1981; Taylor et al., 1987). The cancelled-out index (COI) is calculated dividing the output ratio between the strain expressing two effectors and the strain expressing one effector, by their input ratio (Macho et al., 2010a). Competitive and cancelled-out indices shown are the mean of three replicates displaying typical results from at least three independent experiments. Errors bars represent standard error. Each CI or COI was analyzed using a homoscedastic and 2-tailed Student's t-test and the null hypothesis: mean index is not significantly different from 1, or from other mean value (P value < 0.05).

Fluorescent labelling of bacterial strains

Constitutively expressed fluorescent reporter genes (eCFP or eYFP [enhanced cyan, and yellow fluorescent proteins, respectively]) were introduced into the chromosome of *Pph* strains 1448A and 1449B using a Tn*7* delivery system (Lambertsen et al., 2004): plasmids used are listed in Table 3 of chapter 1. Plasmids were introduced into *Pph* strains by tetraparental mating, as previously described (Lambertsen et al., 2004). PCR using primers Tn*7*-*GlmS* and Tn*7*R109 (Lambertsen et al., 2004), as well as Southern blot analysis using *aacC1* (Gm^R) as a probe, were used to confirm the correct and unique insertion of the transposon within the genome.

Bacterial strains carrying chromosome-located transcriptional fusions of the *hrp* genes *hrpL, hrcU* and *hopAB1* to a promoterless *gfp* gene were generated using an adaptation

of Zumaquero et al. (2010). The *hrpL* and *hopAB1* genes are encoded as monocistronic units, whereas *hrcU* is the last gene of an operon (Rahme et al., 1991; Xiao and Hutcheson, 1994; Jackson et al., 2000). For each gene, two fragments of approximately 500 pb were amplified from *Pph* 1448A genomic DNA using iProof High-Fidelity DNA Polymerase (Bio-Rad, USA); one fragment corresponding to the 3' end of the ORF, including the STOP codon, and the other corresponding to the sequence immediately downstream the STOP codon. The reverse primer for the first fragment and the forward primer for the second share a 16 bp overlapping region, including the T7 primer sequence and an *Eco*RI restriction site, providing homology and a cloning site between both fragments. All primers used are listed in Table 2 of chapter 2. Each reaction was carried out at 94ºC for 3 min, followed by 20 cycles at 94ºC for 20s, 55ºC for 30s, and 72ºC for 50s, followed by 7 min at 72ºC, and the reaction mixture contained 0.64 mM deoxynucleoside triphosphate (dNTP) mix, 5% dimethylsulfoxide (DMSO), 0.4 ng of each primer, 1 ng of genomic DNA, the appropriate enzyme buffer, and commercial ultrapure water (Nalgene, Rochester, NY, USA). Five µl of each gel-purified PCR product were used, without additional primers or template, in a PCR reaction consisting of 8 cycles at 94ºC for 30s, 52ºC for 1 min, and 72ºC for 1 min, finishing with 7 min at 72ºC. Five µl of this reaction, containing a single fragment of approximately 1 Kb, was used as a template for an additional amplification with the forward primer from the first amplified fragment and the reverse from the second (0.4 M of each), 0.64 mM dNTP mix, 5% DMSO, the corresponding buffer, and ultrapure water, for a reaction consisting of 20 cycles at 94°C for 20 s, 53°C for 30 s, and 72°C for 1 min, finishing with 7 min at 72°C. The resulting fragments, including the end of each ORF and its downstream sequence separated by an *Eco*RI site, were A/T cloned into pGEM-T (Promega, USA) and fully sequenced to discard mutations, giving raise to pDLM3 (p*hopAB1-Eco*RI), pDLM4 (p*hrcU-Eco*RI), and pDLM5 (p*hrpL-Eco*RI).

Plasmid pZEP07 (Hautefort et al., 2008) was used as template for PCR-amplification of a fragment containing a promoterless *gfp* gene carrying its own ribosomal-binding site (Willmann et al., 2011), followed by an *Eco*RV site and a chloramphenicol resistance cassette. This fragment was A/T cloned into pGEM-T (Promega, USA) generating pDLM1. A fragment containing the *nptII* kanamycin resistance gene, flanked by FRT sites (Flipase Recognition Target), was PCR-amplified using iProof High-Fidelity DNA Polymerase (Bio-Rad, USA), pDOC-K (Lee et al., 2009) as a template, and the

corresponding primers, and clone into the *Eco*RV site from pDLM1, to generate pDLM2. Plasmid pDLM2 was used as a template to amplify a fragment containing the promoterless *gfp* gene with its RBS, the kanamycin resistance gene, and the chloramphenicol resistance gene, and this fragment cloned into pDLM3, pDLM4 and pDLM5, digested with *Eco*RI and blunt-ended by treatment with the Klenow polymerase fragment (Takara, Japan) generating plasmids pDLM6, pDLM7 and pDLM8, respectively. These resulting plasmids were introduced by electroporation into *Pph* 1448A, as previously described (Zumaquero et al., 2010), and the transformation plated into LB plates supplemented with kanamycin. Replicas of the resulting colonies were carried out on LB plates supplemented with ampicillin (300 μg/ml) to determine which clones were the result of plasmid integration (a single recombination event), and which the result of allelic exchange (a double recombination event). Southern blot analysis, using the *nptII* gene as a probe, was used to confirm that allelic exchange occurred at a single and correct position within the genome.

Microscopy

Sections of inoculated *P. vulgaris* leaves (approximately 5 mm^2) were excised with a razor blade, and mounted onto slides in double-distilled H_2O (lower epidermis toward objective) under a 0.17 mm coverslip. Images of the leaf mesophyll were taken using the Leica SP5 II confocal microscope (Leica Microsystems GmbH, Germany). Variable AOTF filters were used for the visualization of the following fluorophores (excitation/ emission): eYFP (514 nm/ 525 to 600 nm), eCFP (458/ 465 to 505 nm), plant autofluorescence (458/ 605 to 670 nm) and VENUS (515 nm/ 525 to 600 nm). Z series imaging were taken at 1 mm or 10 mm intervals when using 40x or 10x objectives respectively. Images were processed using Leica LAS AF (Leica Microsystems). CCID analyzes were performed as described in Godfrey et al. (2010) using Fiji distribution of ImageJ software.

Apoplast-extracted bacteria were stained with FM4-64 following instructions from the provider (Life Technologies), and analyzed using the Leica DMR fluorescence microscope (Leica Camera).

For Bimolecular Fluorescence Complementation (BiFC), leaf sections were excised with a razor blade at 20 hours after *Agrobacterium tumefaciens* inoculation (described below) and mounted into slides in distillated water.

Flow Cytometry and Cell Sorting

Five hundred µl of an overnight *P. syringae* culture in LB was washed twice into $MgCl_2$, and added to 4.5 ml of Hrp-inducing medium (HIM, with 10 mM fructose and pH 5.7; (Huynh et al., 1989)). Bacterial cultures at the indicated growth stage, as well as apoplast-extracted bacterial suspensions, were analyzed using a Cytomics FC500-MPL cytometer (Beckman Coulter).

Stationary cultures were sorted using a MoFloTM XDP cytometer (Beckman Coulter). Cultures of wild type *Pph* 1448A or *Pph hopAB1::gfp* were analyzed, and based on this analysis, gates were drawn to separate the cells displaying fluorescence levels overlapping those of a 1448A non-GFP bacterial population used as a negative control, from cells expressing higher GFP levels. From each gate, cells were collected into a sterile tube. Immediately before sorting, cells were spun at 12,000 *g* for 10 min, and the resulting pellets resuspended into 10mM $MgCl_2$, and bacterial concentration adjusted to 10^6 cfu/ml, and inoculated into bean plants. An aliquot of sorted cells was analyzed again at the cytometer to visualize the differences in expression of the separated populations. Data were analyzed with FlowJo Software.

Generation of point mutations

HopZ1a^{K289R} point mutation was generated following the instructions of the QuikChange Lightning Multi Site-Directed Mutagenesis Kit (Agilent Technologies) using the vector pAME30 (Macho et al, 2010) as template. The primers used were Z1aM1 (CCGGTGGATTTTTATAGGCATGGCGCTTCGCTG) and Z1aM2 (CAGCGAAGCGCCATGCCTATAAAAATCCACCGG). The mutation was verified by sequencing.

To generate MKK7^{K74R} and MKK7^{K167R}, primers used are listed in Chapter 4, Table 3, and NZYMutagenesis kit (NZYtech, Portugal) was used, following the instructions provided, and pENTR-MKK7 as template. Point mutations were verified by sequencing.

Plasmid generation

Plasmids used in this work are listed in Table 2 of each chapter. All the PCR were performed using Q5 High-Fidelity DNA Polymerase (New England Biolabs, USA), unless otherwise stated.

For COI assays, a fragment containing a gentamicin resistance cassette was excised from pMGm using *Kpn*I and cloned into the corresponding site of pAME30 (HopZ1a), pAME27 (HopZ1a$^{C216A)}$, and pMAM1 (HopZ1a^{K289R}), to generate pAME30Gm, pAME27Gm and pMAM1Gm, respectively. The gentamicin resistance cassette allowed antibiotic selection of strains carrying these plasmids versus strains carrying plasmids conferring kanamycin resistance.

For the expression of proteins used in the *in vitro* acetylation assays, HopZ1a, HopZ1a^{C216A} and HopZ1a^{K289R} were amplified by PCR, using plasmids pAME30, pAME27, and pMAM1 as templates, and primers Z1pET-F (AACATATGGGAAATGTATGCGTCG) and Z1pET-R (AAGGATCCTTAGCGCTGCTCTTCGGC). PCR-amplified DNA fragments, encoding the corresponding ORFs were digested with *Nde*I and *BamH*I and cloned into the corresponding sites of expression vector pET28a(+). The resulting vectors pET28-Z1a, pET28-C2 and pET28-K2 express HopZ1a, HopZ1a^{C216A}, and HopZ1a^{K289R} as 6xHis N-terminal fusion proteins, respectively.

For GST fusion proteins, MKK7 ORF was PCR amplified from *Arabidopsis* genomic DNA using the primers MKK7-F and MKK7-R1, and cloned into pGEX-5X-1 (GE Healthcare, UK) in *Bam*HI and *Eco*RI restriction sites.

For *in planta* transient expression assays, 6xHis-HopZ1a, 6xHis-HopZ1a^{C216A} and 6xHis-HopZ1a^{K289R} ORFs were excised from pET28-Z1a, pET28-C2, and pET28-K2 using *Xba*I and *BamH*I, and cloned into the corresponding sites of binary vector pBINX1: the resulting vectors were designated pBINZ1, pBINZ2 and pBINZ3, respectively.

To generate Gateway-cloning intermediates, HopZ1a and HopZ1a^{C216A} were amplified by PCR using plasmids pAME30 and pAME27 as templates, and primers Z1a pENTR-F and Z1a pENTR-R. MKK7 was amplified from *Arabidopsis* genomic DNA using the primers MKK7 pENTR-F and MKK7 pENTR-R. All these fragments were digested with AscI and NdeI and cloned into the corresponding sites on pENTR/D (Invitrogen,

USA). After sequencing validation, fragments were cloned into their respective destination vectors using the Gateway LR Clonase II Enzyme mix (Invitrogen, USA).

PR1 detection assays

For PR1 detection, approximately 100 µg of leaf tissue were harvested, frozen into liquid nitrogen and grounded into 100 µl of extraction buffer (10 mM Tris-HCl pH 7.4, 150 mM NaCl and EDTA-free plant protease inhibitor cocktail (Roche, Mannheim, Germany)). The resulting homogenate was centrifuged at 16 000 *g* for 10 min at 4ºC. Soluble supernatant was separated and centrifuged again to ensure absence of insoluble debris. Protein concentration within the supernatant was determined using a BioRad protein assay (BioRad, Hercules, USA). Unless otherwise stated, 10 µg of each protein sample, were separated by electrophosesis on 12% acrylamide SDS-PAGE gels (Mini protean, BioRad) and transferred onto PVDF membranes (Millipore, Billerica, USA). Western blots for immunodetection of PR-1 were carried out using standard methods, with a 1:5000 dilution of anti-PR-1 antibody and 1:10000 dilution of a secondary Anti-Rabbit antibody (SIGMA, St. Louis, MO, USA). Membranes were developed using the BioRad Clarity Western ECL Substrate (BioRad, Hercules) following the instructions provided. Anti-PR-1 serum used has been described by Wang and collaborators (2005). Membranes were stained with Coomassie blue as loading control.

Systemyc acquired resistance (SAR) assays

For measuring SAR impact on *Pto* DC3000 growth, the fourth and fifth *Arabidospsis* younger-fully expanded leaves were inoculated with either 10 mM $MgCl_2$ (mock), DC3000 or DC3000-expressing effectors at $5x10^5$ cfu/ml. After 2 dpi, the 3 youngest-fully expanded leaves were infiltrated with a $5x10^4$ cfu/ml DC3000 suspension. Growth of DC3000 in the secondary leaves was measured by 4 dpi, as already described.

To measure the PR1 accumulation in distal tissue, two *Arabidopsis* fully expanded leaves were inoculated with either 10 mM $MgCl_2$ (mock) or a 10 mM $MgCl_2$ bacterial suspension at $5x10^5$ cfu/ml of the strain to be tested. After 48 hours, two distal-young leaves were collected and frozen into liquid nitrogen. Protein extraction and western blot were performed as already described.

Hypersensitive Response assays

For macroscopic HR assays, fully expanded leaves of 4- to 5-week old *Arabidopsis* plants were inoculated using a blunt syringe with a $5x10^7$ cfu/ml bacterial suspension, and symptoms were documented at 20 to 24 h post-inoculation (hpi). A minimum of 30 leaves was infiltrated per strain and plant genotype.

***Nicotiana benthamiana* transient expression assays**

For transient expression assays in *N. benthamiana*, 5-week old plants were infiltrated with an *Agrobacterium tumefaciens* C58C1 solution at OD_{600} 0.5 in 10 mM $MgCl_2$, 10 mM MES (SIGMA, St. Louis, MO, USA), 200 µM 3′,5′-Dimethoxy-4′-hydroxyacetophenone (acetosyringone) (SIGMA, St. Louis, MO, USA) carrying the corresponding binary plasmids.

For immunoprecipitation assays, strains expressing either protein were co-inoculated at OD_{600}= 0.5 each. Samples were collected at 20-30 hours post inoculation, before the onset of visible cell death.

Plants were monitored for development of macroscopic cell death and photographed at 24-48 hours post-inoculation.

Protein expression and purification

All proteins were expressed in *E. coli* NCM631 after induction with 0,1 mM IPTG at 20ºC for 6 hours. His-tagged proteins were purified using Ni-NTA agarose (Quiagen, USA). GST and GST-tagged proteins were purified using Glutathione Sepharose 4B (GE Helathcare, USA). Protein concentrations were determined by the Bio-Rad protein assay (Bio-Rad, USA).

***In vitro* acetylation assays**

For *in vitro* acetylation assays using Western blot, 3 µg of each 6xHis-HopZ1a, 6xHis-HopZ1a^{C216A} and 6xHis-HopZ1a^{K289R} purified protein were incubated in acetylation buffer containing 50mM HEPES pH 8, 10% Glycerol, 1mM DTT and 1mM PMSF, with 100nM inositol hexakisphosphate (IP6 or phytic acid, SIGMA, USA) and 50µM Acetyl-CoA (SIGMA, USA). The reaction was incubated for 1 hour at 30ºC, and

stopped by adding 3X Laemmli buffer and boiling at 95ºC for 5 min. Twenty µl of each sample were separated by SDS-PAGE, and autoacetylation was detected using an anti-Acetylated-Lysine Antibody (Ac-K-103, Cell Signaling Technology, USA). As a loading control 20 µl of the same samples were separated by SDS-PAGE and stained with Coomassie.

For ^{14}C-based acetylation assays, 3 µg of the effector (6xHis-HopZ1a, 6xHis-HopZ1a^{C216A} and 6xHis-HopZ1a^{K289R}) and 5 µg of the substrate (GST, GST-MKK7, GST-MKK7^{K167R}) were incubated in acetylation buffer containing 50 mM HEPES pH 8, 10% Glycerol, 10 mM Sodium butyrate, 1 mM DTT and 1 mM PMSF, with 100 nM inositol hexakisphosphate (IP6 or phytic acid, SIGMA, USA) and 22 nCi Acetyl-CoA (PerkinElmer, USA). The reaction was incubated for 1 hour at 30ºC, and stopped by adding Laemmli buffer and boiled at 95ºC for 5 minutes. 20µl of each sample were separated by SDS-PAGE, and proteins were transferred to a PVDF membrane. Acetylation was detected by autoradiography. As a loading control 20µl of the same samples were separated by SDS-PAGE and stained by Coomassie

Dexamethasone treatment

Five weeks-old DEX-*MKK7* plants were infiltrated with 10 µM dexamethasone (SIGMA; USA) 0.1% ethanol (DEX+), or water 0.1% ethanol (DEX-) for growth assays and callose deposition. Three hours post-infiltration, same leaves were inoculated with the corresponding bacterial suspension for PR1 assays.

Flg22-responses assays

For callose deposition assays, leaves pretreated with or without dexamethasone were infiltrated after 24h with 100 nM flg22. After 15 hours, leaves were cleared in alcoholic lactophenol (1 volume of phenol: glycerol: lactic acid: water and 2 volumes of ethanol) at 65ºC for 30 min, rinsed in water and stained with aniline blue 0.01% in 150mM K_2HPO_4. Samples were mounted in 50% glycerol and examined under UV fluorescence microscope. Four pictures were taken per leaf, and 6 leaves per treatment (2 leaves per plant). Callose deposition was measured using Fiji distribution of ImageJ.

Oxidative burst was quantified as previously described (Macho et al, 2014). Plant discs were incubated overnight with 30 µM dexamethasone 0.1% ethanol, or water 0.1%

ethanol. ROS was elicited with 100 nM flg22 (GeneScript, USA). Twenty leaf discs from 4-week-old plants were used for each condition. Luminescence was measured using a Luminometer.

To detect activation of MAP Kinases, DEX-MKK7 plants were germinated in MS medium, and, transferred after 7 days to liquid MS, where they were kept for another 7 days. MS was changed by DEX+/DEX- treatment (as described before), and after 24 hours plants treated with 100nM flg22. Plant samples were taken at the indicated time points and frozen into liquid nitrogen. Samples were grounded into 100 µl extraction buffer (100mM TRIS pH 7.5, 150mM NaCl, 5mM EDTA, 10% glycerol, 1X protease inhibitor cocktail (SIGMA, USA) and 1X phosphatase inhibitor (Cell Signaling, USA). After a 10 min centrifugation at 16,000 *g*, supernatants were transfered into fresh tubes, and proteins quantified using a BioRad protein assay (BioRad, Hercules, USA). Ten µg of proteins were loaded per lane in a SDS-PAGE, and transferred to a PVDF membrane. MAP kinase activation was detected using an anti-p42/p44-erk antibody (Cell Signalling, USA), and membrane was stained with Coomassie blue.

Immunoprecipitation assays

For immunoprecipitation assays, 1 g of leaf tissue was homogenized into liquid nitrogen, with 2 ml of extraction/washing buffer (50mM Tris-HCl pH 7.5, 150mM NaCl, 0.1% Triton, 0.2% NP-40, 6mM BME and 1X protease inhibitor cocktail [SIGMA, USA]). The resulting homogenate was centrifuged at 16,000 *g* for 20 min at 4ºC, and the supernatant collected into a new tube. Twenty µl of pre-equilibrated anti-HA agarose (SIGMA, USA) were added to each tube, and incubated for 3 hours at 4ºC in an end-over-end shaker. After incubation, tubes were spun down (900 *g*) and beads washed 3 times. To elute the proteins, beads were boiled 5 min at 95ºC in 20 µl 3X Laemmli buffer.

In vitro kinase assay

For *in vitro* kinase assays, 1 µg of GST, GST-MKK7, GST-MKK7^{K74R}, or GST-MKK7^{K167R} plus 1 µg of the Myelin Basic Protein (MBP) (SIGMA, USA) were incubated into phosphorylation buffer containing 50 mM Tris-HCl pH 7.4, 5 mM $MnCl_2$, 5 mM $MgCl_2$, 1 mM DTT, 1 µM cold ATP and 5 µCi [γ^{32}P] - ATP

(PerkinElmer, USA). The reaction was incubated for 30 minutes at 30ºC, and stopped by adding Laemmli buffer and boiling at 95ºC for 5 minutes. Ten µl of each sample were separated by SDS-PAGE, and phosphorylation detected by autoradiography. As a loading control, 10 µl of the same samples were separated by SDS-PAGE and stained with Coomassie blue.

Chapter 1: Dynamics of heterogeneous populations of *Pseudomonas syringae* within plant tissues reveal a diversity of interactions

José S. Rufián, Alberto P. Macho, David S. Corry, John W. Mansfield, Dawn L. Arnold, Carmen R. Beuzón.

Introduction

Plants are continuously under attack by a myriad of microorganisms, often by a mixture of them simultaneously. The different defense mechanisms that plants use to resist such attacks have been the subject of extensive study for years, where much of this research has focused on the interaction between bacterial pathogens and the plant host (Dodds and Rathjen, 2010). These studies, mostly carried out in laboratory conditions, analyze the interaction in a one-to-one basis, one pathogen at a time. However, field infections are likely to be more complex. The interaction between the plant and a given pathogen can be influenced by additional interactions of the plant with the same or different pathogens. Contact with some pathogens, for instance, can induce systemic acquired resistance or SAR (Cameron et al., 1994). Induction of SAR determines a restriction of growth of a newly incoming pathogen in systemic tissues, by determining the pre-activation of defense responses in uninfected tissues, such as accumulation of salycilic acid (SA), or pathogenesis-related proteins (PRs). Plant-associated bacteria can also determine pre-activation of defenses in systemic tissues in a SA-independent, jasmonic acid (JA)-dependent process known as induced systemic resistance (ISR) (van Loon et al., 1998).

Even in the context of a seemingly single infection, genomic changes within the population have been shown to give raise to genetic variants, which can differ in their interaction with the plant. Only within the *P. syringae* complex the strain diversity is overwhelming, with many variants of a pathogen originated through horizontal gene transfer (HGT), mutation, chromosomal re-organisation, and unknown events giving raise to phase variation within the populations, and to the differentiation of variants with important differences on host adaptation (Ma et al., 2006; Godfrey et al., 2011). At the center of the process of host adaptation of *P. syringae* is the T3SS and the T3Es (Alfano and Collmer, 1997). Evolution of the T3SS and that of its effectors has been mostly driven by HGT (Rohmer et al., 2004; Sarkar et al., 2006).

An example of how variants of a given pathogen with different virulence capabilities can meet within the plant is found in the bean pathogen *P. syringae* pv. *phaseolicola* (hereafter referred to as Pph*).* Inoculation of Pph 1302A into resistant bean plants activates the HR, which in turns triggers the excision of the bacterial PPHGI-1 locus, a genomic island encoding a T3E, HopAR1 (formerly AvrPphB), responsible for triggering the HR in this cultivar (Pitman et al., 2005). Once excised from the

chromosome PPHGI-1 is maintained as a circular episome in which gene expression is severely reduced (Godfrey et al., 2011). As excision of PPHGI-1 takes places in a number of cells during an incompatible interaction, the bacterial population bifurcates into two subpopulation differing in whether they express, or not HopAR1. In a host carrying the resistance gene against HopAR1, these two subpopulations have a very different interaction with the host, since those carrying a genomic copy of the island will induce a strong HopAR1-triggered HR, and those carrying its episomal version will not (Godfrey et al., 2011).

Little is known about how mixed populations of a given pathogen interact and develop with the host plant. Work in the 1960s showed that inoculation of a *P. syringae* strain capable of triggering strong plant defenses (avirulent strain) may result in the limitation of a co-inoculated virulent strain (Klement and Lovrekovich, 1961; Omer and Wood, 1969). However, a population of a non-pathogenic strain may also benefit from co-inoculation with a pathogenic one, reaching a larger population size than if inoculated alone (Young, 1974). More recently, following the lead of research in animal pathogens, where mixed infections are used to analyze bacterial virulence (Beuzón and Holden, 2001), our laboratory set up the conditions to use competitive index in mixed infections as a means to assay virulence (Macho et al., 2007). This work showed that co-inoculated *P. syringae* strains affected each other's growth or not, depending on the concentration of the inoculum. Thus, when high inoculation doses were used, it was possible to detect dominant negative effects of avirulent strains on the growth of virulent, or complementation of growth defects of non-pathogenic by pathogenic co-inoculated strains, such as those previously described. These interferences were not detected at lower inoculation doses, like those expected to take place within a natural infection.

In this work, we apply fluorescent confocal microscopy to analyze how mixed bacterial populations of *P. syringae*, with key differences in their virulence capacity, develop within the plant host. We take advantage of the improvements in the biophysical properties of fluorophores and confocal microscopic imaging technology, which allows to minimize the background auto-fluorescence detection from both healthy, and most importantly, plant tissue undergoing the HR (Godfrey et al., 2010). These advances make possible the application of confocal microscopy to follow distribution and growth of *P. syringae* strains labeled with eYFP or eCFP inside the

leaf. We analyze the cellular basis that determine whether co-existing *P. syringae* bacteria with different virulence capabilities affect each other's growth, and discuss the potential implications for host adaptation.

Table 1. Strains used and generated in this work.

Strain	Genotype	Reference
1448A	*P. syringae* pv. *phaseolicola* wild-type strain race 6	(Teverson, 1991)
1449b	*P. syringae* pv. *phaseolicola* wild-type strain race 7	(Teverson, 1991)
IOM1	1448A *ΔhrcV*, KmR	(Macho et al., 2007)
JRP8	1448A Tn*7*-eGFP, Gm^R	This work
JRP9	1448A Tn*7*-eYFP, Gm^R	This work
JRP10	1448A Tn*7*-dsRFP, Gm^R	This work
JRP11	1448A Tn*7*-eCFP, Gm^R	This work
JRP12	1448A *ΔhrcV* Tn*7*-eYFP, Gm^R	This work
JRP15	1449b Tn*7*-eYFP, Gm^R	This work
JRP17	1449b Tn*7*-eCFP, Gm^R	This work
RW60	1449b Vir^-, $pAV511^-$, Rif^R	(Jackson et al., 1999)
JRP18	RW60 Tn*7*-eYFP, Gm^R	This work

Table 2. **Plasmids used in this work**.

Name	Description	Reference
pUXBF13	Helper plasmid, providing the Tn*7* transposase proteins, Amp^R	Bao et al. (1991)
pRK2013	Conjugation helper plasmid, Km^R	Figurski et al. (1979)
AKN132	dsRFP, Amp^R, Gm^R	Lambertsen et al. (2004)
AKN100	eGFP, Amp^R, Gm^R	Lambertsen et al. (2004)
AKN069	eYFP, Amp^R, Gm^R	Lambertsen et al. (2004)
AKN033	eCFP, Amp^R, Gm^R	Lambertsen et al. (2004)

Results

Development of mixed *versus* single micro-colonies within the plant apoplast

Since our previous work showed that interference between co-inoculated largely depended on the concentration of the inoculum (Macho et al., 2007), ,we set out to apply confocal microscopy to analyze the cellular basis for that observation. We generated fluorescently labeled derivatives of the bean pathogen *P. syringae* pv. *phaseolicola* 1448A wild type strain (Table 1), and followed their distribution and growth within the leaf apoplast after inoculation at different concentrations. All fluorescent derivatives expressed the fluorophores, and in keeping with previous reports (Godfrey et al., 2010), the clearest differences in mixed cultures between labeled strains were detected when combining eCFP and eYFP-labeled bacteria (data not shown). Examination by light and fluorescent microscopy of mixed cultures of 1448A eYFP and 1448A eCFP showed that every bacteria tagged with a given fluorophore emitted the corresponding fluorescence at a similar level, both in laboratory medium and *in planta* (Figures 1A and 1B). Growth of 1448A eYFP as well as symptom induction were confirmed to be wild type-like in all conditions tested (Table 3). Growth of 1448A eCFP showed a slight delay compared to wild type, both in laboratory medium and *in planta* (Table 3), but virulence was not affected, since the induction of symptoms was similar to that of 1448A eYFP (Figure 1D), and the number of colonies observed for these two strains was similar following mixed inoculation (Figure 1C). The size of the 1448A eCFP colonies in leaves was somewhat smaller than that of 1448A eYFP colonies, in keeping with the observed delay of growth observed both within the plant and in laboratory medium (Figure 1C and Table 3). Thus, confocal microscopy of leaves inoculated with 1448A eYFP and 1448A eCFP can accurately reflect wild type growth dynamics within the host.

Table 3. CI analysis of fluorescent *P. syringae* strains.

Mixed Strains	^{LB}CI (±SE)	$^{in\ planta}$CI (±SE)
1448a wt *vs*. 1448a YFP	0,97 ± 0,06	-
1448a wt *vs*. 1448a CFP	0,61 ± 0,1*	-
1448a YFP *vs*. 1448a CFP	0,59 ± 0,03*	0,64 ± 0,04*
RW60 YFP *vs*. 1449b CFP	0,74 ± 0,06*	-
1449b YFP *vs*. 1449b CFP	-	0,82 ± 0,02*

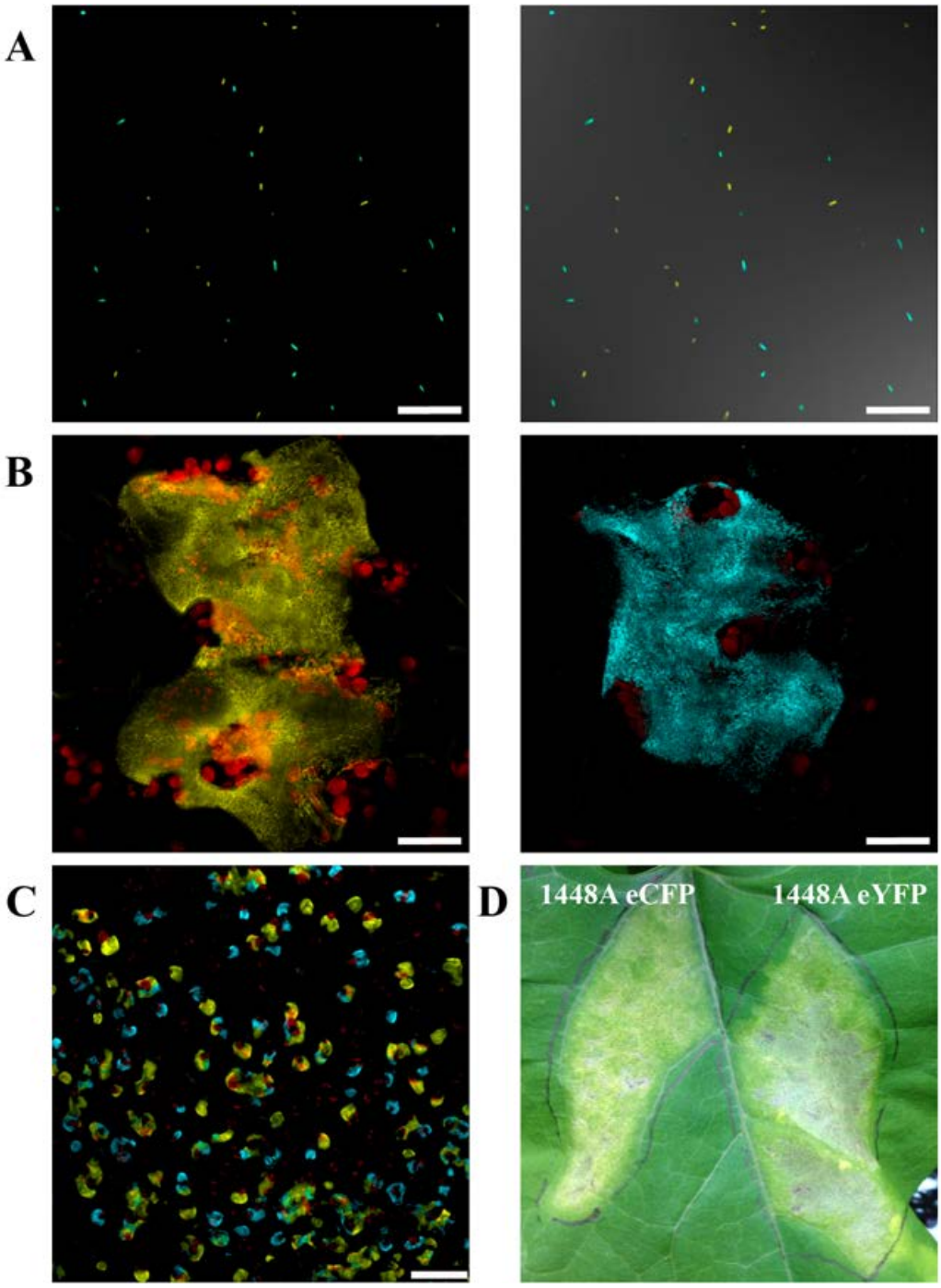

Figure 1. Expression of either eYFP or eCFP in Pph 1448A is constitutive and does not affect virulence. (**A**). Left panel: Fluorescence microscopy image showing constitutive expression of eYFP and eCFP from bacteria grown within rich medium. Right panel: Merged fluorescence (eYFP, eCFP) and phase-contrast microscopy images. (**B**) Confocal fluorescence microscopy image of bean leaf sections 3 days post-inoculation (dpi) with a $5x10^5$ cfu/ml suspension of 1448a eYFP (Left) or 1448a eCFP (Right). Bacterial microcolonies and even individual bacteria can be visualized within the plant apoplast. (**C**) Confocal fluorescence microscopy image of a bean leaf sections 2 days post-inoculation (dpi) with a $5x10^5$ cfu/ml bacterial suspension containing equal amounts of 1448a eYFP and 1448a eCFP. Differently labeled wild type bacteria can be distinguished within single- or mixed-colored colonies. Red in images in B and C corresponds to auto-fluorescence emitted by chloroplasts. (**D**) Symptoms developed by either 1448A eCFP and 1448a eYFP X dpi with $5x10^5$ cfu/ml. Scale bar: A and B: 25 µm. C: 100 µm.

Derivatives of 1448A expressing either eYFP or eCFP were co-infiltrated into bean leaves at different concentrations ($5x10^7$, $5x10^6$, $5x10^5$ and $5x10^4$ cfu/ml), and leaf sections were taken at different days post-inoculation (1 to 5 dpi) and observed by confocal microscopy (Figure 2). Numerous colonies could be observed as early as 1 dpi in leaves inoculated with $5x10^7$ cfu/ml (Figure 2A). The majority of these colonies displayed a mixture of eYFP and eCFP. By 2 dpi, many of the colonies merged as they grew in size. Longer time points showed tissue damage too extensive to be examined by microscopy, as severe disease symptoms had already started to develop. In leaves inoculated with $5x10^6$ cfu/ml, colonies were clearly visible by 2 dpi, and although a considerable proportion of them showed both eYFP and eCFP, single-colored colonies could be detected as well (Figure 2B). As time increased, this trend became clearer despite the fact that confluence led to the appearance of merged colonies. To quantify this trend, we counted single-colored *versus* bicolored colonies, in three independent experiments (three fields per sample and experiment), and calculated the ratio between them. The ratio single- to bicolored colonies was 0.68±0.25, 2 days post-inoculation with $5x10^7$ cfu/ml, supporting the observation of a minority of single-colored colonies at the highest inoculum concentration. However, this ratio was almost 20-fold higher (12.25+/-4.35) 3 days post inoculation with $5x10^6$ cfu/ml, indicating an increase in single-colored colonies associated to lower inoculum concentrations. In short, a 10-fold decrease in the concentration of the inoculum led to a 20-fold increase in the ratio between single-colored *versus* bicolored colonies, from a minority of single-colored colonies, to a majority. Following this trend, leaves inoculated with $5x10^5$ cfu/ml contained a vast majority of single-colored colonies by 3 dpi (Figure 2C). In fact, almost no bicolored colonies could be observed regardless of the time analyzed. In these conditions, equal numbers of both types of single-colored colonies could be observed, although the average size of the eCFP colonies was generally smaller than that of the eYFP colonies, as expected with the growth delay observed for the eCFP strain. As before, a later time point (4 dpi) was associated to an increment in the number of colonies where confluent growth had lead to large single-colored colonies merging (image shown in the back cover of this thesis).

Lastly, when leaves were inoculated with $5x10^4$, the inoculation dose most commonly use for competitive assays (Macho et al., 2007; Macho et al., 2016), we were

unable to observe any bicolored colonies by 4 dpi, and only a few merged, seemingly due to confluent growth of close single-colored colonies colonies by 5 dpi (Fig. 2D).

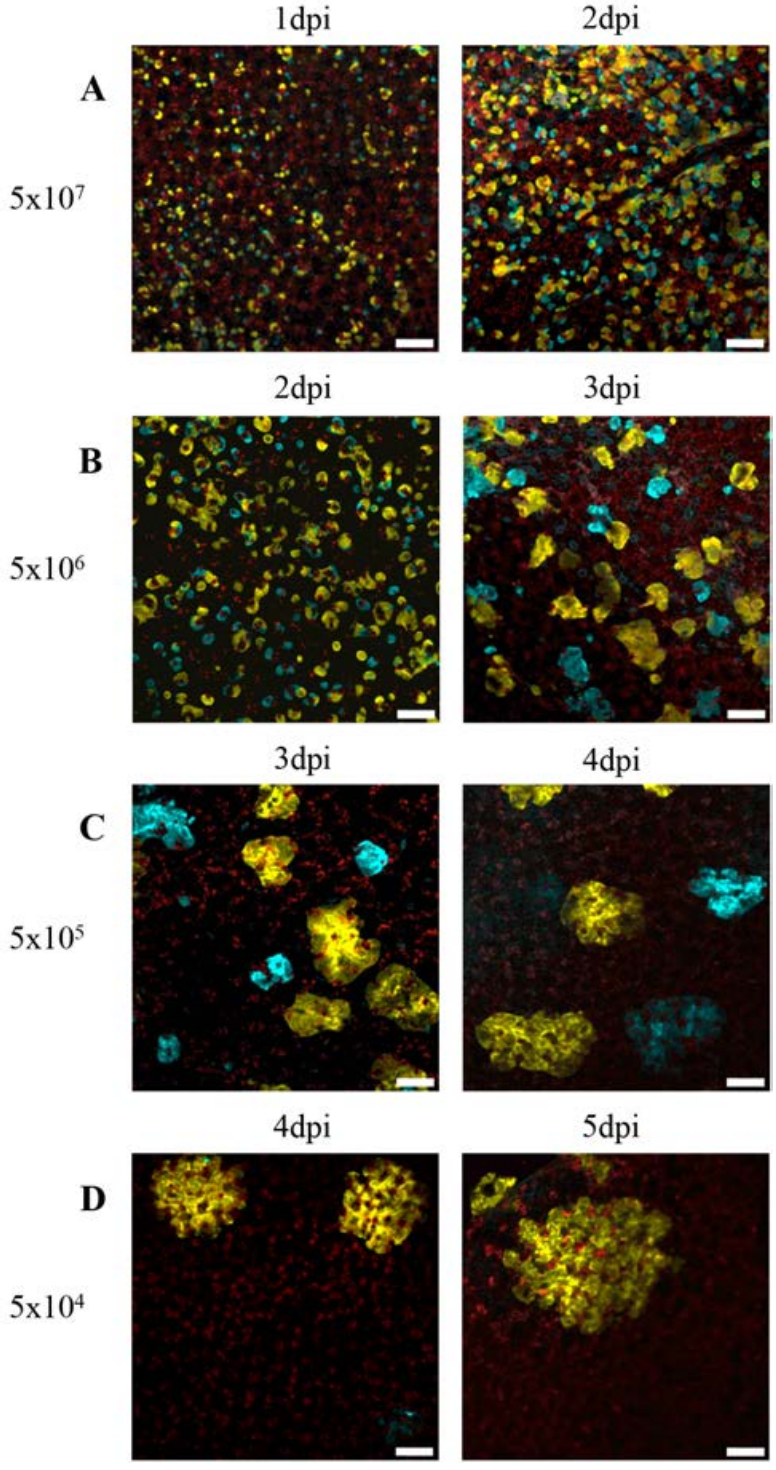

Figure 2. Co-inoculation of 1448a eYFP and 1448a eCFP at different concentrations determines different dynamics of colony development. Wild-type Pph 1448A eYFP (yellow) or Pph 1448A eCFP (cyan) were co-inoculated in equal amounts at the indicated dose (left numbers, cfu/ml) and leaf sections taken and visualize at different dpi. Some time points were not displayed either because only a few and scattered bacteria could be observed, or the inoculated leaf tissue was too damaged due to the progress of the infection. Scale bars: 100 µm

Close proximity to a pathogenic strain promotes growth and spreading of a non-pathogenic strain.

Previous work including our own have shown that when inoculated at high concentratetions pathogenic strains can complementation growth of a non-pathogenic strain (Young, 1974; Macho et al., 2007). We co-infiltrated 1448A eCFP and its non-pathogenic mutant derivative, Δ*hrcV* (eYFP) (Table 1) into bean leaves at different concentrations ($5x10^7$, $5x10^6$ and $5x10^5$ cfu/ml). Leaf sections were taken at 3 dpi and observed by confocal microscopy (Figure 3). The *hrcV* gene encodes an essential component of the Hrp T3SS (Cornelis and Van Gijsegem, 2000), required for development of infection in compatible hosts (Alfano and Collmer, 1997). As previously seen in Figure 2, images display differences in the rate of bicolored *versus* single-colored colonies depending of the concentration of the inoculum used: higher concentrations ($5x10^7$ cfu/ml) lead to a higher rate of bicolored colonies (Figure 3). Three days post-inoculation with $5x10^7$ cfu/ml, growth of Δ*hrcV* eYFP, estimated as the amount of yellow fluorescence, was very similar to that of pathogenic 1448A eCFP (blue fluorescence) (Figures 3A and B). We confirmed these results using CI assays (Figure 3C). CIs result from dividing the output ratio between the two strains by their input ratio (should be close to 1:1), thus a CI close to 1.0 indicates that the co-inoculated strains are growing similarly.. In these experiments, yellow fluorescence associated to the mutant non-pathogenic strain (Δ*hrcV* eYFP) was rarely detectable in single-colored colonies and almost only found in association to blue (1448A eCFP), in bicolored colonies (Figure 3A).. As the inoculum concentration decreased, the rate of bicolored colonies decreased too (Figure 3A), as did growth of Δ*hrcV* eYFP (Figures 3B and C) reaching its maximal difference with pathogenic wild type 1448A eCFP, over 100-fold, in leaves inoculated with $5x10^4$ cfu/ml. These results indicate that close proximity to pathogenic 1448A promotes growth of the non-pathogenic Δ*hrcV* strain

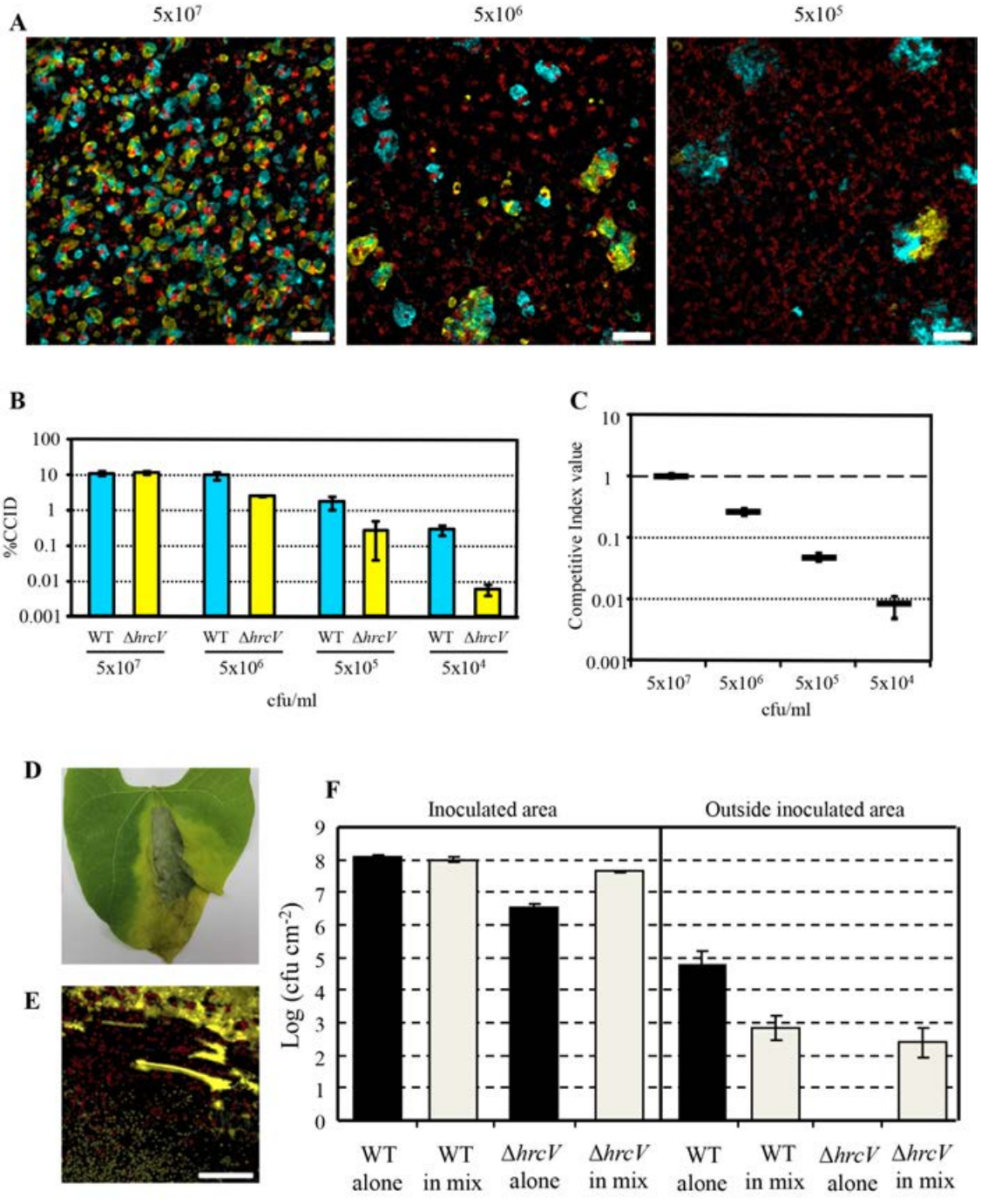

Figure 3. Close proximity with pathogenic bacteria complements growth of non-pathogenic. (A) Confocal microscope images showing growth of 1448a eCFP and Δ*hrcV* eYFP within bean leaves inoculated at different concentration (top numbers, cfu/ml). Scale bars: 100 µm. (**B**) Quantification of Confocal Colony Image Data (CCID) from images obtain for A. (**C**) Competitive Index (CI) assay of mixed inoculum of 1448a eCFP and Δ*hrcV* eYFP at the indicated doses. (**D**) Image showing disease symptoms spreading outside the area inoculated with 1448a at 10^6 cfu/ml by 7 dpi. (**E**) Image shows 1448a eYFP bacterial scattered outside the area inoculated with $5x10^7$ cfu/ml by 2 dpi. **(F**) Bacterial growth at 4 dpi within and outside the tissue inoculated with $5x10^7$ cfu/ml of either 1448a, Δ*hrcV* or both. Error bars in B, C and F indicate standard error.

Having established that close proximity can determine complementation of growth of a non-pathogenic strain by a pathogenic one, we questioned the extent of such

complementation. When leaves are inoculated with $5x10^6$ cfu/ml of the wild type strain symptoms appear initially on the inoculated tissue, spreading with time onto non-inoculated tissue (Figure 3D), as disease progresses and bacteria spreads outside of the inoculated area (Figure 3E). We determined the extent of the spread of 1448A and Δ*hrcV* beyond the inoculated area, in leaves inoculated with $5x10^7$ cfu/ml of either single or mixed inocula (Figure 3F). Wild type bacteria could be consistently detected outside the inoculated area by 5 dpi, independently of whether it was individually or co-inoculated with Δ*hrcV* bacteria. However, mutant bacteria could only be detected outside the inoculated area when co-inoculated with the wild type pathogenic strain (Figure 3F). It is noteworthy that the amount of wild type bacteria found outside the inoculated area was in fact 100-fold lower when co-inoculated with Δ*hrcV* bacteria, raising the possibility of systemic defense responses triggered by the non-pathogenic strain having a negative impact on the systemic spread of the wild type.

Bacterial entry and bacterial growth in mixed inoculations.

Although infiltration is the means of inoculation most commonly used for virulence assays, in the field, bacteria gains access to the plant apoplast mainly through natural openings such as stomata or occasional wounds (Melotto et al., 2008). Inoculations using a bacterial suspension to dip the leaf into, or to spray it, are used in the laboratory when trying to reproduce the natural route of inoculation. These means of inoculations are much less effective than infiltration, rendering maximal initial concentrations of bacterial within the apoplast similar to the concentrations obtained by infiltrating with $5x10^4$ cfu/ml, the lower inoculation dose used in the previous experiments (Macho et al., 2012). Since the formation of mixed colonies following infiltration with $5x10^4$ cfu/ml was shown to be severely reduced, and formation of mixed colonies necessary for growth interference between strains, natural inoculations could perhaps not lead to situations in which different bacteria could interfere with each other. However, whereas infiltration of a bacterial solution into the plant leaf forcefully spreads bacteria evenly throughout the apoplast of the infiltrated area, inoculation by dipping could result in higher local concentration of bacteria associated to the entry points, which could therefore act as concentrators promoting the close proximity required for growth interference. If this was the case, natural entry could potentially

lead to a higher rate of interference within heterogeneous populations, *i.e*. interference with fewer bacteria, than initially predicted from our infiltration assays.

We analyzed the bacterial distribution within the leaf apoplast, 2 hours after dip-inoculation with 1448A eYFP, but we could detect any clear increase in bacterial concentration in relation to stomata (Figure 4A). Unexpectedly, a high bacterial concentration could be found close to the base of trichomas (Figure 4B). Trichomas may represent a structural weak point for mechanical damage and thus offer an additional entry point for *P. syringae* as it would also help to accumulate the inoculating solution (or rainwater). One additional observation regarding bacterial distribution at this time point was their clear concentration close to the vascular bundles (Figure 4C). Interestingly, although *P. syringae* is not a vascular pathogen, it has been recently shown to localize and even move through the vascular bundles in *Arabidopsis* and *Nicotiana benthamiana* (Misas-Villamil et al., 2011; Yu et al., 2013). In any case, when leaves dip-inoculated with a mixed suspension of 1448A eCFP and 1448A eYFP were observed at 5 dpi, the majority of the colonies observed were bicolored colonies, interestingly located close to the vascular bundles (Figure 4D). Notably, a clear concentration of bacterial colonies could be observed close to the edges of the leaves, were hydatodes are located (Figure 4E). Hydatodes are a known port of entry for other leaf pathogens and can also act as such for *P. syringae* (Hugouvieux et al., 1998; Yu et al., 2013)**.** These results support that inoculation by dipping (and presumably rainwater) does generate high local concentrations of bacteria.

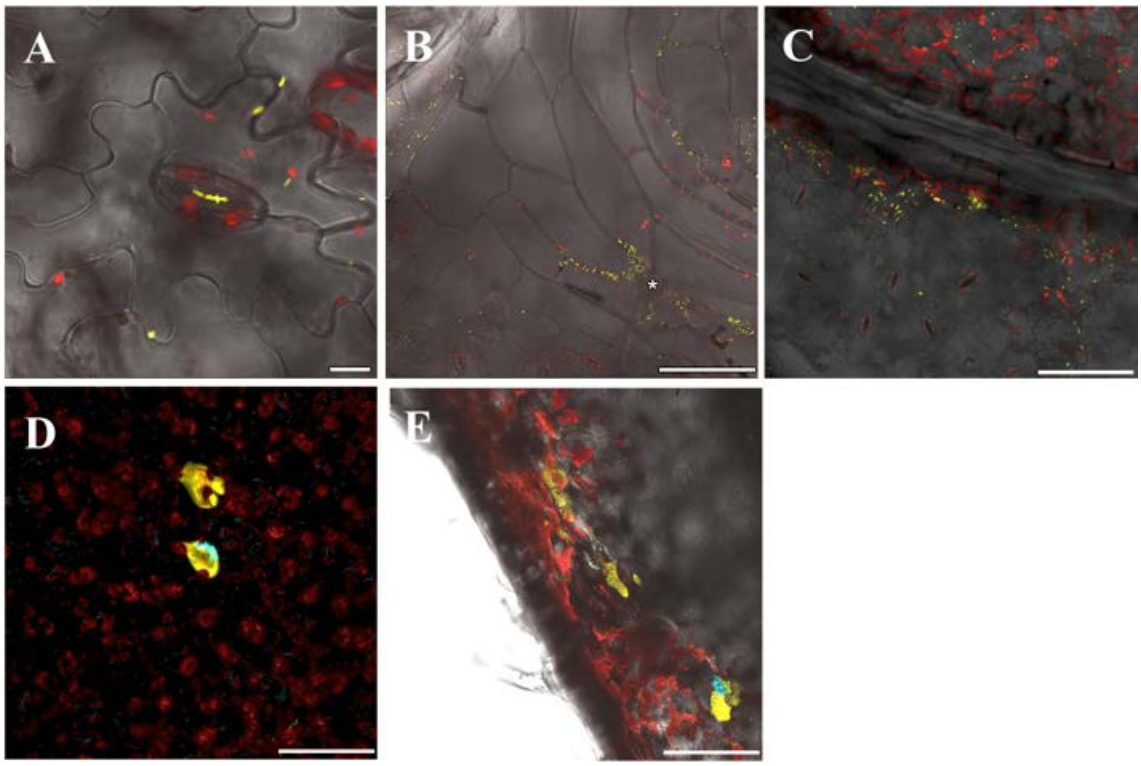

Figure 4. Bacterial entry into the apoplast promotes close vicinity. Dip inoculation of 1448A eYFP allows bacteria to enter through stomata (**A**), thricoma (marked with a star)-associated wounds (**B**) or hydatodes (**E**). Bacteria tend to concentrate close to vascular bundles (**C**). Dip inoculation increases the formation of bi-colored colonies (**D** and **E**). Scale bars: A: 10 µm; B, C, D, and E: 100 µm.

Close proximity between virulent and avirulent bacteria can lead to dominant negative effects and/ or *in trans* defense suppression.

Previous reports from our group and others (Klement and Lovrekovich, 1961; Averre and Kelman, 1964; Omer and Wood, 1969; Macho et al., 2007) had shown that inoculation with a strain capable of triggering a strong defense response (avirulent strain) could restrict growth of a co-inoculated virulent strain. We investigated the basis for this type of interference by analyzing the dynamics of colony development of 1449b eCFP, a wild type representative of *P. syringae* pv. *phaseolicola* race 7, and its avirulent derivative, RW60, expressing eYFP (Table 1). Strain 1449b is fully virulent in plants of the Canadian Wonder bean cultivar. RW60 is a plasmid-cured 1449b derivative that has lost a type III effector (HopAB1, formerly known as VirPphA) capable of suppressing the hypersensitive response (HR) triggered by other type III effector(s) from this strain (Jackson et al., 1999; Tsiamis et al., 2000). Thus, RW60 triggers the HR in cv. Canadian Wonder, which determines a severe restriction of bacterial growth within the plant. Our previous results showed that in leaves co-inoculated with 1449b and RW60 at the relatively low inoculum concentration of $5x10^4$ cfu/ml, growth of wild type 1449b

was more than a five-fold lower than in leaves where it was inoculated alone (Macho et al., 2007). Thus, we co-inoculated 1449b eCFP and RW60 eYFP by infiltrating a $5x10^4$ cfu/ml into bean leaves and analyzed tissue sections taken by 5 dpi using confocal microscopy. An area of plant cells displaying pale green-blue/ yellow fluorescence in their outlines surrounded most single-colored RW60 eYFP colonies but did, not do so around single-colored 1449b eCFP colonies (Figure 5A). Auto-fluorescence in these cells is due to the accumulation of phenolic auto-fluorescent compounds associated to tissue collapse (Bennett et al., 1996; Yu et al., 1998) and liberation of antimicrobial compounds (Whalen et al., 1991; Jambunathan et al., 2001; Wright and Beattie, 2004) during the HR. Bicolored or closely located single-colored colonies could be classified into several types in regards to their association to surrounding auto-fluorescence. We found small colonies formed by virulent 1449b eCFP, closely located to colonies of avirulent RW60 eYFP, both surrounded by a large area of auto-fluorescence, covering many plant cells (Figures 5B and C). The appearance of this type of colonies, likely originated by a dominant negative effect of the defenses triggered by RW60 bacteria on the growth of closely located virulent wild type bacteria, would be in keeping with growth results previously reported (Klement and Lovrekovich, 1961; Omer and Wood, 1969; Macho et al., 2007). However, we also found larger colonies of wild type virulent 1449b eCFP, closely located or even merged with colonies of avirulent RW60 eYFP, without any evidence of defense activation in the surrounding plant cells (no auto-fluorescent cellular outlines) (Figures 5B and D). This type of colonies could result from virulent bacteria either suppressing the activation or the onset of defenses against closely located avirulent RW60 bacteria. Lastly, closely located or merged colonies were also found that displayed auto-fluorescence only in a few plant cells surrounding the virulent colony or its area in the merged colonies, away from virulent eCFP wild type bacteria. These cases could be explained by the wild type colony having successfully suppressed the defense response only in the closest surrounding cells (Figures 5B and E). These last two types of colonies would indicate the ability of the wild type strain to locally suppress *in trans* the defense response triggered by RW60.

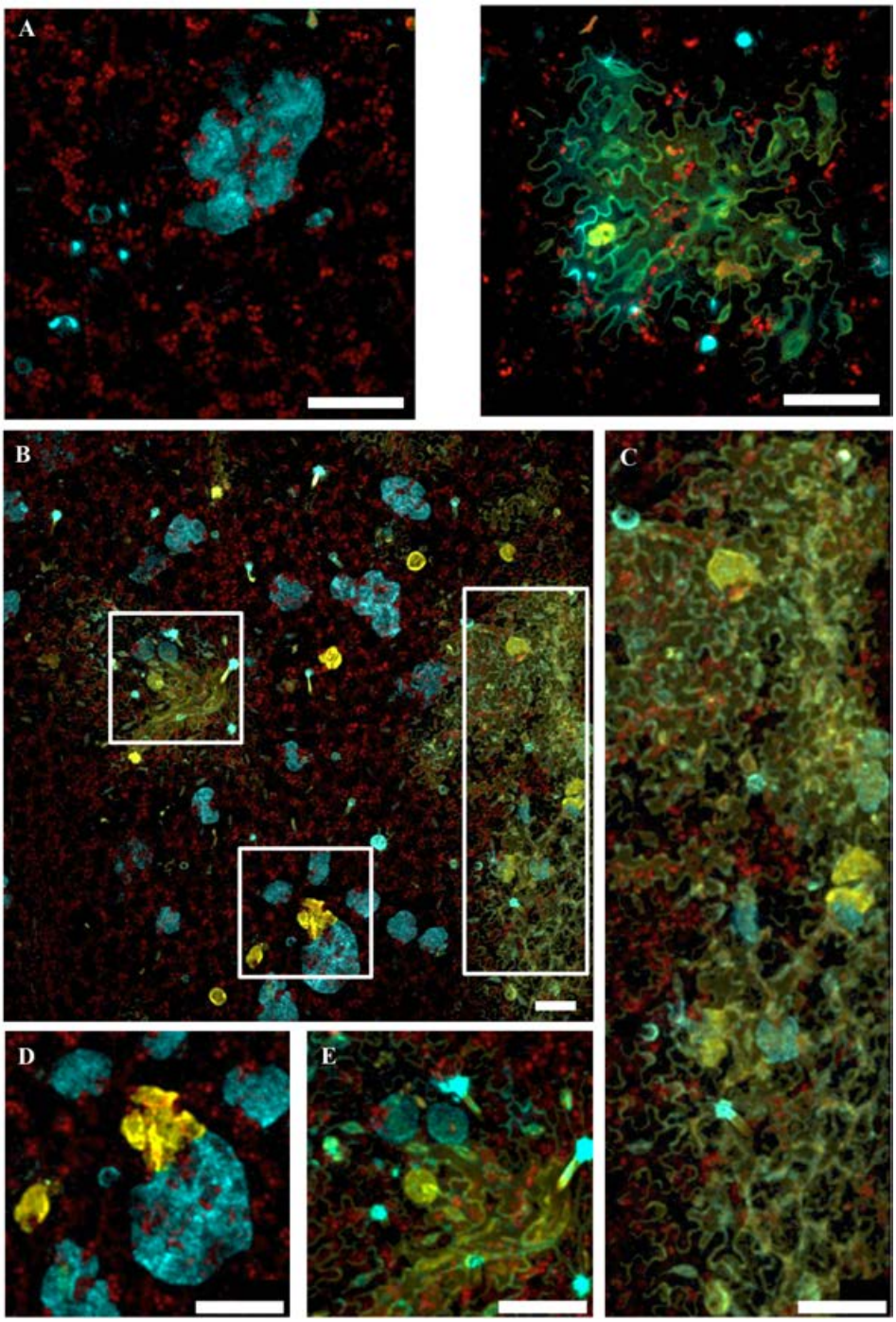

Figure 5. Co-inoculation of virulent and avirulent strains leads to a diversity of interactions. Confocal microscopy images of leaf sections 5 dpi with a bacterial suspension at either $5x10^4$ cfu/ml (**A**) or $5x10^5$ cfu/ml (**B, C, D, and E**), containing equal numbers of virulent wild-type 1449b eCFP (**A,** left panel; blue colonies in all other panels) and avirulent RW60 eYFP (**B,** right panel; yellow colonies in all other panels). **C**, **D**, and **E** are close ups of the different types of colonies displayed in **B**, as classified according to their association to fluorescent plant cell outlines associated to local activation of the defense response: (**C**) Growth of virulent 1449b eCFP is limited as small blue microcolonies can be seen fully surrounded by a large auto-fluorescent area due to the activation of the HR against closely located virulent RW60 eYFP microcolonies. (**D**) Avirulent RW60 eYFP microcolonies not surrounded by autofluorescence, seemingly protected by closely located large numbers of virulent eCFP bacteria. (**E**) Closely located microcolonies of virulent 1449b-CFP and avirulent RW60 eYFP were activation of plant defenses is restricted to the vicinity of avirulent bacteria, away from wild type virulent bacteria. .Size bars represent 100 µm.

Discussion

In this study we have used confocal microscopy to analyze how *P. syringae* pv. *phaseolicola* distributes and grows within the plant apoplast, and to show an array of different scenarios taking place when strains displaying differences on their virulence meet within the plant. We confirm our previous results that the outcome of the individual interaction between a given strain and the host may have a strong impact on the development of a co-inoculated strain in certain conditions. We demonstrate that the interferences observed between strains co-inoculated at high bacterial concentrations, are due to close proximity, rather than to the overall high bacterial load on the inoculated area. This conclusion is supported by the fact that similar bacterial concentrations within the apoplast at the onset of the experiment, display different distribution within the inoculated area leading to differences in growth depending on the means of inoculation (i.e. infiltration *versus* dip-inoculation).

In trans defense suppression within a mixed infection

Interestingly, although complementation of non-pathogenic strains can only be clearly observed in mixed or merged colonies, interferences between virulent and avirulent strains (i.e. dominant-negative effects on wild type growth, or defense suppression) can also be observed between bacterial colonies located near, but not in direct contact. Thus, different types of interference seem to require a different degree of proximity to take place. In support of this conclusion, while no complementation of growth of the Δ*hrcV* mutant can be detected following inoculation by infiltration at $5x10^4$ cfu/ml, a mild dominant negative effect (five-fold decrease of growth) can be detected on a wild type strain when co-inoculated with its avirulent derivative RW60 at the same concentration (Macho et al., 2007). These results could reflect that cell-to-cell signaling between host cells may have a stronger role in the establishment of ETI than in the establishment of other type of defense responses, for which a more direct contact may be necessary both for its activation and its suppression.

Another interesting result in regard to defense suppression within mixed infections is that *in trans* complementation of the Δ*hrcV* by the co-inoculated wild type allows the mutant to spread beyond the inoculated area. It has been reported that ETI in

Arabidopsis and PTI in *N. benthamiana* stop vascular transport through the xylem (Oh and Collmer, 2005; Freeman and Beattie, 2009), which *P. syringae* may use to colonize distant tissues (Misas-Villamil et al., 2011). On these bases, it has been proposed that vascular defenses may play a role in restricting pathogen spread (Misas-Villamil et al., 2011). Our results indicate that close proximity between pathogenic and non-pathogenic bacteria allows the later to colonize distant tissues, and this could be achieved through *in trans* suppression of either local or vascular defenses involved in restricting ssystemic colonization.

Here, we have analyzed interference between co-inoculated strains in the leaf apoplast of Canadian Wonder bean plants, but the relation between bacterial proximity and each type of interference detected could vary in specific microenvironments within different plant tissues, or in different hosts, depending on the intensity of the defenses involved. In relation to this, we previously observed that mixed populations of the pathogen *Ralstonia solanacearum* have very different dynamics depending on where they were inoculated within the plant: the same dose of inoculum triggered strong complementation in the stem, but not in the leaf (Macho et al., 2010b). One possible explanation was that in inoculation within the stem, rendered higher local concentration of bacteria, but it is also possible that differences in plant defenses in vascular *versus* parenchyma cells allow for differences in complementation.

Bacterial entry into the plant apoplast during dip-inoculation

Infiltration forces bacteria into the apoplast through the applied pressure, whereas, as in nature, bacteria have to gain entry through their own means when spray or dip-inoculated. We have observed that different means of inoculation lead to differences in how bacteria distribute within the apoplast upon entry. Whereas dip-inoculation leads to a clear concentration of bacteria around trichomas, which could constitute a weak structural point prone to tissue damage, facilitating bacterial entry through the associated wounds, it did not lead to bacterial concentration around stomata. Stomata are largely considered to be the main port of entry of *P. syringae* into the plant apoplast (Melotto et al., 2006). However, this conclusion is largely based on the study of the interaction between *P. syringae* pv. tomato and other coronatine-producing *P. syringae* strains, and *Arabidopsis* and/ or tomato plants (Melotto et al., 2008). These studies have shown that despite inmediate closure of the stomata upon detection of conserved

patterns in the pathogen, such as flagelling, the production of the phytotoxin coronatine allows these bacteria to re-open stomata, allowing further and more efficient invasion of the leaf. However, how other *P. syringae* strains may reach the apoplast is less clear. *P. syringae* pv. *tabaci* has also been shown to re-open stomata even though it does not produce coronatine (Melotto et al., 2006), suggesting other virulence factor(s) encoded by this strain can either inhibit stomata closure or re-open them. However, it has also been suggested that pathogens lacking the ability to re-open stomata may favor other ports of entry, such as is the case for the foliar pathogen *Xanthomonas campestris* pv. *campestris*, which mainly enters the leaf through hydathodes, water-exuding pores at the edge of leaves (Hugouvieux et al., 1998). Thus, since *P. syringae* pv. *phaseolicola* does not produce coronatine, the absence of bacterial concentration around stomata in the dip-inoculated bean leaves could be an indication of this pathogen lacking the ability to re-open stomata. In support of this notion, we observed a clear concentration of bacterial colonies located close to the edges of the leaves, were hydathodes are located (Figure 4E). Interestingly, hydathodes has been recently shown as an alternative route of entry for the coronatine-producing *P. syringae* pv. tomato DC3000 in Arabidopsis (Yu et al., 2013). Nonetheless, our observation could reflect a bacterial preference for *P. syringae* pv. phaseolicola entry through hydathodes rather than stomata, or be simply a consequence of the distribution of the inoculating solution (and perhaps rainwater) on the leaf surface.

But the most relevant result obtained when dip-inoculating bean leaves is that co-inoculated strains interfere with each other at lower intra-apoplast concentrations than needed following infiltration. These results supports that the incidence of these type of interferences can be relevant for adaptation to the host in nature, where inoculation occurs mostly through rainwater, with high local epiphytic concentration of bacteria taking place (Kinkel et al., 2000; Lindow and Brandl, 2003).

Mixed infection assays reveal a new phenomenon

We initially set out to analyze how meeting within the plant would affect the fate of bacteria with different virulence capabilities, and chose to do so using mixed infection assays, normally used as a sensitive assay to measure virulence attenuation (Beuzón and Holden, 2001; Macho et al., 2007; Macho et al., 2010b; Feng et al., 2012). However, through these assays we detected such a variety of interactions between co-

inoculated bacteria within a single experiment that lead us to explore the possible source for such phenotypic heterogeneity. These results (Figure 5) show that different types of interferences do take place between virulent and avirulent bacteria within the same infection. The dominant negative effect previously detected in growth assays (Macho et al., 2007) would thus be the net resultant of all of these types of interferences. These different scenarios between the co-inoculated strains could arise from differences in the timing of the arrival and establishment of bacteria to a given tissue location. But they could also take place if the bacterial population was not homogeneously expressing the genes involved in determining the interaction with the plant (e.g. the genes encoding the effectors triggering the HR, or the genes encoding the T3SS): if there were cell-to-cell differences in the expression of a virulence gene(s) within each bacterial clonal population.

Chapter 2: A bistable switch controls virulence of bacterial plant pathogen *Pseudomonas syringae*

José S. Rufián, María A. Sánchez-Romero, Diego López-Márquez, Alberto P. Macho, John W. Mansfield, Dawn L. Arnold, Javier Ruiz-Albert, Josep Casadesús, Carmen R. Beuzón.

Introduction

Infectious processes involve spatial and temporal gene expression changes that follow the migration of bacterial pathogens from the point of invasion to the target tissues of the host. Pathogen progression through the host is accompanied by adjustments in transcription and phenotype to respond to different stimuli and microenvironments. However, the sources of variation may not always be deterministic, directly correlated to stimuli. Stochastic events may cause cell-to-cell transcriptional and phenotypic differences between genetically identical individuals, and may take place within the same microenvironment. This leads to a probabilistic determination of gene transcription and phenotype generally known as phenotypic heterogeneity or variation. Phenotypic heterogeneity has been known to take place within microbial clonal populations for decades (Bigger, 1944; Novick and Weiner, 1957). Moreover, a heterogeneous unimodal pattern of gene expression may become bimodal, bifurcating into two distinct patterns, in a process known as bistability that leads to the formation of bacterial subpopulations or lineages. Genetically identical bacterial subpopulations formed without the involvement of environmental cues may be even viewed as a programmed event.

Bistability on gene expression can be generated within a heterogeneous population by a positive feedback loop, as described by Novick and Weiner (1957) in the *E. coli lac* operon, or by a double negative feedback loop as in the lysis/lysogeny decision of bacteriophage lambda. The literature on bacterial bistable switches has been enriched with interesting examples in the last decade (Davidson and Surette, 2008; van der Woude, 2011; Sanchez-Romero and Casadesus, 2014; van Vliet and Ackermann, 2015). For instance, bistability is known to occur in the acquisition of competence for DNA uptake and in the formation of a sporulating subpopulation in *Bacillus subtilis* (Chai et al., 2008). Despite these examples, microbiological studies of pathogens growing in tissue sites have largely relied on averaging microbial responses for entire populations. The recent advent of single cell analysis has enabled a shift in perspective allowing detection and analysis of cell-to-cell non-genetic variation.

The importance of analyzing phenotypic heterogeneity in pathogen populations has been very recently highlighted in the context of antibiotic exposure for several animal and human pathogens including *Salmonella enterica* (Helaine and Holden, 2013; Arnoldini et al., 2014; Campbell-Valois et al., 2014; Claudi et al., 2014; Diard et al.,

2014; Sanchez-Romero and Casadesus, 2014; Manina et al., 2015). The formation of distinct bacterial lineages has also been proposed to play a role in the colonization of animals by some bacterial pathogens. In *Salmonella enterica*, phenotypic heterogeneity has been observed at several stages of host colonization. During intestinal infection, flagella are necessary for swimming and also facilitate invasion of intestinal cells (Stecher et al., 2004). However, intestinal populations of *Salmonella* are a mixture of flagellated and non-flagellated bacteria (Saini et al., 2010b; Stewart and Cookson, 2012). Formation of a non-flagellated subpopulation may be viewed as a stealth strategy because flagellin is highly immunogenic (Josenhans and Suerbaum, 2002). Another phenotypic bifurcation during *Salmonella* infection is observed in systemic infection: upon entry into macrophages the *Salmonella* population splits into two subpopulations, one of which replicates while the other enters a dormant-like state (Helaine and Holden, 2013). Colonization of the gall bladder by *Salmonella* involves also lineage formation: a subpopulation invades the gall bladder epithelium, while another subpopulation remains in the gall bladder lumen (Baumler et al., 2011). The potential relevance of phenotypic heterogeneity in the development of bacterial infections is further supported by recent reports showing within-host bistable expression of major virulence traits, such as the cholera toxin in *Vibrio cholerae* (Nielsen et al., 2010), the SPI1 type III secretion system (T3SS) in *S. enterica* (Stecher et al., 2008; Saini et al., 2010a; Diard et al., 2013), or NO-detoxification in *Yersinia pseudotuberculosis* (Davis et al., 2015).

Despite the increasing evidence supporting the notion of bacterial pathogens exploiting non-genetic variation to adapt to mammalian hosts, little is known about the occurrence or potential impact of these processes in the adaptation of bacteria to non-animal niches. In this work, we have addressed this question using the plant pathogen *Pseudomonas syringae*, an archetype considered by many the most relevant plant pathogenic bacteria (Mansfield et al., 2012). *P. syringae* is relevant both academically, as a model pathogen, and economically, for its increasing impact in agriculture, with the recent resurgence of old diseases (Shenge, 2007), and the emergence of new infections of worldwide importance (Green et al., 2010).

In plants, *P. syringae* can be found in the surface of leaves, from where it enters the leaf through natural openings and wounds to reach the intercellular spaces of the leaf parenchyma, the apoplast, where it replicates causing disease. The plant presents a two-tiered response against *P. syringae* (Jones and Dangl, 2006).

In this study, we analyzed the molecular mechanism behind the phenotypic heterogeneity observed during bacterial colonization of the plant host. We demonstrate that expression of key structural and regulatory components, as well as expression of a translocated effector of the *P. syringae* T3SS is bistable within the plant apoplast. Bistability also takes place within the homogeneous environment of the laboratory, during exponential growth in nutrient-limited, T3SS-inducing medium, and it is a dynamic, reversible and non-heritable process. Furthermore, it has consequences for bacterial adaptation to the plant host since populations sorted by their T3SS expression levels display differences in virulence. Genetic analysis of the regulatory elements controlling expression of the T3SS in *P. syringae* identifies the HrpV/HrpG double negative regulatory loop as the bistable switch involved in turning heterogeneity into bistability, requiring the transcriptional activator HrpL, and enhanced by the contribution of HrpA, the main component of the T3SS pilus, involved in a positive feedback loop. To our knowledge, this is the first example of bacterial heterogeneity and bistability of a major virulence determinant shown within a non-mammalian host.

Table 1. Strains used and generated in this work.

Strain	Genotype	Reference
1448A	*P. syringae* pv. *phaseolicola* wild-type strain race 6	(Teverson, 1991)
JRP9	1448A Tn*7*-eYFP, Gm^R	This work
JRP11	1448A Tn*7*-eCFP, Gm^R	This work
DLM1	1448A *hrpL::gpf*, Km^R	This work
DLM2	1448A *hrcU::gpf*, Km^R	This work
DLM3	1448A *hopAB1::gpf*, Km^R	This work
IOM49	1448A Δ*hrpA*	(Ortiz-Martin et al., 2010a)
JRP-F1	1448A Δ*hrpA; hrpL::gpf*, Km^R	This work
JRP-F2	1448A Δ*hrpA; hopAB1::gpf*, Km^R	This work
IOM57	1448A Δ*hrpG*	(Ortiz-Martin et al., 2010b)
IOM48-F	1448A Δ*hrpV*	Ortiz-Martín et al., 2010b
IOM58	1448A Δ*hrpG* Δ*hrpV*	Ortiz-Martín et al., 2010b
JRP-F3	1448A Δ*hrpG; hopAB1::gpf*, Km^R	This work
JRP-F4	1448A Δ*hrpV; hopAB1::gpf*, Km^R	This work
JRP-F5	1448A Δ*hrpG* Δ*hrpV; hopAB1::gpf*, Km^R	This work

Table 2. **Plasmids used in this work**.

Name	Description	Reference
pAME8	pAMEX derivative, contains the *avrRpt2* effector expressed from the *nptII* promoter	(Macho et al., 2009)
pIOM22	pBBR1-MCS-4 derivative, contains a promotorless *hrpL* gene expressed from the *lacZ* promoter	(Ortiz-Martín et al., 2010a)
pIOM92	pBBR1-MCS-4 derivative, contains a	(Ortiz-Martín et al.,

	promotorless *hrpG* gene expressed from the *lacZ* promoter	2010b)
pIOM53	pBBR1-MCS-4 derivative, contains a promotorless *hrpV* gene expressed from the *lacZ* promoter	(Ortiz-Martín et al., 2010b)

Table 3. **Primers used in this work**.

Name	Description	Restriction site
HrpL A1	CGGTATCCGTCAACTGACGG	NA
HrpL A2	GAATTCTATCCACTCAGGCGAACGGG	*Eco*RI
HrpL B1	TGAGTGGATAGAATTCTCTGTCTGGAACCAACTCGC	*Eco*RI
HrpL B2	ATGGGCGACCATCGGATCC	NA
HrcU A1	GTGATTCTGGGGTTGCTGC	NA
HrcU A2	GAATTCAGCTCCCAGCTTAAAGCTCC	*Eco*RI
HrcU B1	AGCTGGGAGCTGAATTCGCAAGCCAGGCGTAACAGG	*Eco*RI
HrcU B2	TTCTACTACAACGTCGCTGC	NA
HopAB1 A1	GCATCCTTTATAACTGACCC	NA
HopAB1 A2	GAATTCCTGAAATCAGTTCAGCTTAACG	*Eco*RI
HopAB1 B1	CTGATTTCAGGAATTCTCGTTGTAGTGGCCGG	E*co*RI
HopAB1 B2	GGACAGGTCGTAGTAGAGCG	NA
Zep07F	GAATTCTAAGAAGGAGATATACATATGAG	NA
Zep07F	GAATTCTTATCACTTATTCAGGCGTA	NA

Results

P. syringae displays bistable expression of the T3SS within the plant

Using confocal microscopy to follow the dynamics of fluorescently labelled *P. syringae* populations during colonization of the plant apoplast, we often observe a clear heterogeneity on the size of the bacterial microcolonies (Figure 1 and Chapter 1). Heterogeneity even extends to the intensity of the plant defenses activated around individual microcolonies, as can be followed through the accumulation of auto-fluorescent phenolic compounds (Figure 1 and Chapter 1) (Bennett et al., 1996). In order to investigate the source of the observed heterogeneity at a molecular level, we generated transcriptional fusions to *gfp* on the chromosome-located native copies of three genes encoding different elements of the major virulence determinant of *P. syringae*, its T3SS, required for activation and suppression of plant defenses, and virulence. The *loci* selected included the gene encoding HrpL, an alternative sigma factor of the extracytoplasmic factor (ECF) family (Fouts et al., 2002). HrpL activates expression of more than 50 genes within the nutrient-limited plant leaf apoplast (Ferreira et al., 2006; Lam et al., 2014; Mucyn et al., 2014), including the *hrp/hrc* genes that encode the T3SS, and the effector genes (Xiao et al., 1994; Fouts et al., 2002). We also selected two HrpL-regulated genes: *hrcU*, the last gene of the *hrcQRSTU* operon, encoding a structural component of the T3SS required for secretion and translocation (Charkowski et al., 1997), and *hopAB1* (previously known as *virPphA*), encoding a type III-translocated effector (T3E) involved in suppression of effector-mediated plant defenses (Jackson et al., 1999). Expression of *hrcU* is abolished in a Δ*hrpL* mutant, while expression of *hopAB1* is severely reduced but still detectable (Thwaites et al., 2004). Expression of these fusions was examined by fluorescence microscopy both in apoplast-extracted bacteria and within the plant tissue 4 days post inoculation (dpi) (Figure 2A and data not shown). Clear differences in *gfp* fluorescence were observed for the highly expressed *hopAB1::gfp* gene fusion in apoplast-extracted bacteria, indicating that expression of this gene displays phenotypic heterogeneity during bacterial growth within the plant (Figure 2A). Flow cytometry analyses were then carried out on apoplast-extracted bacteria for all three genes. Expression of both *hrpL::gfp* and *hopAB1::gfp* reached bistability following a bimodal distribution, and all three genes displayed expression heterogeneity (Figure 2B).

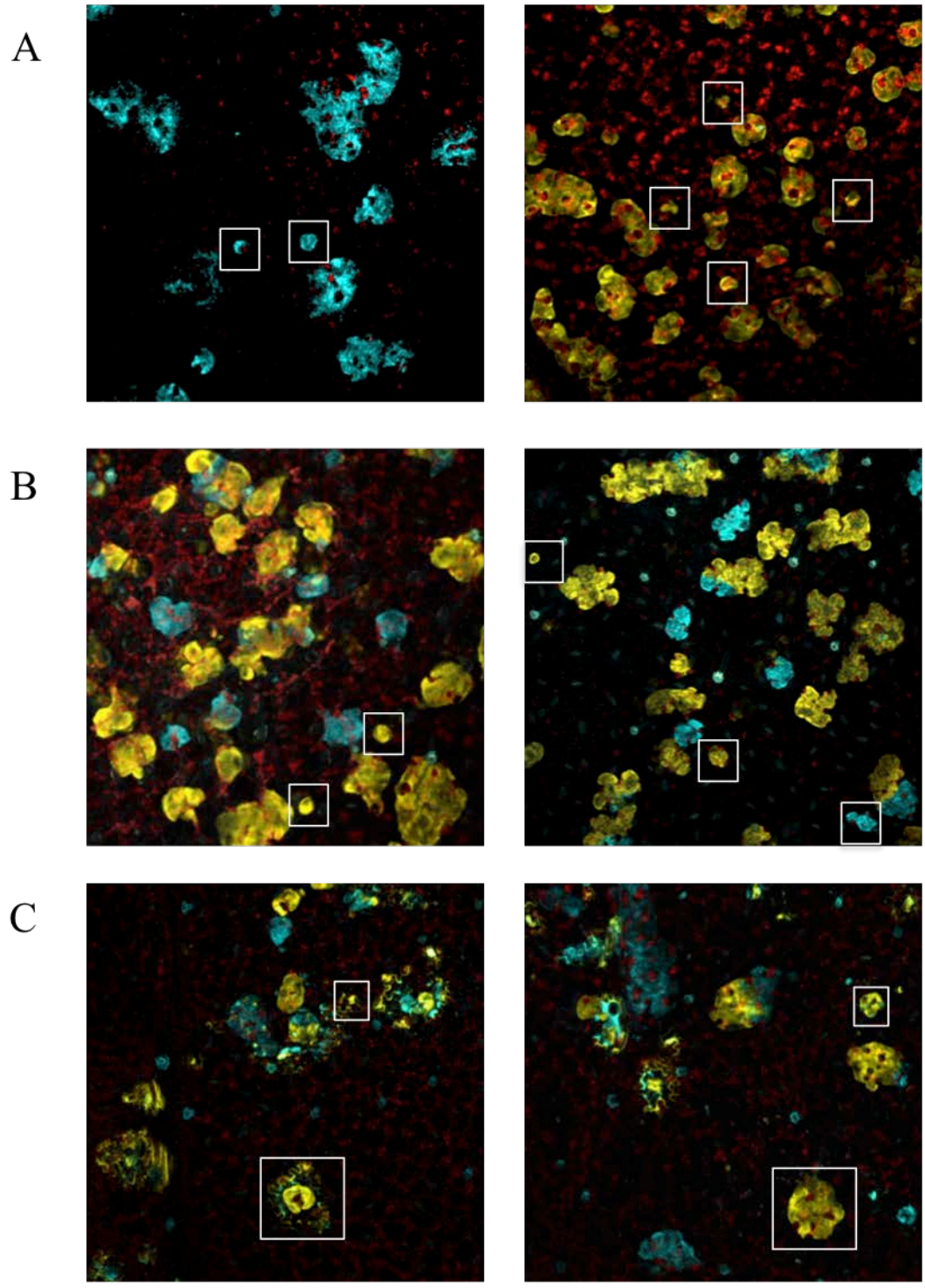

Figure 1. Bacterial growth and activation of defenses displays heterogeneity during *P. syringae* colonisation of the plant apoplast. (**A**) Confocal microscopy images of bean leaves inoculated with $5x10^6$, cfu/ml of either wild type 1448a eCFP (left panel) or 1448a eYFP (right panel) at 3 dpi. (**B**) Confocal microscopy images of bean leaves inoculated with $5x10^6$, cfu/ml of a bacterial suspension containing equal numbers of 1448a eCFP and 1448a eYFP at 3 dpi. Boxes highlight small colonies of either strain found among typically larger colonies (**C**) Confocal microscopy images of bean leaves inoculated with $5x10^5$, cfu/ml inoculum, containing equal amounts of 1448a eCFP and 1448a eYFP expressing AvrRpt2, at 3 dpi. AvrRpt2 triggers the hypersensitive response leading to the accumulation of auto-fluorescent (yellow and blue) phenolic compounds that accumulate in the cell wall. Boxes highlight large and small colonies of 1448a eYFP expressing AvrRpt2 surrounded or not by defense-related auto-fluorescence, regardless of their size. Red corresponds to auto-fluorescence generated by chloroplasts.

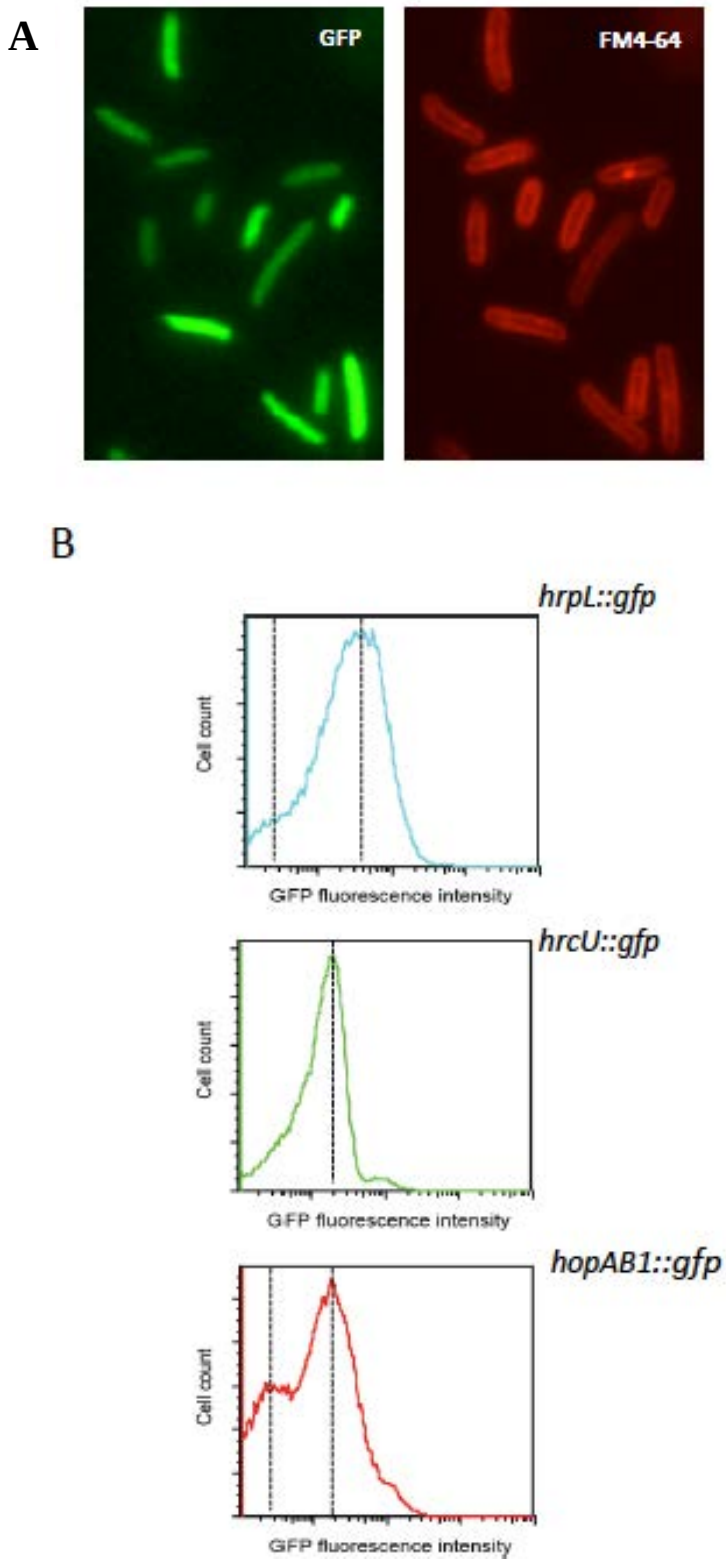

Figure 2. Expression of *hrpL::gfp* and *hopAB1::gfp* is bistable within the plant. (**A**) Fluorescence microscopy images apoplast-extracted bacteria from bean leaves inoculated with a $5x10^5$ cfu/ml inoculum of a strain carrying *hopAB1::gfp* at 5 dpi. Left panel shows GFP fluorescence. Right panel shows bacteria strain stained with the membrane dye FM4-64 (**B**) Flow cytometry analysis of apoplast-extracted bacteria carrying either *hrpL::gfp*, *hrcU::gfp* or *hopAB1::gfp*, obtained from bean leaves inoculated with a $5x10^5$ cfu/ml inoculum of each strain at 5 dpi. Dotted lines indicate the mode(s) for each gene and condition. All data were collected for 100,000 events per sample.

Expression of T3SS genes bifurcates into two subpopulations in a highly dynamic and reversible manner

A number of factors could explain these observations, *e.g*. differences could reflect spatial differences between microenvironments within the apoplast. However, they could also result from stochastic events, such as an uneven distribution of regulators during cell division leading to cell-to-cell transcriptional differences within the same microenvironment. A previous report on the necrotrophic plant pathogen *Dickeya dadantii* showed that a plasmid-cloned type III secretion promoter could display phenotypic heterogeneity in laboratory conditions (Zeng et al., 2012b). Although the T3SS is not as relevant for virulence in necrotrophic pathogens as it is in biotrophic or hemibiotrophic pathogens, such as *P. syringae*, (Glazebrook, 2005; Davidsson et al., 2013), this report led us to analyze if the bistabiity on the expression of the T3SS genes observed *in planta* could take place in the homogeneous environment of laboratory medium.

Expression of all three genes was induced in bacteria growing in nutrient-limited HIM (Hrp-inducing medium) (Huynh et al., 1989) (Figure 3). The expression curves for all three genes were heterogeneous in this medium, with heterogeneity being larger in exponential than stationary phase bacteria. A detectable proportion of all cultures, particularly in those corresponding to exponentially growing bacteria, displayed fluorescence levels overlapping those of the non-GFP control bacteria (Figure 3). Remarkably, expression of both *hrpL::gfp* and *hopAB1::gfp* was found to be bimodal during exponential growth (Figure 3A). The mode for one of the subpopulations observed for *hrpL::gfp* coincided with the mode of the population of non-GFP control bacteria (Figure 3). Bistability was no longer detected in stationary phase cultures supporting a reversible and non-genetic origin for the differences observed between these subpopulations (Figure 3B).

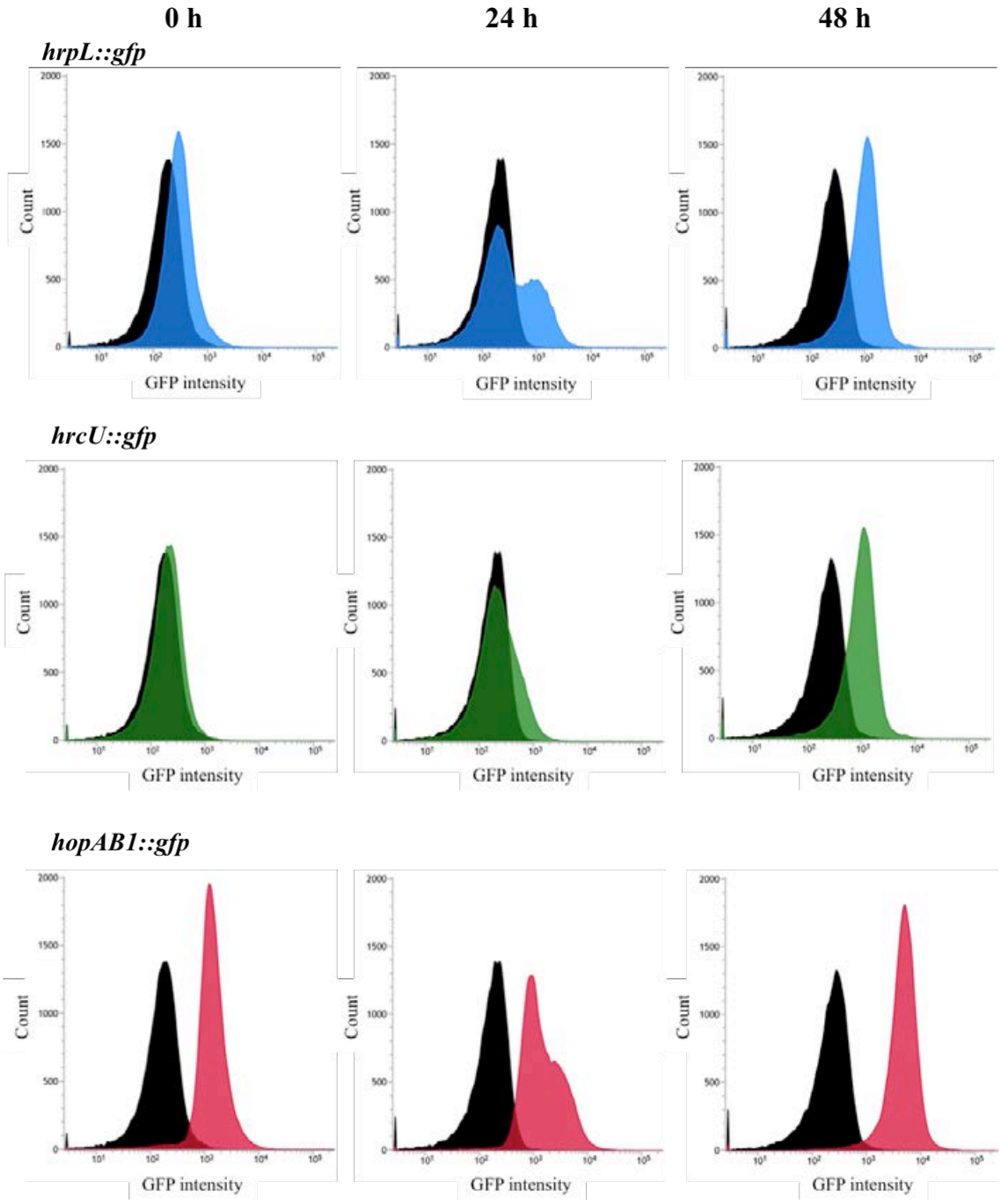

Figure 3. Expression of *hrpL::gfp* and *hopAB1::gfp* is bistable during exponential growth in Hrp-inducing medium. Flow cytometry analysis of strains carrying chromosome-located transcriptional fusions to the T3SS genes *hrpL*, *hrcU* or *hopAB1*, growing in HIM (Hrp-inducing medium). Histograms show GFP fluorescence distribution in strains growing at, either 0h (immediately after a 1:10 dilution of an overnight LB culture), 24h (exponential phase) or 48h (stationary phase). Black histograms show non-fluorescent 1448A included as a reference. All data were collected for 100,000 events per sample.

Differences in gene expression correlate with differences in virulence

Since the T3SS is essential to suppress basal defenses and without it *P. syringae* cannot multiply within the plant or cause disease (Alfano and Collmer, 1997), bacterial

subpopulations differing in their expression of *hrpL* and T3SS-related genes are expected to differ in how they interact with the plant host. To validate this notion, we went back into the plant to analyze the development of disease in leaves inoculated with two different bacterial subpopulations, sorted according to their level of expression of *hopAB1* (Figure 4A, upper panel). Disease symptoms developed faster, and were stronger, in leaf areas inoculated with the population expressing higher levels of *hopAB1* (Figure 4B). The symptoms also spread sooner beyond the area inoculated with the high-expressing subpopulation. Thus, differences in gene expression correlate with differences in virulence.

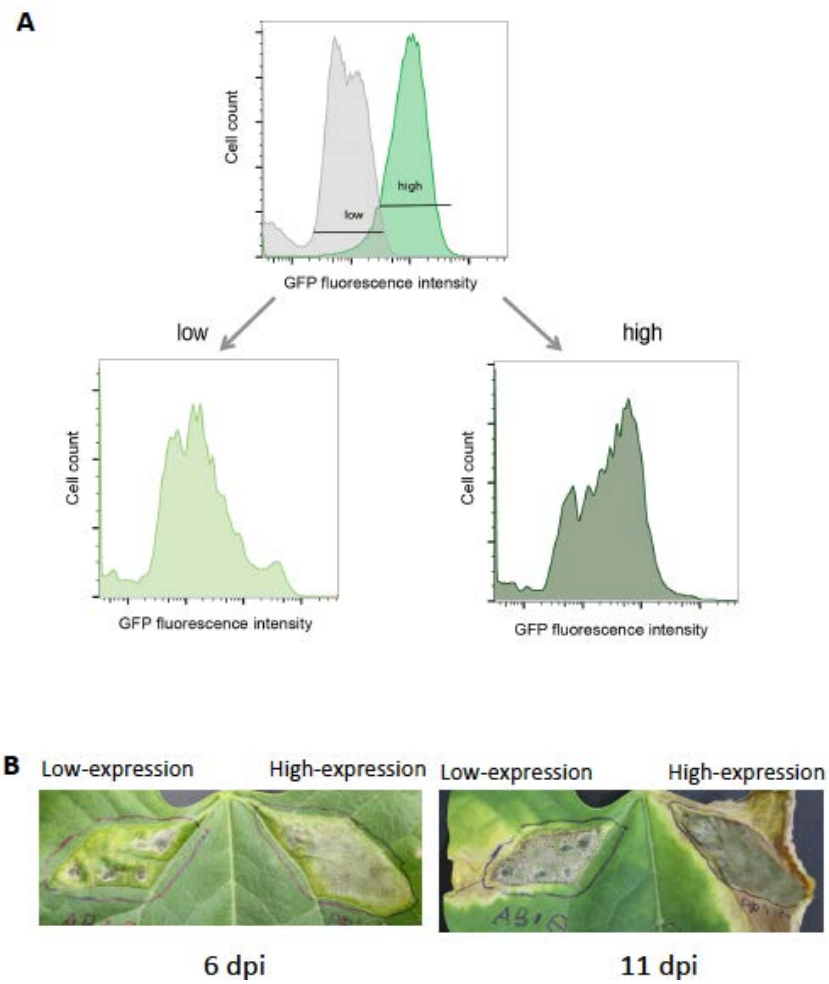

Figure 4. The level of *hopAB1* expression correlates with virulence. (**A**) Flow cytometry analysis of strain carrying *hopAB1::gfp*. GFP fluorescence intensity is shown as a green histogram. Gates were drawn to separate *hopAB1::gfp* bacteria displaying fluorescence levels overlapping the 1448A non-GFP bacterial population (indicated with a line marked as low), used as a negative control (Grey histogram), from cells expressing high GFP levels (indicated with a line marked as high, and including the mode for the expressing population). After sorting, aliquots of sorted cells were run again at the cytometer to confirm the efficacy of the sorting process (below), and bacterial concentration adjusted to 1 x 10^6 cfu/ml. Some overlap caused by the dynamic and reversible nature of the process can be detected (**B**) Disease symptom progression in bean leaves inoculated with 1 x 10^6 cfu/ml of each of the sorted populations at 6 and 11 days post inoculation (dpi).

Bistability of the T3SS genes is established at the level of HrpL by the action of HrpA, and HrpV/HrpG regulatory loops

HrpL regulates expression of *hopAB1* (Xiao and Hutcheson, 1994). Thus, the bistability displayed by *hopAB1* is likely to originate from that affecting *hrpL* expression. To test this hypothesis, a plasmid carrying a copy of *hrpL* under the control of the *lacZ* promoter, constitutive in *P. syringae* (Ortiz-Martin et al., 2010a) was introduced in the strains carrying the *hrpL::gfp* or *hopAB1::gfp* fusions and its effect in *gfp* expression analyzed by flow cytometry. Figure 5A shows how the bimodal distribution of *hrpL::gfp* becomes unimodal in the presence of constitutively expressed HrpL, and that of *hopAB1::gfp* strongly reduced, displaying a shift towards a more activated state, supporting the central role of HrpL in the establishment of bistability in the system.

The establishment of bistability usually requires the action of at least one feedback loop (either a positive or a double negative regulatory loop) to turn quantitative differences originated through heterogeneous expression, into qualitative differences and a bimodal distribution of expression (Veening et al., 2008). Two such feedback loops regulate the expression of the T3SS genes in *P. syringae* a positive feedback loop carried out HrpA the main component of the T3SS pilus (Roine et al., 1997 2000), and a double negative feedback loop carried out by HrpV, an anti-activator of the T3SS genes that binds to HrpS the enhancer-binding protein required for HrpL expression, and HrpG, which binds HrpV acting as an anti-anti-activator (Wei et al., 2005). We analyzed the roles of these two regulatory loops in the establishment of bistability using mutants and/ or plasmids encoding the corresponding genes. Bistability in both *hrpL::gfp* and *hopAB1::gfp* was reduced but not abolished in an Δ*hrpA* mutant background (Figure 5B), supporting a non-essential contribution for HrpA to the bistable phenotype. Bistability of *hopAB1::gfp* was completely abolished in a Δ*hrpG* (Figure 6A), where in the absence of its repressor, HrpV establishes a negative feedback loop expected to dampen noisy and heterogeneous expression. In the absence of HrpV, expression increased and bistability was also increased, regardless of the presence of HrpG, since the phenotype of the Δ*hrpV* mutant was identical to that of a double mutant Δ*hrpV* Δ*hrpG* (Figure 6A). The epistatic effect of the Δ*hrpV* mutation on the phenotype of Δ*hrpG* supports the notion of HrpG exerting its role in regulation of the expression of the T3SS genes mainly through its role as repressor of HrpV. Constitutive expression of

either regulator from a plasmid lead to reciprocal results, with a stronger bistable phenotype associated to overexpression of HrpG, and the absence of bistability in cells overexpressing HrpV (Figure 6B). Plasmid-expression of these regulators also caused these effects on the expression of *hrpL::gfp.*

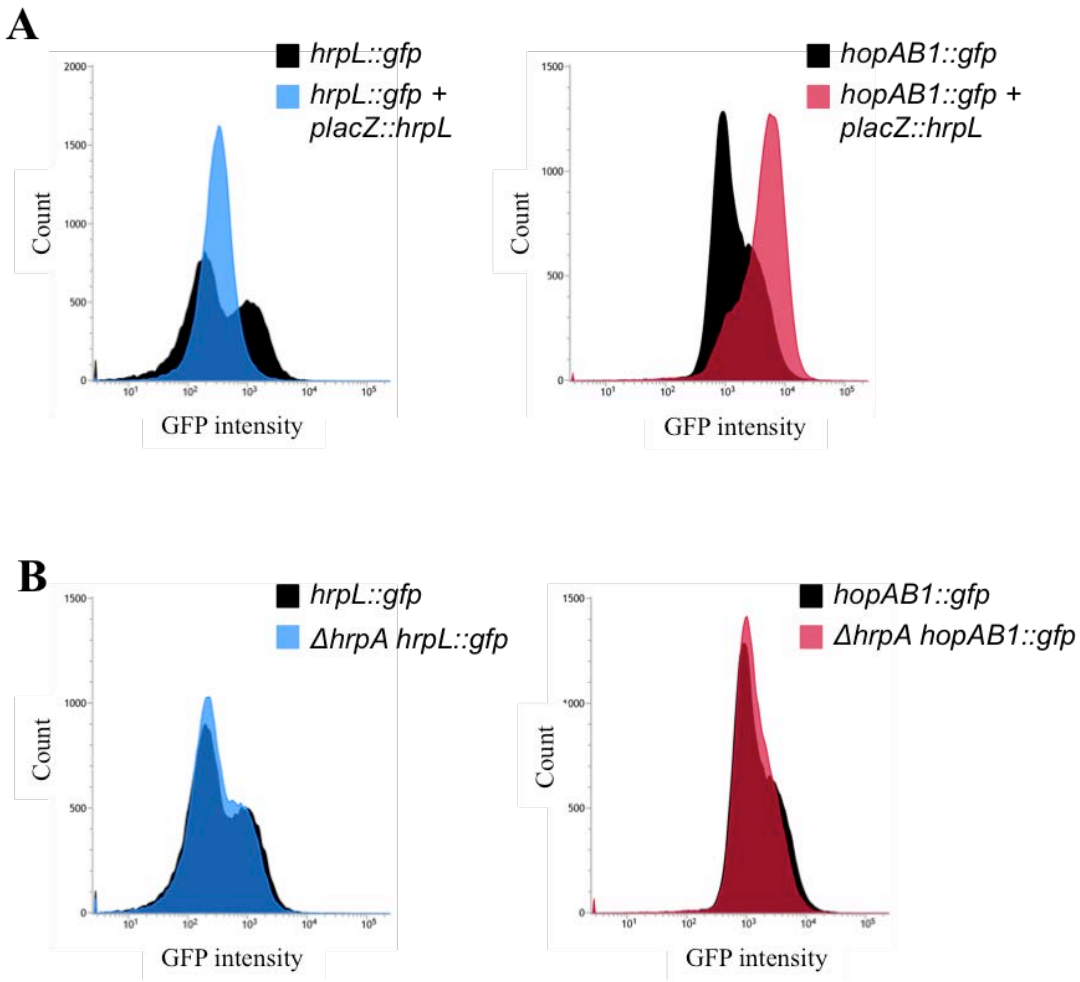

Figure 5. Bistability of *hrpL::gfp* and *hopAB1::gfp* is abolished by constitutive expression of HrpL, and mildly reduced in the absence of HrpA. Flow cytometry analysis of HIM-growing bacterial strains carrying chromosome-located transcriptional fusions to the T3SS genes *hrpL*, *hrcU* or *hopAB1*, in different genetic backgrounds. Histograms show GFP fluorescence distribution in strains growing at 24h. Black histograms show fluorescence of the fusions in the wild type 1448A background. Coloured histograms show fluorescence of the fusions in: (**A**) A strain carrying a plasmid encoding HrpL under the control of a *lacZ* promoter, and (**B**) A strain carrying a Δ*hrpA* mutation. All data were collected for 100,000 events per sample.

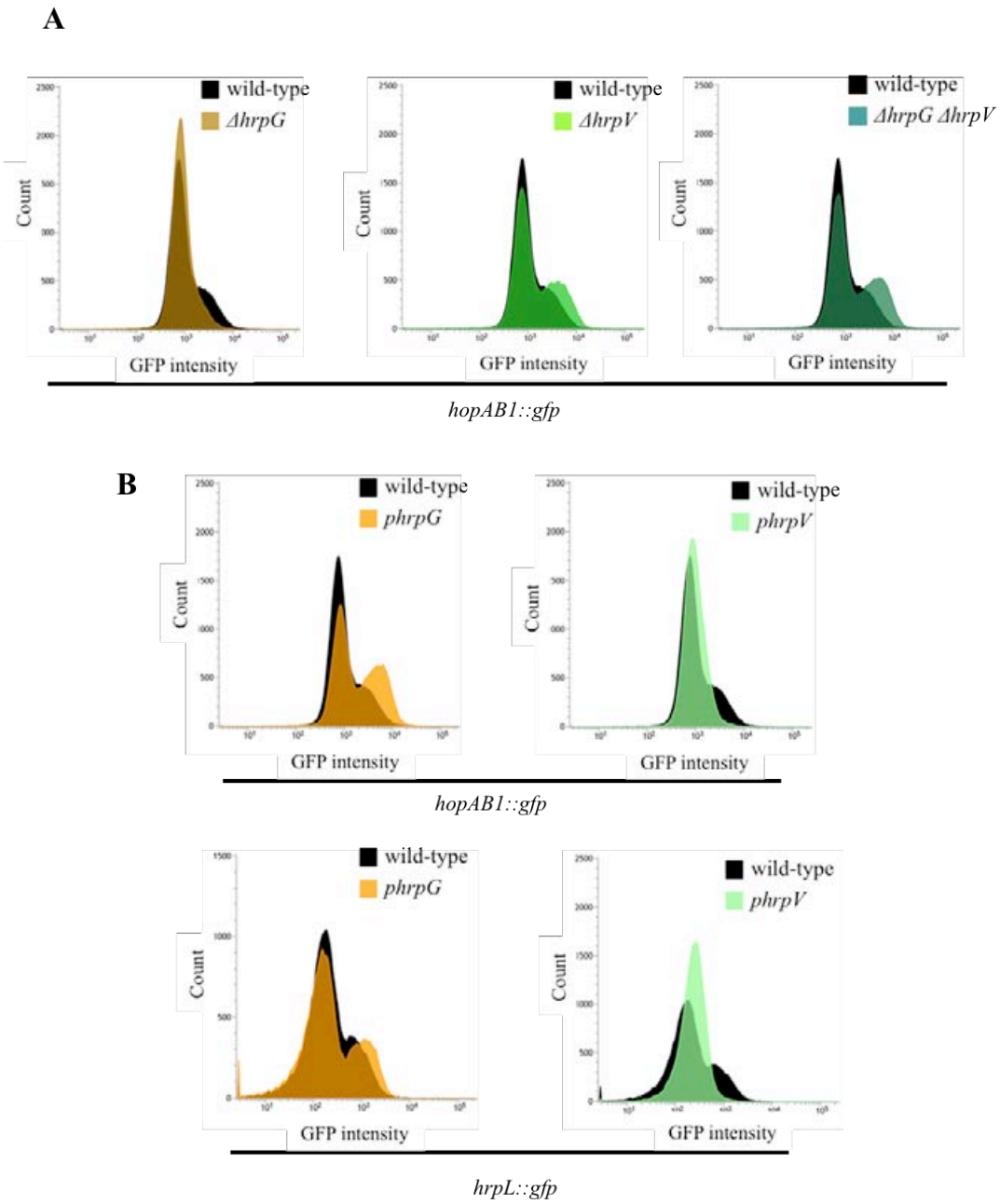

Figure 6. Bistability of *hrpL::gfp* and/ or *hopAB1::gfp* is abolished by deletion of *hrpG* or constitutive expression of HrpV, and enhanced by deletion of *hrpV* or constitutive expression of HrpG. Flow cytometry analysis of HIM-growing bacterial strains carrying chromosome-located transcriptional fusions to the T3SS genes *hrpL, hrcU* or *hopAB1*, in different genetic backgrounds. Histograms show GFP fluorescence distribution in strains growing at 24h. Black histograms show fluorescence of the fusions in the wild type 1448A background. Coloured histograms show: (**A**) Fluorescence of *hopAB1::gfp* in strains carrying mutations in either *hrpG*, *hrpV*, or both; (**B**) Fluorescence of either *hopAB1::gfp* or *hrpL::gfp* in a strain carrying a plasmid encoding either HrpG or HrpV, under the control of a *lacZ* promoter. All data were collected for 100,000 events per sample.

Discussion

This study was undertaken to investigate the molecular mechanisms underlying the heterogeneity observed within the process of colonisation of the plant apoplast. We found that expression of the T3SS genes, the major virulence determinant of *P. syringae*, is heterogeneous and bistable during bacterial growth within the apoplast. The plant apoplast is a complex environment where different factors may alter bacterial responses. Thwaites and collaborators (2004) reported that following leaf extraction, bacteria that remained attached to the plant cell wall displayed higher amounts of T3SS gene transcripts than those found within the apoplastic fluid. However, the heterogeneity hereby described was detected in apoplastic bacteria. The apoplast is a nutrient-limited environment (Rico and Preston, 2008), where unsuppressed plant defenses can still be detected (Mitchell et al., 2015), and can therfore be considered stressful for bacteria. Bacterial stress is accompanied by a reduction in both transcription and translation that has been proposed to increase phenotypic heterogeneity in some systems (Veening et al., 2008). Interestingly, the apoplastic environment has been shown to activate recombination-mediated genomic rearrangements in *P. syringae* that lead to phase variation upon activation of the HR (Lovell et al., 2011). The fact that phenotypic heterogeneity is enhanced in some stressful situations suggests a potential adaptive value. Indeed, theoretical studies proposed that such adaptative advantage may become apparent in changeful and/ or hostile environments (Kussell et al., 2005; Kussell and Leibler, 2005), while later reports have provided experimental evidence supporting this notion for several animal and plant pathogens (Srikhanta et al., 2010; Lovell et al., 2011; Hernandez et al., 2012; Claudi et al., 2014; Sanchez-Romero and Casadesus, 2014; Manina et al., 2015). The differences in virulence established in this work for bacterial subpopulations sorted according to T3SS expression levels further suggests that non-genetic phenotypic heterogeneity can be relevant for bacterial adaptation to plant hosts. On these grounds, a tentative interpretation of our results is that the stressful conditions found within the apoplast may favour phenotypic heterogeneity and confer selective advantage to *P. syringae* populations with heterogeneous and/ or bistable expression of the T3SS and effector genes.

Bacteria not expressing the T3SS could act as ‘cheaters’ benefiting from the T3SS-mediated contribution of those ‘cooperator’ bacteria that express it, in a model

similar to that proposed for complex microbial communities with secreting and no-secreting genotypes (Xavier et al., 2011). Plus, 'cheater' bacteria could gain a potential fitness advantage, being relieved of the metabolic burden of expressing the T3SS. Moreover, activation of expression of the T3SS genes in *P. syringae* has been shown to be associated to repression of housekeeping functions (Ferreira et al., 2006). Such a fitness advantage has been described in animal pathogens such as *S. enterica, P. aeruginosa* and *Yersinia spp* (Wiley et al., 2007; Kohler et al., 2009 2011). Supporting this notion, Barret and collaborators (2011) found unexpectedly high frequencies of polymorphism affecting several virulence traits, including the T3SS, in natural populations of *P. syringae* infecting *Arabidopsis thaliana*, and demonstrated that less aggressive strains increase their growth potential in mixed infections and have a fitness advantage in non-host environments. Hence, reversible phenotypic heterogeneity on the T3SS expression might facilitate adaptation to different agricultural and environmental conditions. Giving strength to this view, Morris and collaborators (2008) found that natural isolates of *P. syringae* from various agricultural and non-agricultural habitats showed changes in the phenotypic but not the genotypic population structure.

Because the apoplast is a complex environment, we turned to an *in vitro* system for further investigation. Since HrpL is the transcriptional activator of the other two genes, *hrcU* and *hopAB1*, and also regulates indirectly its own expression through a positive loop determined by the product of the HrpL-activated *hrpA* gene (Wei et al., 2000), and a double negative loop determined by the products of the HrpL-regulated *hrpG and hrpV* genes (Wei et al., 2005), the simplest explanation for our results was that the phenotypic heterogeneity observed for *hrcU* and bistability of *hopAB1* originated from *hrpL* heterogeneous and bistable expression. The fact that not all three genes display bistability may reflect different thresholds in the response of each gene to HrpL activation. Indeed, different levels of HrpL-regulation have been reported for T3SS-structural and effector genes in *P. syringae* (Zumaquero et al., 2010). It could also be due to additional regulatory loops differentially affecting these genes, dampening or enhancing heterogeneity, *e.g.* an additional negative regulation of structural genes such as *hrcU*. Although no such loops have been described for the *hrcQRSTU* operon, the *hrpC* operon encoding HrcC and HrcF structural components of the T3SS has been reported to display a differential regulation (Ortiz-Martin et al., 2010b). In any case, the fact that bistability requires native expression of HrpL, and it is abrogated when HrpL is

consititutively expressed from a plasmid confirms the central role of this protein in the establishment of this phenotype. Indeed, both the double negative regulation carried out by HrpV and HrpG, and the positive regulation carried out by HrpA, identified as necessary for or contributing to bistability, involved the action of HrpL. The drastic and reciprocal effects of deletion and overexpression of either HrpV or HrpG on bistability of the T3SS genes clearly identifies this pair as the bistable switch involved in turning heterogeneity into bistability. The observation of a link between bistability and growth phase could reflect the need for active cell division to generate stochastic differences in the relative levels of these two proteins through involvement of an additional factor differentially associated to growth phase. Bistable expression of *tcpA* expression in *Vibrio cholerae* is established through the combined effect of the positive auto-regulation of ToxT production and CRP-cAMP, with this complex involved in restricting bistability to stationary phase (Nielsen et al., 2010).

The phenotypic heterogeneity displayed by HrpL could also translate in differences in non-T3SS genes of the HrpL regulon. One system potentially affected by HrpL bistability is the flagella assembly, since HrpL has been shown to downregulate motility (Ortiz-Martin et al., 2010a). In *P. syringae*, differences in motility correlate with differences in adaptation to the host and other environments (Schroth, 1974; Haefele and Lindow, 1987; Hatterman D.R., 1989). In addition, the flagellum is both a costly organelle to assemble (Macnab, 1996) and a strong activator of plant defenses (Felix et al., 1999). In *S. enterica,* the expression of genes encoding the SPI1 T3SS, necessary to induce gut inflammation and to overcome competition from commensal microbiota (Kaiser et al., 2012), as well as that of the flagellar genes, display phenotypic heterogeneity during colonisation of the host (Cummings et al., 2006; Saini et al., 2010a), leading to the different phenotypic combinations to cooperate to promote the infection through the division of labour (Stecher et al., 2008; Diard et al., 2013).

On the basis of these results, we tentatively propose that phenotypic heterogeneity plays a role in the adaptation of *P. syringae* to agricultural and perhaps to non-agricultural, ecologically relevant environments. These findings can potentially impact control strategies to protect economically important crops. Our results provide the first proof of phenotypic variation in a plant bacterial pathogen, adding to the very few examples showing phenotypic variation directly affecting a major virulence factor, and identify the molecular mechanisms involved in turning expression heterogeneity into

bistability and non-genetic lineage formation. Although we cannot rule out additional sources of variation, our results also provide a mechanistic explanation for the presence of bacterial microcolonies displaying phenotypic differences in growth and/ or activation of defenses within the plant apoplast. Finally, they show that phenotypic heterogeneity, as a bacterial strategy to generate within-host diversity, is not restricted to mammalian hosts.

Chapter 3: Auto-acetylation on K289 is not essential for HopZ1a-mediated plant defense suppression

José S. Rufián, Ainhoa Lucía, Alberto P. Macho, Begoña Orozco-Navarrete, Manuel Arroyo-Mateos, Eduardo R. Bejarano, Carmen R. Beuzón, Javier Ruiz-Albert

The results presented in this chapter have been published in:

Rufián JS, Lucía A, Macho AP, Orozco-Navarrete B, Arroyo-Mateos M, Bejarano ER, Beuzón CR and Ruiz-Albert J (2015) Auto-acetylation on K289 is not essential for HopZ1a-mediated plant defense suppression. *Front. Microbiol.* 6:684. doi: 10.3389/fmicb.2015.00684

Introduction

Many Gram-negative pathogenic bacteria use a type III secretion system (T3SS) to secrete proteins, known as effectors, directly inside the host cell cytosol. Type III effectors (T3Es) modulate diverse processes inside the host, suppressing plant defense responses triggered upon recognition of the pathogen (Gohre and Robatzek, 2008). One such defense is triggered upon recognition of conserved pathogen-associated molecular patterns (PAMPs) and is known as PAMP-triggered immunity or PTI (Boller and Felix, 2009). T3Es can be directly or indirectly detected by the plant resistance proteins, triggering a second line of defense, a strong response known as effector-triggered immunity (ETI) that is typically accompanied by a type of programmed cell death referred to as the hypersensitive response (HR). The ETI response determines a severe restriction in pathogen growth (Chisholm et al., 2006). Effectors triggering strong immunity were originally named avirulence factors, as their expression by a pathogen determines resistance against the disease (Mansfield, 2009).

Effectors can also suppress ETI, cell death and other HR-associated phenomena, thus promoting pathogen growth and the development of disease (Jones and Dangl, 2006). We have shown that HopZ1a from *Pseudomonas syringae pv. syringae* is one such effector (Macho et al., 2010a). Heterologous expression of HopZ1a from *P. syringae* pv. tomato DC3000 (hereafter DC3000), suppresses RNA and protein accumulation of *pathogenesis related-1* (*PR1*), triggered in *Arabidopsis* by this pathogen (Macho et al., 2010a), and partially suppresses the ETI triggered by the expression of the heterologous effectors AvrRpt2, AvrRps4 and AvrRpm1 (Macho et al., 2010a). These defense suppression activities of HopZ1a are similar to those described for the related *Xanthomonas* effector AvrBsT (Kim et al., 2010; Szczesny et al., 2010; Kim et al., 2013). We have also demonstrated that HopZ1a is capable of suppressing systemic acquired resistance (SAR) triggered by either virulent or avirulent bacteria (Macho et al., 2010a). All these virulence activities are fully dependent on HopZ1a C216 catalytic residue. In turn, HopZ1a triggers SA and EDS1-independent immunity in *Arabidopsis* (Lewis et al., 2010; Macho et al., 2010a) upon recognition by the *ZAR-1* resistance gene (Lewis et al., 2010).

HopZ1a is a member of the YopJ/HopZ effector superfamily, whose members share a conserved catalytic triad (C/H/D) and have been shown to perform numerous biochemical activities, mainly as proteases and/or acetyltransferases, with some

effectors such as YopJ displaying up to three different biochemical functions concurrently (Orth et al., 2000; Mukherjee et al., 2006; Sweet et al., 2007). To explain such multiplicity of activities, it has been suggested that acetyltransferases and proteases might use the same catalytic mechanism on different substrates (Mukherjee et al., 2007). HopZ1a has been described to display cysteine protease activity (Ma et al., 2006), but also acetyltransferase activity on lysine residues of a number of plant target proteins, with the latter activity requiring the plant cofactor phytic acid (Lee et al., 2012; Jiang et al., 2013; Lewis et al., 2013). HopZ1a catalytic triad cysteine (C216) is essential for all described virulence and avirulence functions, as well as for its biochemical activities, and a HopZ1a^{C216A} mutant behaves as a catalytically inactive mutant (Ma et al., 2006; Lewis et al., 2008; Macho et al., 2010a; Lee et al., 2012). *Xanthomonas* AvrBsT, the only other effector of the YopJ/HopZ superfamily with ETI-suppressing activity, shares with HopZ1a the biochemical activities, cofactor requirements, and catalytic triad dependence on its virulence and avirulence functions (Szczesny et al., 2010; Kim et al., 2013; Cheong et al., 2014). HopZ1a has also been shown to autoacetylate in a lysine residue (K289) conserved in some related effectors, with the HopZ1a^{K289R} mutant phenocopying the catalytically inactive HopZ1a^{C216A} mutant in respect to the acetyltransferase activity, and also to its avirulence and some of its virulence functions (Lee et al., 2012). Autoacetylation of such conserved lysine residue was originally described for another member of the YopJ/HopZ superfamily, *Ralstonia* effector PopP2 (Tasset et al., 2010). Autoacetylation of PopP2 is required to trigger a defense response mediated by RRS1-R, a plant resistance protein that interacts with PopP2 but is not acetylated by this effector (Tasset et al., 2010).

In this work, we analyze the requirement of HopZ1a K289 acetylation for HopZ1a suppression of ETI and SAR, as well as its avirulence function, *i.e*. HopZ1a induction of ETI. We have found that expression of HopZ1a^{K289R} suppresses accumulation of PR1 in local tissue, as well as SAR in distal tissues, although the suppression activities of the mutant effector are not as efficient as those achieved by expression of wild type HopZ1a. Our results indicate that autoacetylation of this residue is important for full activity but not essential for suppression of either ETI or SAR. Interestingly, we also found that the K289R mutation does not abolish the onset of ETI upon HopZ1a recognition, although it is required for full immunity. The K289R mutation reduces but does not prevent HopZ1a-mediated immunity from restricting

growth of DC3000, in contrast with mutation of the C216 catalytic residue. Similarly, the K289R mutation reduces but does not abolish HopZ1a induction of macroscopic HR, and more importantly, it does not eliminate HopZ1a ability to effectively protect *Arabidopsis* against infection with DC3000. Our results indicate that this residue is important but not essential for HopZ1a activity, since its mutation does not abrogate the effector virulence and avirulence activities.

Table 1. Plasmids used in this work

Name	Promoter	Expressed effectors	Resistance	Reference
pAME30	*nptII*	HopZ1a	Amp, Km	(Macho et al., 2010a)
pAME27	*nptII*	HopZ1a^{C216A}	Amp, Km	(Macho et al., 2010a)
pMAM1	*nptII*	HopZ1a^{K289R}	Amp, Km	This work
pAME8	*nptII*	AvrRpt2	Amp, Km	(Macho et al., 2009)
pAME33	*nptII*	HopZ1a + AvrRpt2	Amp, Km	(Macho et al., 2010a)
pAME34	*nptII*	HopZ1a^{C216A} + AvrRpt2	Amp, Km	(Macho et al., 2010a)
pJRU10	*nptII*	HopZ1a^{K289R} + AvrRpt2	Amp, Km	This work
pMGm	-	-	Gm	(Murillo et al., 1994)
pAME30Gm	*nptII*	HopZ1a	Amp, Km, Gm	This work
pAME27Gm	*nptII*	HopZ1a^{C216A}	Amp, Km, Gm	This work
pMAM1Gm	*nptII*	HopZ1a^{K289R}	Amp, Km, Gm	This work
pET28a(+)	T7	-	Amp	Novagen (USA)
pET28-Z1a	T7	6xHis-HopZ1a	Amp	This work
pET28-C2	T7	6xHis-HopZ1a^{C216A}	Amp	This work
pET28-K2	T7	6xHis-HopZ1a^{K289R}	Amp	This work
pBINX1	CaMV35S	-	Km	(Sanchez-Duran et al., 2011)
pBINZ1	35S	6xHis-HopZ1a	Km	This work
pBINZ2	35S	6xHis-HopZ1a^{C216A}	Km	This work

pBINZ3	35S	6xHis-HopZ1a^{K289R}	Km	This work

Results

HopZ1a^{K289R} suppresses local PR1 accumulation triggered by DC3000

We have previously shown that HopZ1a suppresses DC3000-triggered PR1 protein accumulation, and that this suppression requires its catalytic cysteine C216 residue (Macho et al., 2010a). To analyze the potential effect of the K289R mutation on HopZ1a activity, we inoculated *Arabidopsis* Col-0 plants with DC3000, DC3000 expressing HopZ1a, or DC3000 expressing either the catalytically inactive HopZ1a^{C216A} mutant or the HopZ1a^{K289R} mutant, and compared the levels of PR1 accumulation in local tissue 48 hours after infection (hpi).

In keeping with our previous results (Macho et al., 2010a), PR1 accumulated to similar levels in leaves inoculated with DC3000 or DC3000 expressing HopZ1a^{C216A}, while PR1 accumulation was clearly reduced in plants inoculated with DC3000 expressing HopZ1a (Figure 1). When leaves were inoculated with DC3000 expressing the HopZ1a^{K289R} mutant protein, PR1 levels were slightly reduced compared to those observed following inoculation with DC3000 or DC3000 expressing HopZ1a^{C216A}, however this reduction was not as substantial as that achieved by the wild type version of the effector (Figure 1). These results indicate that the HopZ1a^{K289R} mutant is still able to suppress local PR1 accumulation elicited by virulent bacteria in the context of a compatible interaction, and suggest that the K289R mutation does not render the effector inactive, in contrast to the C216A mutation.

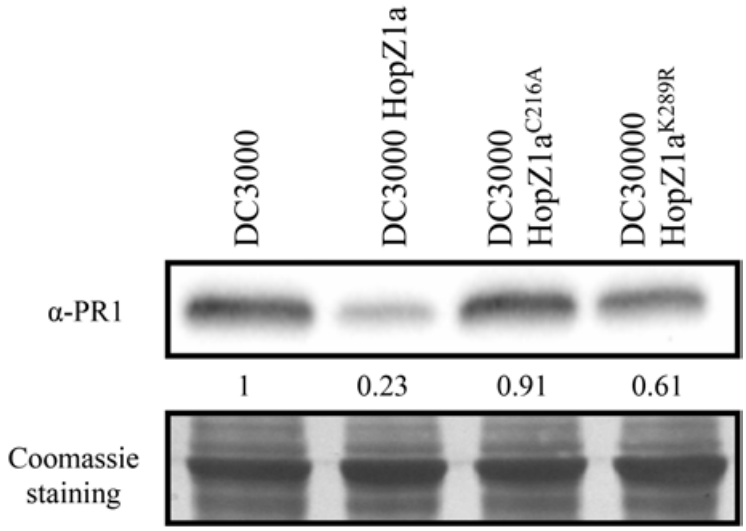

Figure 1. HopZ1a-mediated suppression of local DC3000-triggered PR1 accumulation is reduced but not abolished by the K289R mutation. Western blot showing PR1 accumulation in Col-0 leaves inoculated with 5 x 10^5 cfu/ml of DC3000, DC3000 expressing HopZ1a (pAME30), or DC3000 expressing the mutant derivatives HopZ1a^{C216A} (pAME27) or HopZ1a^{K289R} (pMAM1). Ten micrograms of total protein were loaded per sample, and Coomassie staining is shown as loading control. The signal intensity for each band was quantified using Fiji distribution of ImageJ software and is shown below the blot. The experiment was repeated three times with similar results.

HopZ1a^{K289R} suppresses AvrRp2-triggered immunity

We have also described previously that HopZ1a suppresses the local accumulation of PR1 that accompanies the onset of the ETI triggered by the expression of the heterologous effector AvrRpt2 by DC3000 (Macho et al., 2010a). HopZ1a suppression of AvrRpt2-induced PR1 accumulation is a virulence activity that also depends on the HopZ1a catalytic cysteine C216 (Macho et al., 2010a). To analyze the potential effect of the K289R mutation on HopZ1a activity, we inoculated *Arabidopsis* Col-0 plants with DC3000 expressing AvrRpt2, or DC3000 co-expressing AvrRpt2 and either HopZ1a, HopZ1a^{C216A}, or HopZ1a^{K289R}, and compared the levels of PR1 in the inoculated tissue at 24 hpi.

PR1 accumulated to similar levels in leaves inoculated with DC3000 expressing AvrRpt2 or DC3000 co-expressing AvrRpt2 and HopZ1a^{C216A}, while PR1 accumulation was clearly reduced in leaves inoculated with DC3000 co-expressing AvrRpt2 and HopZ1a (Figure 2A). In leaves inoculated with DC3000 co-expressing AvrRpt2 and the HopZ1a^{K289R} mutant protein, we could not detect differences in PR1 accumulation in comparison to leaves inoculated with either DC3000 expressing AvrRpt2 alone or with HopZ1a^{C216A} (Figure 2A)

HopZ1a suppression of AvrRpt2-triggered defense responses has also been demonstrated in *Arabidopsis* by directly comparing the growth attenuation determined by the individual expression of each effector, with the growth attenuation determined by their simultaneous expression (Macho et al., 2010a). Thus, we also analyzed the impact of the K289R mutation on the suppression of AvrRpt2-triggered growth restriction. To do so we performed mixed infections and calculated the cancelled-out index (COI), a modification of the competitive index (Beuzón and Holden, 2001), previously applied to this purpose (Macho et al., 2010a). COIs directly measure the differences in growth, within the same plant, between a strain expressing one of the effectors and a strain co-expressing both effectors, *i.e.* differences in growth of co-inoculated DC3000 expressing HopZ1a and DC3000 co-expressing HopZ1a and AvrRpt2. Thus, we can directly compare how expression of AvrRpt2 affects growth of DC3000 in the presence of HopZ1a or any of its mutant derivatives, with growth of DC3000 expressing only the HopZ1a version. As HopZ1a is expressed in both strains, the growth reduction it causes in Col-0 is cancelled out as it equally affects both strains (Macho et al., 2010a), and any difference in growth detected between the strain expressing both effectors and the strain expressing only the HopZ1a version, would be due to a growth restriction determined by the unsuppressed defenses triggered against AvrRpt2. A diagram illustrating this analysis is included as supplementary material (Figure S1).

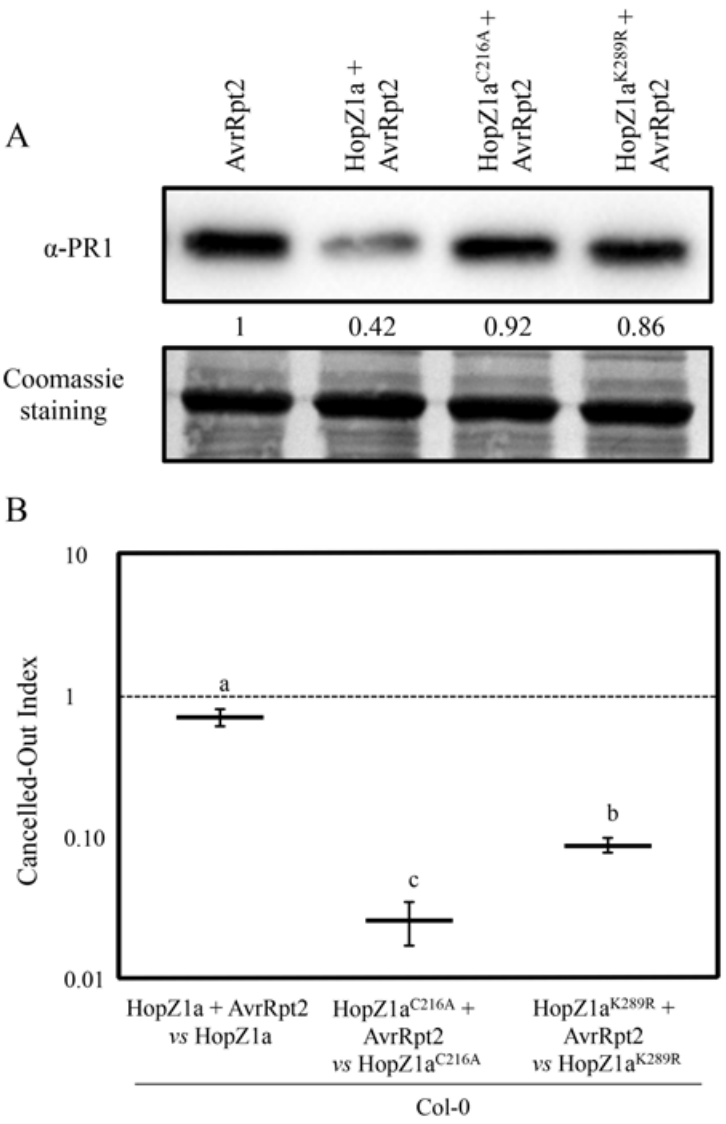

Figure 2. **HopZ1a^{K289R} partially suppresses AvrRpt2-triggered immunity**. (**A**) Western blot showing PR1 accumulation in Col-0 leaves inoculated with 5 x 10^5 cfu/ml of DC3000 expressing AvrRpt2 (pAME8) alone or co-expressing AvrRpt2 with HopZ1a (pAME33), HopZ1a^{C216A} (pAME34) or HopZ1a^{K289R} (pJRU10). Ten micrograms of total protein were loaded per sample, and Coomassie staining is shown as loading control. The experiment was repeated twice with similar results. (**B**) Cancelled-out indices (COIs) measuring growth within a mixed infection of DC3000 co-expressing AvrRpt2 and any of the three HopZ1a variants: wild-type HopZ1a (pAME33), HopZ1a^{C216A} (pAME34) or HopZ1a^{K289R} (pJRU10) , in relation to growth of DC3000 expressing only the corresponding HopZ1a: wild-type HopZ1a (pAME30Gm), HopZ1a^{C216A} (pAME27Gm) or HopZ1a^{K289R} (pMAM1Gm). COIs are calculated as the output ratio between the strain expressing both effectors and the strain expressing just one, divided by their input ratio. Each COI value represents the means of 2 independent experiments with 3 biological replicates each. Error bars represent the standard error. Mean values marked with the same letter are not significantly different from each other as established by Student's t-test ($P<0.05$).

As previously reported (Macho et al., 2009; Macho et al., 2010a) DC3000 co-expressing AvrRpt2 and HopZ1a displayed a small although significant growth attenuation compared to that of co-inoculated DC3000 only expressing HopZ1a

(COI=0.69±0.09) (Figure 2B, Figure S1), despite the fact that AvrRpt2 alone triggers a 50-100 fold growth attenuation when expressed by DC3000 from the same plasmid. This result is expected since HopZ1a is capable of partially suppresing the defense response triggered by AvrRpt2 in *Arabidopsis* (Macho et al., 2010a). Accordingly, growth of DC3000 co-expressing AvrRpt2 and the HopZ1a^{C216A} catalytic mutant was almost 50 fold lower than the growth of DC3000 expressing HopZ1a^{C216A} alone (COI=0.03±0.01) (Figure 2B, Figure S1). However, growth of DC3000 co-expressing AvrRpt2 and the HopZ1a^{K289R} mutant was only a 10-fold lower than growth of the strain expressing HopZ1a^{K289R} alone (COI=0.09±0.01). These results indicate that mutation K289R decreases, but does not abrogate, HopZ1a ability to suppress AvrRpt2-triggered restriction of growth, since co-expression of AvrRpt2 and HopZ1a^{K289R} causes a smaller attenuation of growth than co-expression of AvrRpt2 and the HopZ1a^{C216A} catalytic mutant or expression of AvrRpt2 alone (Figure 2B).

Our results (Figure 2B) indicate that, unlike the catalytically inactive HopZ1a^{C216A} mutant derivative, HopZ1a^{K289R} mutant is still able to suppress AvrRpt2-triggered immunity, since it still suppresses AvrRpt2-triggered restriction of growth. The fact that we do not detect suppression of PR1 protein in plants inoculated with DC3000 expressing the HopZ1a^{K289R} mutant may indicate that our assay is not sensitive enough, or that the association between the PR1 accumulation and growth restriction associated to AvrRpt2-triggered immunity is not linear. To this regards, a similar lack of linearity in the association between PR1 accumulation and growth restriction during induction of SAR has been previously shown (Macho et al., 2010a).

HopZ1a partially suppresses AvrRpt2-triggered immunity in *zar1-1* mutant plants

Results presented in Figure 2B are in agreement with our previous report concluding that HopZ1a partially suppresses AvrRpt2-triggered ETI in *Arabidopsis* (Macho et al., 2010a). However, it has been recently reported that HopZ1a transgenic expression in *zar1-1* plants does not interfere with AvrRpt2-induced macroscopic HR (Lewis et al., 2014). HopZ1a-triggered immunity in *Arabidopsis* is dependent on the ZAR1 resistance protein (Lewis et al., 2010). In the light of this report we decided to analyze the ability of HopZ1a to suppress AvrRpt2-triggered immunity in the absence of HopZ1a-triggered immunity. To this purpose, we analyzed HopZ1a impact on AvrRpt2-triggered restriction of growth in a *zar1-1* plant genotype (Lewis et al., 2010).

Using CI assays, we compared growth of DC3000 expressing HopZ1a or AvrRpt2 with growth of DC3000 in *zar1-1* plants, to determine the growth restriction associated to ETI responses against each of these effectors in the mutant background (Figure 3). Growth of DC3000 expressing HopZ1a was very similar to growth of DC3000 in *zar1-1* plants (CI=0.72±0.09) (Figure 3). Whereas, as expected since AvrRtp2-triggered immunity is independent of ZAR1, the expression of this effector in DC3000 still determined a strong attenuation of growth (CI=0.03±0.01) (Figure 3). However, co-expression of AvrRpt2 and HopZ1a in *zar1-1* plants caused significantly less growth attenuation (CI=0.10±0.03) than that caused by expression of AvrRpt2 alone (Figure 3), demonstrating that HopZ1a suppression of AvrRpt2-triggered immunity takes place in the absence of HopZ1a-triggered immunity, and is not caused by an overlap or interference between the two ETI pathways.

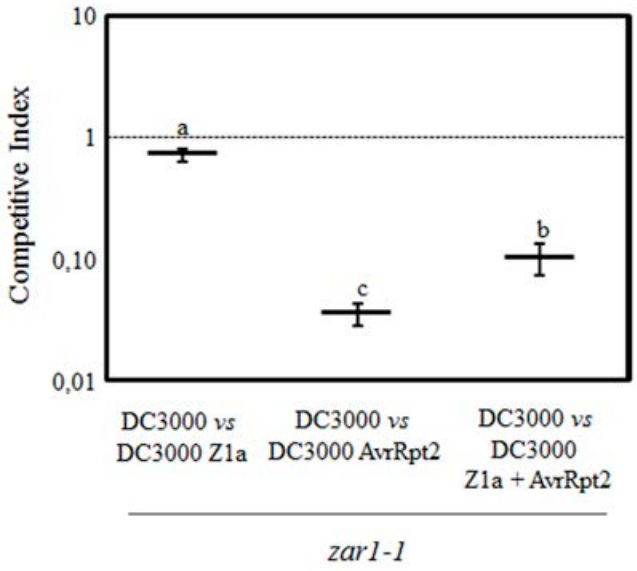

Figure 3. HopZ1a suppresses AvrRpt2-triggered ETI in *zar1-1* plants. Competitive indices (CIs) measuring growth within a mixed infection of DC3000 expressing HopZ1a (Z1a, pAME30), AvrRpt2 (pAME8) or co-expressing both (Z1a + AvrRpt2, pAME33) in relation to growth of DC3000. CIs are calculated as the output ratio between the strain expressing the effector(s) and DC3000, divided by their input ratio. Each CI value represents the means of 3 independent experiments with 3 biological replicates each. Error bars represent the standard error. Mean values marked with the same letter were not significantly different from each other as established by Student's t-test (P<0.05).

HopZ1a^{K289R} retains the ability to suppress Systemic Acquired Resistance (SAR) triggered by DC3000 infection

Both virulent and avirulent bacteria can trigger SAR, a defense response elicited in distal (systemic) tissues as a result of local infection. Activation of SAR determines both systemic accumulation of PR1, and restriction of growth of newly incoming bacteria (Cameron et al., 1994). We have previously shown that HopZ1a expression suppresses SAR triggered by DC3000, and that such suppression requires HopZ1a catalytic cysteine C216 (Macho et al., 2010a). To determine whether the HopZ1a^{K289R} mutant retained HopZ1a ability to suppress SAR, we first analyzed the effect of the mutation K289R in HopZ1a ability to suppress SAR-associated restriction of growth of newly incoming bacteria. We inoculated primary leaves with either 10 mM $MgCl_2$ (mock), DC3000, or DC3000 expressing HopZ1a or the corresponding mutant derivatives HopZ1a^{C216A} or HopZ1a^{K289R} (Figure 4A). Two days after inoculation of primary leaves, distal leaves were inoculated with DC3000, and 4 days after this second inoculation we monitored the growth of DC3000. Figure 4A shows that, as previously described, pre-inoculation of primary leaves with either DC3000 or DC3000 expressing the catalytically inactive mutant HopZ1a^{C216A} triggered SAR to equivalent levels, since growth of DC3000 in distal leaves was similarly attenuated in both cases. In contrast, pre-inoculation with DC3000 expressing HopZ1a did not result in detectable attenuation of growth of DC3000 in distal leaves, since it did not show significant differences with that observed in mock pre-inoculated leaves, thus confirming the reported HopZ1a suppression of SAR (Macho et al., 2010a). Systemic leaves from plants pre-inoculated with DC3000 expressing HopZ1a^{K289R} displayed DC3000 cfu values significantly different to those reached in plants pre-inoculated with DC3000 expressing HopZ1a^{C216A}, but similar to those reached in plants pre-inoculated with DC3000 expressing HopZ1a (Figure 4A), supporting the notion that autoacetylation of HopZ1a on K289 is not required for suppression of SAR in *Arabidopsis*.

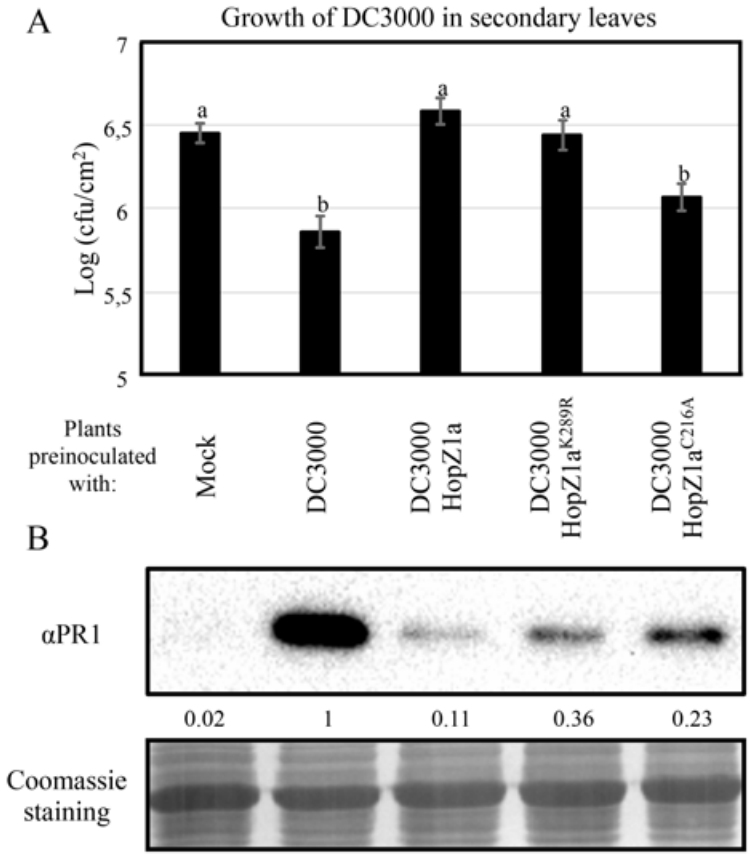

Figure 4. HopZ1a-mediated suppression of SAR is reduced but not abolished by the K289R mutation. (A) Growth of DC3000 inoculated in secondary leaves of plants pre-inoculated in primary leaves by infiltrating either a 10 mM $MgCl_2$ solution (Mock), or 5 x 10^5 cfu/ml of DC3000, DC3000 expressing HopZ1a (pAME30), or DC3000 expressing the mutant derivatives HopZ1a^{C216A} (pAME27) or HopZ1a^{K289R} (pMAM1). Two days post-inoculation of primary leaves, secondary leaves were inoculated with 5 x 10^4 cfu/ml of DC3000, and growth was measured at 4 days post-inoculation of the secondary leaves. The experiment was repeated four times with similar results, and the results shown correspond to a representative experiment. The values shown represent the means of 5 biological replicates. Error bars represent the standard error. Values marked with the same letter were not significantly different from each other as established by Student's t-test ($P<0.05$). (B) Western blot analysis for immunodetection of PR1 on distal non-inoculated leaves, 2 days after inoculating primary leaves with either 10 mM $MgCl_2$ (Mock), or 5 x 10^5 cfu/ml of DC3000, DC3000 expressing HopZ1a (pAME30), or DC3000 expressing the mutant derivatives HopZ1a^{C216A} (pAME27) or HopZ1a^{K289R} (pMAM1). Ten micrograms of total protein were loaded per sample, and Coomassie staining is shown as loading control. The experiment was repeated twice with similar results.

To determine how the HopZ1a^{K289R} mutant ability to suppress SAR correlates with suppression of PR1 accumulation in systemic tissue, we used western blot analysis to analyze accumulation of PR1 in systemic leaves of plants pre-inoculated with DC3000 or DC3000 expressing the different versions of HopZ1a. In keeping with previous results (Macho et al., 2010a), expression of HopZ1a in DC3000 suppresses PR1 accumulation in systemic tissues, since distal leaves of plants pre-inoculated with DC3000 expressing HopZ1a displayed a strong reduction of PR1 accumulation when

compared to plants pre-inoculated with DC3000 (Figure 4B). This suppression is dependent on HopZ1a catalytic cysteine, since systemic leaves of plants pre-inoculated with DC3000 expressing HopZ1a^{C216A} displayed PR1 levels that were higher than those observed in plants pre-inoculated with DC3000 expressing HopZ1a (Figure 4B). As previously reported (Macho et al., 2010a) the C216A mutation did not entirely abolish HopZ1a ability to suppress PR1 accumulation, since the systemic levels of PR1 in plants pre-inoculated with DC3000 expressing HopZ1a^{C216A} did not reach the levels observed in plants pre-inoculated with DC3000 (Figure 4B). Interestingly, when primary leaves were inoculated with DC3000 expressing HopZ1a^{K289R}, the accumulation of PR1 in distal leaves reached levels that were intermediate between those elicited by DC3000 expressing HopZ1a^{C216A} and DC3000 expressing wild type version of the effector (Figure 4B). These results indicate that the HopZ1a^{K289R} mutant is still able to partially suppress systemic accumulation of PR1 in response to DC3000.

HopZ1a^{K289R} triggers ETI in *Arabidopsis* and *N. benthamiana*

Inoculation of *Arabidposis* leaves with a 5x10^7 cfu/ml of DC3000 expressing HopZ1a induces macroscopic HR symptoms in *Arabidopsis* leaves, which are absent in leaves inoculated with the same dose of DC3000 expressing the HopZ1a^{C216A} catalytic mutant (Lewis et al., 2008; Macho et al., 2010a). It has been reported that the mutation K289R completely prevents HopZ1a-triggered HR, which cannot be detected when expressing the mutant effector under the control of its own promoter (Lee et al., 2012). However, considering that our results presented above indicate that such mutation does not render the effector entirely inactive, we wondered whether HopZ1a^{K289R} could still be able to trigger immunity in *Arabidopsis*.

To analyze whether the HopZ1a^{K289R} mutant was able to trigger macroscopic HR in *Arabidopsis*, we inoculated leaves with 5x10^7 cfu/ml of DC3000, DC3000 expressing HopZ1a, or DC3000 expressing either HopZ1a^{C216A} or HopZ1a^{K289R} mutant derivatives, and monitored HR development by 20–24 hpi (Figure 5A). Development of macroscopic HR requires a rather strong ETI response, which might not be reached by lower levels of effector expression (Macho et al., 2009), thus we expressed HopZ1a and its mutant derivatives under the control of the strong constitutive *nptII* promoter, to factor in the chance of an stronger effector expression allowing detection of a mild ETI. In keeping with previous reports (Lewis et al., 2008; Macho et al., 2010a), a clear HR

was detected in plants inoculated with DC3000 expressing HopZ1a, while no HR could be detected in leaves inoculated with either DC3000 or DC3000 expressing HopZ1a^{C216A} (Figure 5A). Interestingly, leaves inoculated with DC3000 expressing HopZ1a^{K289R} displayed noticeable macroscopic HR (Figure 5A). As expected from previous reports (Lewis et al., 2010) (Lewis et al., 2014), inoculation of *zar1-1* leaves with these strains did not induce any visible cell death symptom (Figure S2).

The ETI triggered in Arabidopsis against HopZ1a in *Arabidopsis* determines a strong restriction of bacterial growth that can be measured using competitive index assays (CIs), in mixed infections of DC3000 co-inoculated with DC3000 expressing HopZ1a (Macho et al., 2009; Macho et al., 2010a). To further investigate the impact of the K289R mutation in HopZ1a activation of ETI in *Arabidopsis*, we performed CI assays by co-inoculating *Arabidopsis* plants with DC3000 and DC3000 expressing HopZ1a, HopZ1a^{C216A}, or HopZ1a^{K289R} (Figure 5B). As previously described (Macho et al., 2010a), a clear growth attenuation was measured for DC3000 expressing HopZ1a in comparison with co-inoculated DC3000 (CI=0.03±0.01), while no significant attenuation was detected for DC3000 expressing HopZ1a^{C216A} catalytically inactive (CI=0.91±0.10) (Figure 5B). In contrast, DC3000 expressing HopZ1a^{K289R} displayed a small attenuation of growth (CI=0.46±0.10), significantly smaller than that measured for DC3000 expressing HopZ1a, but significantly different from the absence of attenuation observed for HopZ1a^{C216A}-expressing DC3000 bacteria (Figure 5B).

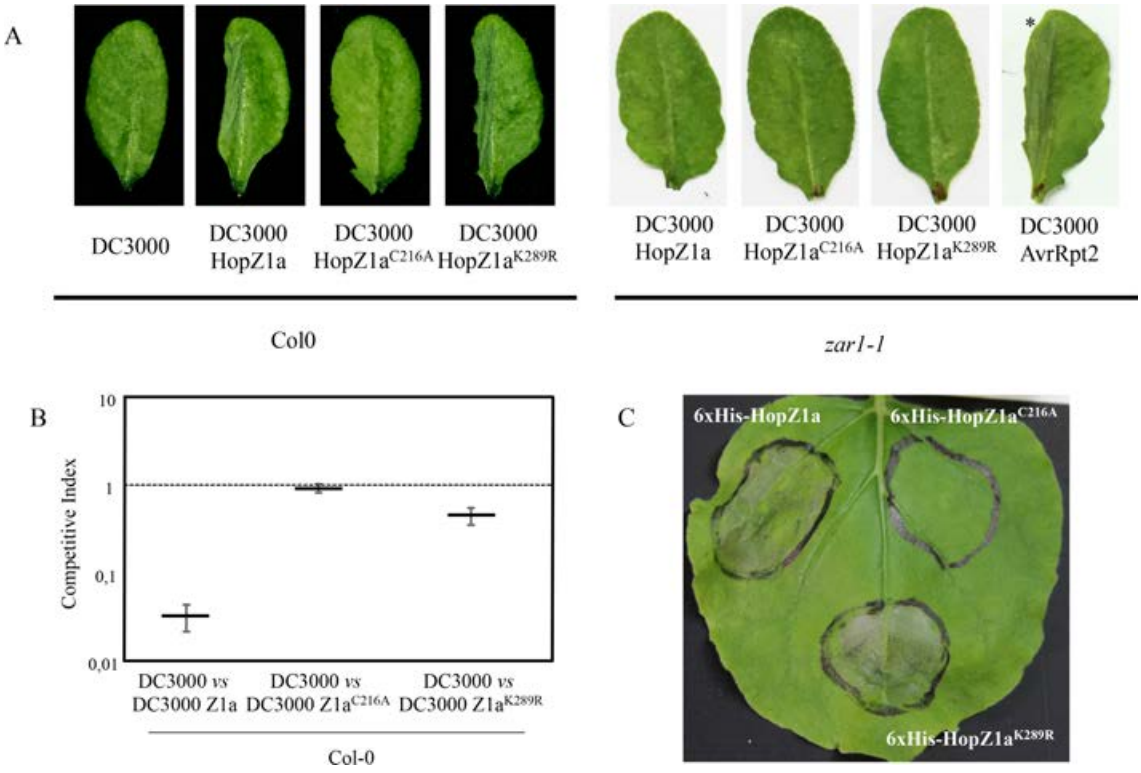

Figure 5. **HopZ1a^{K289R} triggers ETI**. (A) Hypersensitive response (HR) to hand-infiltration of Col-0 leaves with bacterial suspensions containing 5 x 10^7 cfu/ml of DC3000 alone or DC3000 expressing HopZ1a (pAME30), or each of its mutant derivatives HopZ1a^{C216A} (pAME27) or HopZ1a^{K289R} (pMAM1). Photographs were taken 24 hours post-inoculation. Images are representative of at least 30 inoculated leaves per strain and experiment. The experiment was repeated twice with similar results. (B) Competitive indices (CIs) measuring growth within a mixed infection of DC3000 expressing HopZ1a (Z1a, pAME30), or each of its mutant derivatives HopZ1a^{C216A} (Z1a^{C216A}, pAME27) or HopZ1a^{K289R} (Z1a^{K289R}, pMAM1), in relation to growth of DC3000. CIs are calculated as the output ratio between the strain expressing the effector and DC3000, divided by their input ratio. Each CI value represents the means of 3 independent experiments with 3 biological replicates each. Error bars represent the standard error. Mean values marked with the same letter were not significantly different from each other as established by Student's t-test ($P<0.05$). (C) Development of HR following transient expression of either 6xHis-HopZ1a (pBINZ1) or each of its mutant derivatives 6xHis-HopZ1a^{C216A} (pBINZ2) or 6xHis-HopZ1a^{K289R} (pBINZ3). *Nicotiana benthamiana* leaves were inoculated with *Agrobacterium tumefaciens* C58C1 carrying binary plasmids encoding the corresponding effector genes. Pictures were taken 48 hours post inoculation. The experiment was repeated 3 times with similar results.

In addition to triggering HR in *Arabidopsis*, HopZ1a has been shown to trigger macroscopic HR in *Nicotiana benthamiana* leaves when transiently expressed using *Agrobacterium* (Ma et al., 2006); (Lewis et al., 2008). We expressed HopZ1a and its mutant derivatives HopZ1a^{C216A} and HopZ1a^{K289R} in *N. benthamiana* leaves, under the control of a constitutive promoter, by using *Agrobacterium*-mediated transient expression, and monitored HR symptoms at 40 hours after *Agrobacterium* inoculation. While transient HopZ1a^{C216A} overexpression did not result in HR elicitation whatsoever, HopZ1a^{K289R} overexpression elicited an HR of a similar intensity to that elicited by overexpressing HopZ1a (Figure 5C).

Taken together, results shown in Figure 5 indicate that autoacetylation of HopZ1a in its lysine 289 contributes, but it is not essential, to trigger ETI in *Arabidopsis*.

HopZ1a^{K289R}-triggered defenses effectively protects *Arabidopsis* against disease development

We have previously shown that resistance triggered in *Arabidopsis* by the expression of HopZ1a efficiently protects plants from DC3000 infection, resulting in the absence of virulence-associated disease symptoms (Macho et al., 2010a). To analyze whether the defense response triggered against HopZ1a^{K289R} mutant is sufficient to stymie DC3000 disease in *Arabidopsis*, we monitored development of disease symptoms at 4–6 dpi on plants spray-inoculated with DC3000, DC3000 expressing HopZ1a, or DC3000 expressing either HopZ1a^{C216A} or HopZ1a^{K289R} mutant derivatives. As expected from previous results (Macho et al., 2010a), plants sprayed with either DC3000 or DC3000 expressing HopZ1a^{C216A} displayed noticeable disease symptoms, namely chlorosis and stunted growth, while plants sprayed with DC3000 expressing HopZ1a did not (Figure 6). Interestingly, plants sprayed with DC3000 expressing HopZ1a^{K289R} did not display chlorosis and only a slightly reduction in plant growth could be observed (Figure 6).

These results clearly show that the HopZ1a^{K289R} mutant triggered-resistance effectively protects *Arabidopsis* plants from disease.

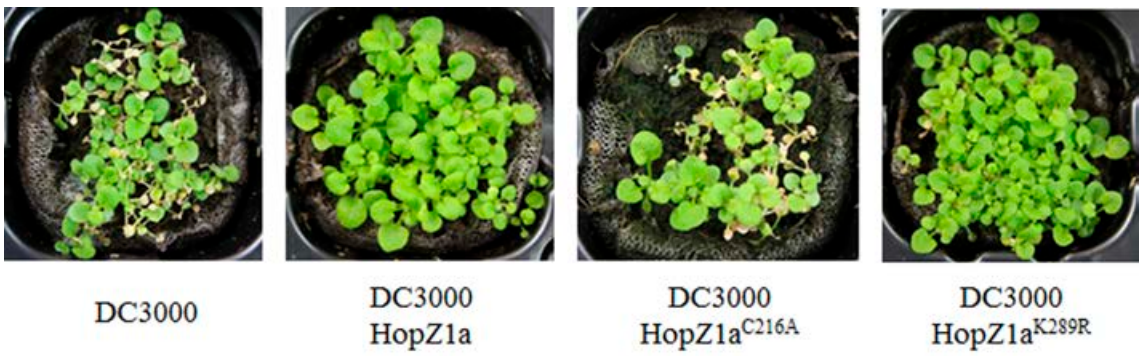

Figure 6. **Expression of HopZ1a^{K289R} from DC3000 protects Col-0 plants against disease**. Virulence symptoms caused by spray-inoculated DC3000, or DC3000 expressing HopZ1a (pAME30), or each of its mutant derivatives HopZ1a^{C216A} (pAME27) or HopZ1a^{K289R} (pMAM1). *Arabidopsis* plants were sprayed with bacterial suspensions containing 5 x 10^7 cfu/ml in 0.02% Silwet L-77, and photographed 6 days post-inoculation. The experiment was repeated three times using 5 plants per strain, and representative images are shown.

HopZ1a^{K289R} is acetylated *in vitro*

Since our results demonstrate that the K289 lysine residue is not essential for HopZ1a activities within the plant, it is possible that an alternative lysine residue may still be acetylated in the absence of K289, thus partially complementing the potential requirement for HopZ1a autoacetylation. Therefore, we decided to reassess HopZ1a^{K289R} acetylation *in vitro*, by incubating wild type HopZ1a and its mutant derivatives HopZ1a^{K289R} and HopZ1a^{C216A} in the presence of acetyl-coenzyme A and the eukaryotic co-factor phytic acid (Mittal et al.), and monitoring lysine acetylation of each effector version by Western blot using an specific antibody. HopZ1a^{K289R} is still acetylated *in vitro* although to a lesser extend that the wild type HopZ1a protein, in contrast to complete absence of acetylation in the catalytically inactive HopZ1a^{C216A} mutant (Figure 7). These results are in contrast to previously published results (Lee et al.; Ma et al., 2015).

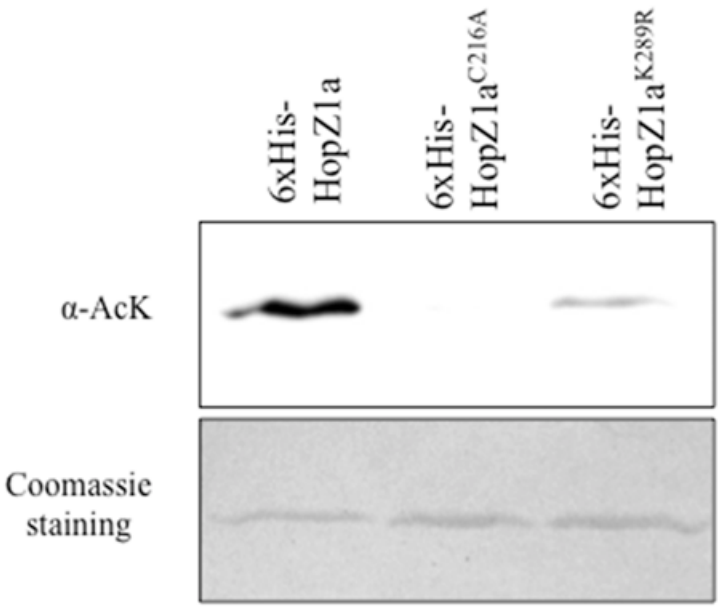

Figure 7. HopZ1a is acetylated on K289 *in vitro*. Western blot analysis for immunodetection of acetylated lysines. 20 ul of the *in vitro* acetylation reaction of 6xHis-HopZ1a (pET28-Z1a), 6xHis-HopZ1a^{C216A} (pET28-C2) or 6xHis-HopZ1a^{K289R} (pET28-K2) were loaded per lane. Coomassie staining is shown as loading control. The experiment was repeated three times with similar results.

Discussion

HopZ1a^{K289R} triggers ETI in *Arabidopsis* and *N. benthamiana* and effectively protects *Arabidopsis* against disease developmen

Results described in this chapter indicate that the HopZ1a^{K289R} mutant is still able to trigger a defense response that induces macroscopic HR (Figure 5) and, more importantly, effectively protects *Arabidopsis* from infection (Figure 6). While our results in respect to HopZ1a^{K289R} mutant triggering macroscopic HR are at variance with those described previously (Lee et al., 2012), this discrepancy can be due to differences in effector levels, since we express HopZ1a under the control of a strong constitutive promoter, and macroscopic HR symptoms can be quite dependent on threshold levels of the eliciting effectors (Macho et al., 2009). While the development of macroscopic HR symptoms after high-dose bacterial inoculation is a good measure of the ability of an effector to trigger a defense response, the protection from infection after a low-dose inoculation may reflect more accurately the physiological significance of such defense response for the plant. In this respect, results shown in Figure 6 support the notion that the K289R mutation does not abrogate HopZ1a avirulence activity. It is important to notice that in neither of these assays, regarding induction of macroscopic HR or protection against disease development, did the catalytically inactive HopZ1a^{C216A} trigger any defense response whatsoever, regardless of being expressed under the control of the same strong promoter, supporting the notion that HopZ1a^{K289R} activity is not an artifact due to overexpression.

HopZ1a^{K289R} suppresses DC3000-triggered basal immunity

Results described in this chapter indicate that the HopZ1a^{K289R} mutant retains its ability to suppress basal immunity triggered by DC3000, since it can partially suppress DC3000-triggered local and systemic PR1 accumulation (Figures 1, 4), as well as DC3000-triggered SAR-dependent restriction of growth in systemic tissues (Figure 4).
The fact that PR1 accumulation against DC3000 requires a functional T3SS (Figure 1) (Macho et al., 2010a) suggests that it is due to weak ETI-like defenses. However, the implication of PTI cannot be ruled out, since the level of PR1 accumulated in response to PAMPs in the attenuated T3SS mutant could be below the level of detection. In regards to this, a recent report demonstrates that HopZ1a can indeed suppress DC3000-triggered PTI response when overexpressed in transgenic *Arabidopsis* plants (Lewis et

al., 2014). Additionally, the related effector AvrBsT can also suppress the PTI triggered by DC3000 infection in tomato, as shown by a lower accumulation of PR1 in the infected plants (Kim et al., 2010).

Previous reports have suggested that the K289R mutation completely abrogates HopZ1a virulence activity, since heterologous expression of the corresponding mutant effector in *Pseudomonas* syringae pv. cilantro 0788-9 did not contribute to the growth of the expressing strain in the *Arabidopsis zar1-1* background (Lee et al., 2012). However, the rather modest growth rate achieved in *Arabidopsis* by *Pseudomonas* strain 0788-9, together with the limited contribution of wild type HopZ1a to such growth, might be limiting the sensitivity of such assay. Using a wider array of virulence assays, we demonstrate that the K289R mutation does not abolish HopZ1a virulence activity.

HopZ1a suppresses AvrRpt2-triggered immunity in the absence of HopZ1a-triggered immunity

Our results demonstrate that HopZ1a suppression of AvrRpt2-triggered immunity takes place in the absence of HopZ1-triggered immunity (Figure 3), and it is therefore not a consequence of an overlap or interference between the defense responses triggered by these effectors. This notion was previously supported by the fact that AvrRpt2 does not alter HopZ1a-triggered restriction of growth in *rps2* plants, where AvrRpt2 does not trigger resistance but still displays virulence activity (Macho et al., 2010a). This is in disagreement with a recent report based on transgenic overexpression of HopZ1a in *zar1-1* plants where it has been shown to suppress PTI, but not to prevent the onset of macroscopic HR (Lewis et al., 2014). However, such a strong suppression of PTI could alter potentially the ETI response of the transgenic lines.

HopZ1a^{K289R} suppresses AvrRpt2-triggered ETI

ETI suppression is a key virulence activity of HopZ1a that is only partly affected by the K289R mutation, while being completely eliminated in the catalytically inactive HopZ1a^{C216A} mutant. The related *Xanthomonas* effector AvrBsT has also been shown to suppress the ETI induced in pepper plants by a second *Xanthomonas* effector, AvrBs1 (Szczesny et al., 2010). In fact, the demonstrations of the ETI-suppressing activities of AvrBsT and HopZ1a were presented simultaneously, becoming the first known effectors belonging to the YopJ / HopZ family to display such virulence function (Macho et al., 2010a; Szczesny et al., 2010). The ETI-suppression ability of AvrBsT is

also dependent on its catalytic cysteine (Szczesny et al., 2010). However, the activity of the AvrBsT mutant equivalent to HopZ1a^{K289R} has only been assayed by heterologous expression in the interaction model based on *Pseudomonas* DC3000 and the *Arabidopsis* Pi-0 ecotype, where it does not display any virulence function (Cheong et al., 2014). In view of the new results presented here, and the similarities between HopZ1a and AvrBsT, it would be interesting to analyze the performance of the AvrBsT^{K282R} mutant in pepper plants, where it displays ETI-suppression abilities.

ZAR1-mediated resistance against HopZ1a

HopZ1a has been reported in turn to slightly enhance the growth of DC3000 in *zar1-1* plants (Lewis et al., 2010) and to slightly decrease it (Jiang et al., 2013), however in both cases differences in growth were within the same log. In our experimental conditions growth of DC3000 expressing HopZ1a was close to that of DC3000 in *zar1-1* plants, albeit slightly decreased (Figure 3), since the CI of DC3000 expressing HopZ1a in mixed infection with DC3000 (CI=0.72±0.09) was statistically different from 1.0. Our results are therefore in agreement with the observations of (Jiang et al., 2013). The disparity with the results from the first report (Lewis et al., 2010) could be due to differences in experimental settings, however the existence of a residual defense against HopZ1a in the *Arabidopsis zar1-1* background cannot be ruled out. Such residual defense could be either due to residual activity of a truncated ZAR1 protein, or to a weak recognition by a second resistance protein, as described for other effectors (Saucet et al., 2015).

HopZ1a acetyltransferase activity

On view of the results presented in this work, the absolute requirement of the K289 lysine residue for HopZ1a activity can be discarded. A recent paper (Ma et al., 2015) support this result, and described two serine residues (S349 and S351) that are also acetylated in HopZ1a. The acetyltransferase activity described for the HopZ/YopJ effector family is based on the Ping-Pong model, which requires an autoacetylated state of the effector prior to the transfer of the acetyl group to the substrate (Mukherjee et al., 2006). Thus, we hypothesize that HopZ1a autoacetylates itself on the two serines described (Ma et al., 2015), and theses acetyl groups are used by the lysine 289 to transacetylate its targets. Our *in vitro* assays (Figure 7) suggest the presence of alternative lysine residues in HopZ1a that can be acetylated, partially complementing

the absence of K289. However, using ^{14}C-labelled acetyl-CoA as acetyl donor, Ma et al. (Ma et al., 2015) observed an increased autoacetylation activity in HopZ1a^{K289R} mutant compared with the wild type. This inconsistent result can only be explained as methodological differences. We use a specific anti-acetylated lysines antibody to detect differences on the lysine-acetylation status of HopZ1a and the K289R mutant. However, the radioactivity-based assay used by Ma et al. (Ma et al., 2015) detects the acetylation of all putative residues in the protein (i.e. lysines, serines and threonines).

However we cannot rule out that autoacetylation of HopZ1a might not be altogether essential for HopZ1a activities within the plant. In fact, it has been suggested in relation to the closely related effector HopZ1c (Lewis et al., 2014) that the C-terminal third of the HopZ family might be dispensable for acetyltransferase activity, or that HopZ1c may use water instead of acetyl-CoA during its enzymatic reaction, resulting in hydrolysis of substrates rather than acetylation, in an alternative catalytic mechanism suggested by (Mukherjee et al., 2007).

Furthermore, although HopZ1a is indeed susceptible of autoacetylation in lysine and serine residues, as shown by Figure 7, Lee et al. 2012 and Ma et al. 2015, it should be noted that the only HopZ1a interacting protein where the acetylated residues have been identified, namely the pseudokinase ZED1, is acetylated on threonine residues rather than lysines (Lewis et al., 2013). Therefore, we cannot rule out that HopZ1a might also display acetyltransferase activity on other amino acid residues, such as serine or threonine, as it is the case with YopJ, the archetypal effector of the YopJ/HopZ superfamily (Mukherjee et al., 2006).

Results presented to date for several YopJ/HopZ effectors do not support a consistent association between their autoacetylation at the conserved lysine residue and their transacetylation activities. For instance, AvrBsT maintains the autoacetylation activity in the absence of the conserved lysine residue, which is however essential for the acetylation of one of its described targets (Cheong et al., 2014). On the other hand, prior autoacetylation of YopJ is not required for acetylation of MEK, one of its described targets (Mittal et al., 2010). This opens the possibility that the said lysine residue and/or its autoacetylation, while contributing to the overall function of the effectors, may not be essential for all their activities *in planta*. Considering the various targets proposed for each of the effectors belonging to the YopJ/HopZ superfamily, and the numerous biochemical activities assigned, sometimes concurrently, to said effectors

(Orth et al., 2000; Hotson and Mudgett, 2004; Ma et al., 2006; Mukherjee et al., 2006; Sweet et al., 2007; Szczesny et al., 2010; Tasset et al., 2010; Zhou et al., 2011; Lee et al., 2012; Jiang et al., 2013; Lewis et al., 2013; Cheong et al., 2014), it is tempting to speculate that their molecular mechanisms *in planta* might be manifold, and therefore that the conserved lysine residue and/or its autoacetylation might not be required for all targets or activities. The resultant of all these activities on numerous targets would be observed as virulence or avirulence manifestations on a given plant model, and might be behind the intermediate phenotypes described for the HopZ1a^{K289R} mutant in this work.

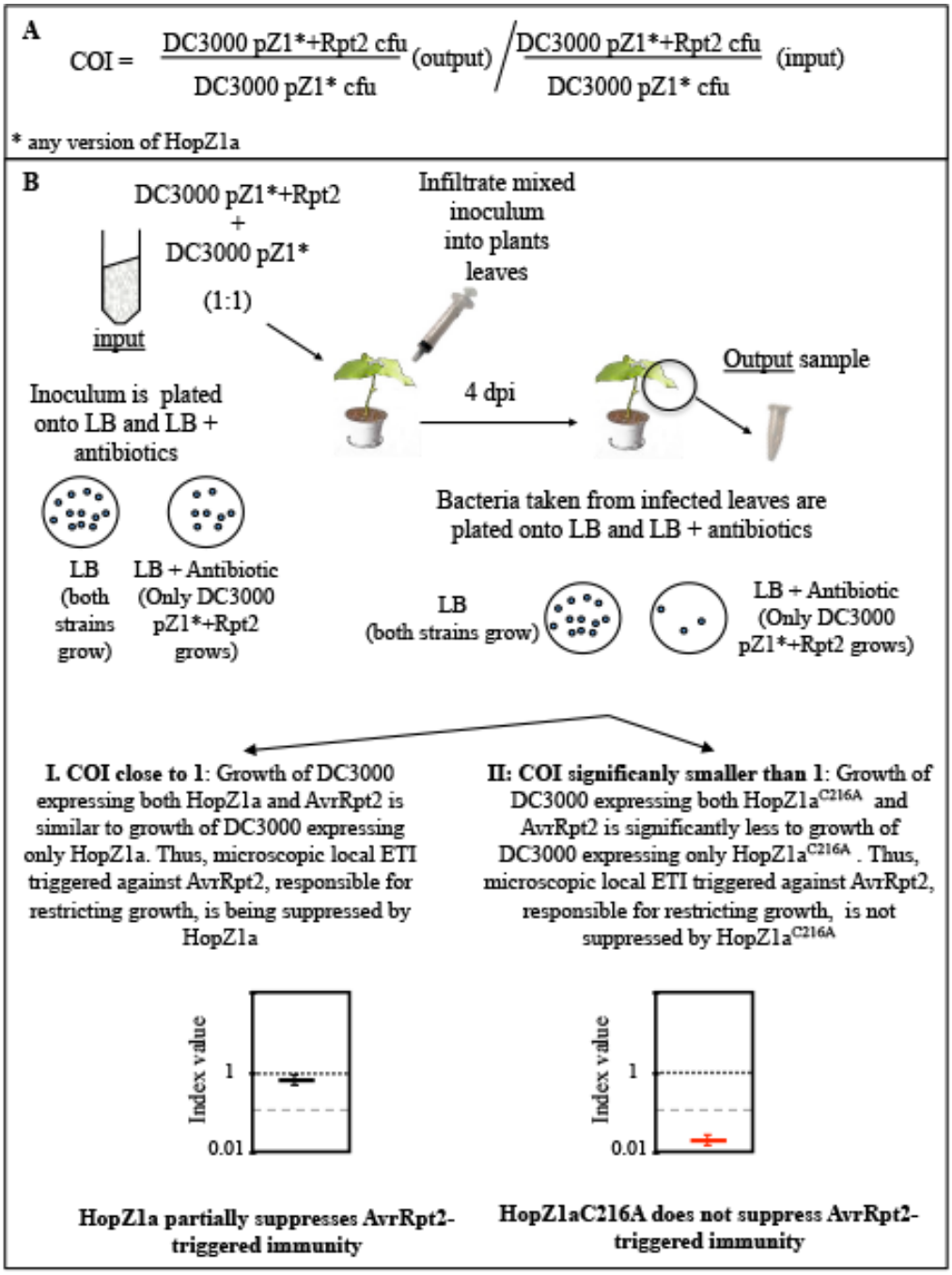

Figure S1. Diagram depicting the cancelled-out analysis carried out in this study. A. COI is defined as ratio between cfu of the the strain expressing both AvrRpt2 and any version of HopZ1a, and the cfu of the strain expressing only the corresponding HopZ1a version in the output sample, divided by their ratio within the input inoculum. **B**. Determination and analysis of COI. A mix inoculum containing an equal bacterial number of both strains is infiltrated into plant leaves. The inoculum is plated onto LB and LB supplemented with antibiotics, to differentiate between the co-inoculated strains, and to establish the input ratio which should be close to 1. Bacteria are recovered from plant leaves at 4 days post inoculation (dpi), and plated into LB and LB supplemented with antibiotics, to differentiate the strains ant to determine their output ration. I and II represent the two control outcomes for the analysis.

Chapter 4: The bacterial effector HopZ1a acetylates MKK7 to suppress plant defense responses

José S. Rufián, Diego López-Márquez, Javier Rueda-Blanco, Carmen R. Beuzón, Javier Ruiz-Albert

Introduction

HopZ1a is a *P. syringae* T3E with the ability to suppress several layers of plant defense. HopZ1a has been shown to suppress in *Arabidopsis* (i) basal resistance or PTI triggered by *P. syringae* pv. tomato DC3000 (Macho et al., 2010a; Lewis et al., 2014) (ii), ETI triggered by the expression of the heterologous effectors AvrRpt2, AvrRps4 and AvrRpm1 (Macho et al., 2010a; Rufian et al., 2015), and (iii) systemic acquired resistance (SAR) triggered by either virulent or avirulent bacteria (Macho et al., 2010a; Rufian et al., 2015). On the other hand, HopZ1a triggers ETI in Col-0 *Arabidopsis* plants upon recognition by the ZAR-1 resistance protein (Lewis et al., 2010), a defense response that is independent of salicylic acid (SA) and EDS1 (Lewis et al., 2010; Macho et al., 2010a).

HopZ1a belongs to the YopJ / HopZ superfamily of T3Es, which includes representatives from both animal and plant pathogens (Ma et al., 2006; Lewis et al., 2010). Many of these T3Es have been described to function as acetyltransferases, among other biochemical activities (Trosky et al.; Zhou et al.; Mittal et al., 2006; Jones et al.; Lee et al., 2012). In fact, HopZ1a has been shown to display acetyltransferase activity, with varying degrees of efficiency, on some of its proposed plant targets (Lee et al., 2012; Jiang et al., 2013) or decoys (Lewis et al., 2013). HopZ1a acetyltransferase activity is completely dependent on the integrity of the catalytic triad cysteine (C216), since a HopZ1a^{C216A} mutant behaves as a catalytically inactive mutant (Lee et al., 2012). Likewise, residue C216 is essential for all described HopZ1a virulence and avirulence functions *in planta* (Ma et al., 2006; Lewis et al., 2008; Macho et al., 2010a; Lewis et al., 2014; Rufian et al., 2015). HopZ1a has also been described to auto-acetylate in two serine residues (S349 and S351) that are required for acetyltransferase activity *in vitro*, virulence activity *in planta*, and interaction with the co-factor IP6 (Ma et al., 2015). In turn, lysine residue K289, which was originally postulated to be the only HopZ1a auto-acetylation site and key for effector activity (Lee et al., 2012), might only partially contribute to trans-acetylation (Ma et al., 2015) and does not seem to be essential for HopZ1a virulence or avirulence activities (Rufian et al., 2015).

A common theme among the majority of T3Es that constitute the YopJ / HopZ superfamily, particularly for those present in animal pathogens, seems to be the interference with MAPK signaling cascades leading to the activation of the immune response. The archetypal member of the superfamily, *Yersinia* effector YopJ, acetylates

key serine and threonine residues of a subset of mitogen-activated protein kinase kinases (MAP2Ks or MKKs) and MAP kinase kinase kinases (MAP3Ks) from several animal models, competing with the phosphorylation of said residues, which in turn leads to inactivation of downstream defense signaling, and suppression of the immune response (Mittal et al., 2010 ; Meinzer et al., 2012). YopJ can also acetylate lysine residues of several of its targets, however this modification does not seem to be essential for its inhibitory function (Mukherjee et al., 2006; Paquette et al., 2012). Within the same superfamily, AvrA from *Salmonella* and VopA from *Vibrio* acetylate key serine, threonine, and lysine residues of their corresponding target MKKs, resulting in inhibition of kinase activity and the suppression of immune responses (Trosky et al.; Jones et al.). YopJ and VopA can also interfere with MAPK modules in yeast, via acetylation of kinases PBS2, MEK1, or Ste7 (Yoon et al., 2003; Trosky et al., 2004; Hao et al., 2008).

In plants, MAPK cascades also constitute signaling networks leading to defense against pathogens, since PRR recognition of PAMPs leads to activation of MAPK modules and ultimately to the corresponding immune response (reviewed by (Pitzschke et al.; Feng and Zhou, 2012)). Interestingly, HopZ1a has been described to suppress MAPK activation in *Arabidopsis* (Lewis et al., 2014). Further, several other T3Es suppress plant defense signaling by targeting mitogen-activated protein kinase (MAPK) cascades at different levels, as in the case of HopAI1 interfering with several MAP kinases (MPKs) (Zhang et al., 2007a; Zhang et al., 2012), or HopF2 blocking the phosphorylation of a MAP kinase kinase, MKK5 (Wang et al., 2010). In fact, a considerable number of T3Es interact with plant kinases, altering their function, which results in the interference of plant defense signaling (Block and Alfano, 2011; Macho and Zipfel, 2015). Some T3Es, such as AvrPto, AvrPtoB, or HopF2, target PRRs or its co-receptors, typically acting on them as kinase inhibitors and suppressing early PTI events (Shan et al., 2008; Xiang et al., 2008; Cheng et al., 2011; Wu et al., 2011; Xiang et al., 2011; Zeng et al., 2012a; Zhou et al., 2014). Other T3Es, such as AvrPphB or AvrAC, act on PRR-associated receptor-like cytoplasmic kinases (RLCKs), inactivating their function to suppress PTI (Zhang et al., 2010; Feng and Zhou, 2012).

Since RLCKs and MAPKs are important components of plant defense signaling targeted by T3Es, they are accordingly guarded by plant resistance proteins that in resistant plants can detect, directly or indirectly, the alterations induced by T3E action

on their targets, and trigger the corresponding ETI defense responses, as those described for AvrPphB or AvrAC when acting respectively on the RLCKs PBS1 (Shao et al., 2003) or PBL2/RIPK (Guy et al., 2013), or for HopAI1 while acting on MPK4 (Zhang et al., 2012). In this sense, the ETI triggered by HopZ1a in *Arabidopsis* seems to be the consequence of the recognition, by the ZAR-1 resistance protein, of HopZ1a acetylation of the RLCK pseudokinase ZED1, which is proposed to act as a decoy (Lewis et al., 2010; Lewis et al., 2013).

In addition to the molecular decoy ZED1, a number of plant proteins have been proposed to be the targets of HopZ1a virulence activity (Zhou et al., 2011; Lee et al., 2012; Jiang et al., 2013).

Zhou et al. (2011) described the interaction of HopZ1 with Glycine max HID1 (GmHID1), an enzyme involved in the biosynthesis of daidzein, a major soybean isoflavone. HopZ1 activity resulted in the degradation of GmHID1, and the suppression of daidzein biosynthesis, which is induced by *P. syringae*. However, the authors failed to find any direct inhibitory effect of daidzein on *P. syringae* growth, therefore the putative role of GmHID1 in PTI was not confirmed, likewise its suppression by HopZ1. It is important to notice that GmHID1 has no putative ortholog in *Arabidopsis*, the plant model were the majority of HopZ1a virulence or avirulence activities have been characterized.

Later on, Lee et al. (2012) described the interaction of HopZ1a with tubulin, using a heterologous *in vivo* screen in human HEK293T cells. In *Arabidopsis*, HopZ1a interacted with tubulin at a higher rate than the unrelated control effector HopF2. HopZ1a expression in *Arabidopsis* seedlings destroyed, with potential consequences on plant basal defense, the microtubule network to a higher extent than expression of the unrelated control effector AvrRpt2, in conditions were both T3Es were triggering ETI to some degree. However, the authors acknowledged that such microtubule destruction might be an indirect effect of HopZ1a acting on a yet unidentified protein, such as a MAPK.

Finally, Jiang et al. (2013) described the interaction of HopZ1a with soybean and *Arabidopsis* JAZ proteins, key negative regulators of jasmonate (JA) signaling. HopZ1a expression induced COI-dependent degradation of JAZ, thus promoting JA-responsive gene expression. The authors hypothesized that, since plant JA signaling is to some

extent antagonistic to SA-dependent plant defense, activation of JA signaling by HopZ1a action might facilitate host defense suppression and pathogenesis.

Remarkably, the aforementioned reports (Zhou et al., 2011; Lee et al., 2012; Jiang et al., 2013) addressed only indirectly, if at all, HopZ1a ability to suppress plant basal defenses in regard to the proposed plant targets, while neither addressed the involvement of HopZ1a in the suppression of ETI or SAR. It is conceivable that HopZ1a interferes with many host proteins, with a number of them yet to be identified behind the unexplained suppression phenotypes. Alternatively, given the broad plant defense suppression abilities of HopZ1a, its host target might be a single key positive regulator of defense, participating in the signaling of different branches of the immune response. Considering the pattern of interference with MKKs displayed by many T3Es of the YopJ / HopZ superfamily leading to defense suppression, the existence of multiple T3Es from plant pathogens interfering with host kinases to suppress immunity, the effect on MAPK activation displayed by HopZ1, and the fact that HopZ1a molecular decoy is indeed a plant kinase, we decided to analyze *Arabidopsis* MKKs as putative targets for HopZ1a.

Arabidopsis genome presents only ten genes encoding MKKs, of which only eight are likely to be expressed (Zhang et al., 2008). Among these, MKK3, MKK4/5, and MKK7 have all been identified as positive regulators of plant defense (Doczi et al., 2007; Zhang et al., 2007a; Xu et al., 2008). Interestingly, while neither MKK3 nor MKK4/5 cascades have been associated to positive signaling of SAR, the suppression of which is a trademark of HopZ1a virulence activity, MKK7 has been proved to be essential for SAR activation, since specific silencing of MKK7 blocks SAR induction and promotes growth of *P. syringae* pv. maculicola and *Xanthomonas campestris* pv. campestris (Zhang et al., 2007b). All things considered,, we decided to investigate MKK7 as a potential target for HopZ1a interference, such a key target that could single-handedly account for all the defense suppression phenotypes described for this effector.

In this work, we demonstrate that MKK7 participates in the signaling of basal defenses restricting DC3000 growth in *Arabidopsis*, validating this model pathosystem for the characterization of MKK7 potential interactors. Our results are the first to show MKK7-dependent accumulation of callose, ROS burst response, and MAPK activation, which eventually restrict the growth of both wild-type DC3000 and the corresponding T3SS null mutant. Furthermore, we demonstrate the participation of MKK7 in the

signaling of the ETI response triggered by AvrRpt2. In regard to HopZ1a interference with MKK7 signaling, we first demonstrate that this effector can suppress the abovementioned MKK7-dependent PTI and ETI defense responses, and continue to prove HopZ1a-MKK7 interaction *in planta*, as well as HopZ1a-dependent acetylation of MKK7 *in vitro*. Finally, we determine that MKK7 acetylation occurs in a conserved lysine residue, which we show to be essential for MKK7 activity *in vitro* and *in planta*, and that such modification reduces MKK7 self-phosphorylation, and abrogates MKK7 trans-phosphorylation activity on a generic susbtrate

Table 1. Plasmids used in this work

Name	Promoter	Expressed protein	Resistance	Reference
pAME30	*nptII*	HopZ1a	Amp, Km	Macho *et al*. (2010a)
pAME27	*nptII*	HopZ1a^{C216A}	Amp, Km	Macho *et al*. (2010a)
pMAM1	*nptII*	HopZ1a^{K289R}	Amp, Km	Rufián et al., (2015)
pAME8	*nptII*	AvrRpt2	Amp, Km	Macho *et al*. (2009)
pAME30Gm	*nptII*	HopZ1a	Amp, Km, Gm	Rufián et al. (2015)
pENTR^{TM}/D-TOPO	-	-	Km	Invitrogen
pENTR-Z1a	-	HopZ1a	Km	This work
pENTR-C2	-	HopZ1a^{C216A}	Km	This work
pENTR-K2	-	HopZ1a^{K289R}	Km	This work
pENTR-GFP	-	GFP	Km	This work
pENTR-MKK7	-	MKK7	Km	This work
pENTR-MKK7^{K167R}	-	MKK7 ^{K167R}	Km	This work
pMD1	*35S*	-	Km	Tai et al., (1999)
pMD-Z1	*35S*	HopZ1a-3xFLAG	Km	Macho *et al*. (2010)
pMD-C2	*35S*	HopZ1a^{C216A}-3xFLAG	Km	This work
pMD-K2	*35S*	HopZ1a^{K289R}-3xFLAG	Km	This work
pMD-GFP	*35S*	GFP-3xFLAG	Km	This work
pMD-MKK7	*35S*	MKK7-HA	Km	This work
pMD-MKK7^{K167R}	*35S*	MKK7 ^{K167R} -HA	Km	This work

pDEST-^{GW}VYNE	*35S*	VENUS-N-term	Km	Gehl et al., (2009)
pDEST-^{GW}VYCE	*35S*	VENUS-C-term	Km	Gehl et al., (2009)
pZ1-VYNE	*35S*	HopZ1a-VENUS-N-term	Km	This work
pC2-VYNE	*35S*	HopZ1a^{C216A}-VENUS-N-term	Km	This work
pK2-VYNE	*35S*	HopZ1a^{K289R}-VENUS-N-term	Km	This work
pMKK7-VYCE	*35S*	MKK7-VENUS-C-term	Km	This work
pET28a(+)	T7	-	Km	Novagen (USA)
pET28-Z1a	T7	HopZ1a	Km	This work (Chapter 3)
pET28-C2	T7	HopZ1a^{C216A}	Km	This work (Chapter 3)
pET28-K2	T7	HopZ1a^{K289R}	Km	This work (Chapter 3)
pGEX-5X-1	tac	GST	Amp	GE Healthcare
pGEX-MKK7	tac	GST-MKK7	Amp	This work
pGEX-MKK7^{K74R}	tac	GST-MKK7^{K74R}	Amp	This work
pGEX-MKK7^{K167R}	tac	GST-MKK7^{K167R}	Amp	This work

Table 2. Primers used in this work

Name	Sequence	Restriction site
pENTR-Z1-F	AAGCGGCCGCCATGGGAAATGTATGCGTCG	NotI
pENTR-Z1-R	AAGGCGCGCCCGCGCTGCTCTTCGGCAAG	AscI
pENTR-MKK7-F	AAGCGGCCGCCATGGCTCTTGTTCGTAAACGC	NotI
pENTR-MKK7-R	AAGGCGCGCCCAAGACTTTCACGGAGAAAAGG	AscI
MKK7-K167R-F	AGAGACATCAGACCTGCGAATC	-
MKK7-K167R-R	TTCGCAGGTCTGATGTCTCTG	-
MKK7 K74R-F	AGATATACGCTCTGAGATCAGTCAACGGCGACATGAGTCC	-
MKK7 K74R-R	GGACTCATGTCGCCGTTGACTGATCTCAGAGCGTATATCT	-
MKK7-F	AAGGATCCCCGCTCTTGTTCGTAAACGCC	BamHI
MKK7-R2	AAGAATTCCTAAAGACTTTCACGGAGAAAAGG	EcoRI

Results

MKK7 participates in the *Arabidopsis* basal defense response to *Pseudomonas syringae*

Recognition of bacterial PAMPs ultimately leads to the restriction of bacterial growth (Zipfel et al., 2004). The role played by MKK7 in plant defense against bacterial pathogens has been previously shown, by monitoring the effect of MKK7 overexpression, or MKK7 silencing, in *Arabidopsis* plants inoculated with *Pseudomonas syringae* pathovar maculicola or *Xanthomonas campestris* pathovar campestris (Zhang et al., 2007b). To confirm that these results were consistent with the interaction model comprising *Pseudomonas syringae* pathovar tomato strain DC3000 (hereafter DC3000) and *Arabidopsis*, a model where HopZ1a characterization has been predominantly accomplished, we set to investigate whether overexpression of MKK7 in *Arabidopsis* limits the growth of this compatible pathogen.

To this purpose, we used transgenic *Arabidopsis* plants expressing the MKK7 gene under the control of the dexamethasone (DEX)-inducible promoter (hereafter MKK7-DEX plants), previously generated by Zhang et al. (2007b). Upon DEX treatment, MKK7-DEX plants display activated Pathogenesis-Related 1 (PR1) gene expression and increased resistance to *P. syringae* pv. maculicola infection (Zhang et al. 2007). It is important to notice that transgenic lines were generated in the wild type Col-0 background (Zhang et al., 2007b), and therefore carry the wild type gene coding for MKK7. We treated MKK7-DEX plants with either 0.1% ethanol (control plants) or DEX (induced plants) 3 hours before inoculation by infiltration with DC3000 at 5 x 10^4 cfu/ml, and measured bacterial growth at 4 days post inoculation (dpi). Bacterial growth in DEX-induced plants was approximately 15-fold lower than that achieved in control plants (Figure 1A) demonstrating that MKK7 expression negatively affects DC3000 growth in *Arabidopsis*.

Furthermore, we analyzed the growth of a DC3000 *ΔhrcV* mutant strain, which is unable to assemble a functional T3SS, triggering PTI, and it is therefore non-pathogenic with *Arabidopsis*, after inoculation into induced on non-induced MKK7-DEX plants. We treated transgenic plants with DEX to induce expression of the corresponding transgenes, 3 hours before inoculation by infiltration with a Δ*hrcV* mutant strain at 5 x 10^5 cfu/ml, and measured bacterial growth at 4 dpi. Bacterial growth of the mutant

strain in DEX-activated plants was approximately 10-fold lower than that achieved in control plants (Figure 1B) suggesting the existence of an MKK7-dependent basal defense against DC3000.

To further characterize the MKK7-dependent basal defense response in *Arabidopsis*, we monitored the accumulation of callose in the cell wall of MKK7-DEX plants, in response to flagellin. In *Arabidopsis*, recognition of this archetypal PAMP by plant receptors eventually leads to the strengthening of the plant cell wall by callose deposition (Gómez-Gómez et al., 1999; Gómez-Gómez and Boller, 2000). To this purpose we infiltrated MKK7-DEX plants, either induced with DEX or non-induced, with the conserved flagellin peptide flg22, and then monitored the average number of callose deposits, as visualized by staining with the fluorescent dye aniline blue (Figure 1C). MKK7-DEX plants induced for MKK7 expression 24h hours before flg22 infiltration presented significantly more foci stained with aniline blue than non-induced plants, which in turn presented more callose deposits than control plants treated with water before flg22 infiltration (Figure 1C).

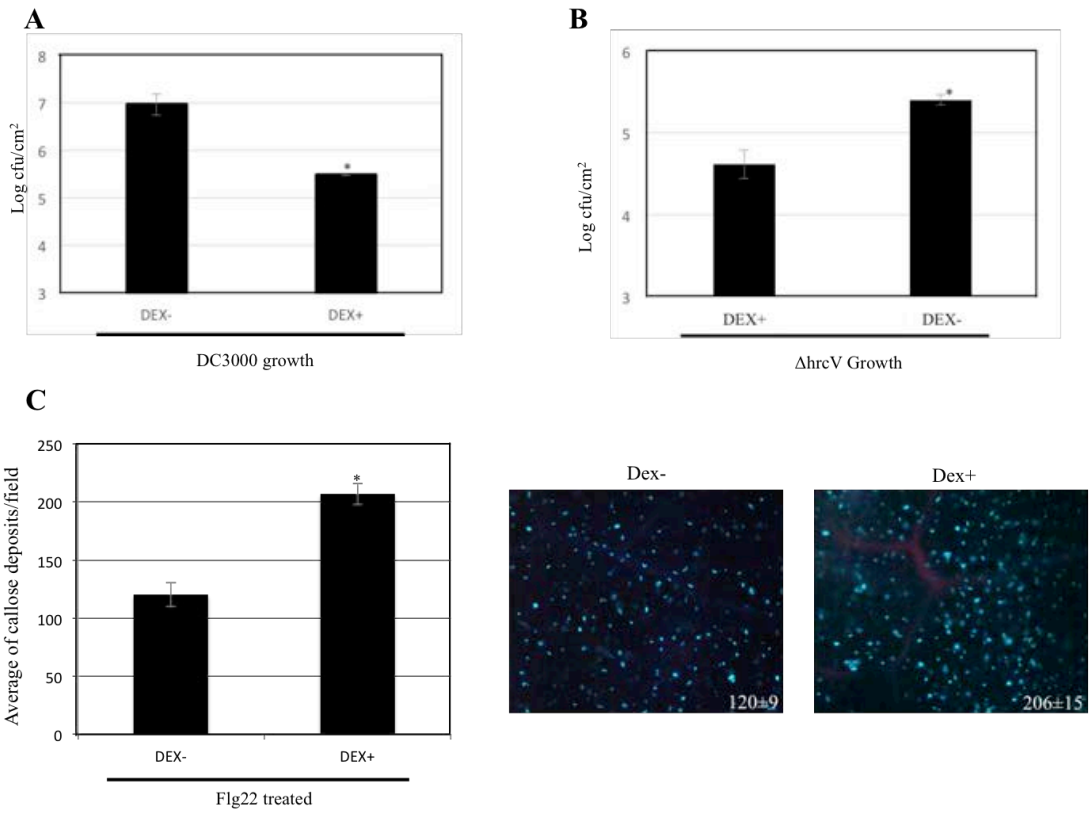

Figure 1. Expression of MKK7 increases disease resistance. (**A**) *P. syringae* pv. tomato DC3000 growth in DEX-MKK7 plants pre-treated with dexamethasone (DEX+) or water (DEX-). Plants were inoculated with a $5x10^4$ cfu/ml bacterial suspension, and bacteria were recovered at 4 dpi. The experiment was repeated 3 times with similar results. (**B**) *P. syringae* pv. tomato Δ*hrcV*. growth in DEX-MKK7 plants induced (DEX+) or uninduced (DEX-). Plants were inoculated with a $5x10^5$ cfu/ml bacterial suspension and bacteria were recovered at 4 dpi. The experiment was repeated twice with similar results. (**C**) Callose deposition in response to flg22-PTI activation. DEX-MKK7 plants were inoculated with dexamethasone (DEX+) or water (DEX-) 24h prior to flg22 treatment. After 15 hours, leaves were stained with aniline blue and observed under UV fluorescence microscope. Left panel show mean quantification of callose deposits in 24 photos. Right panel show representative images. Error bars represent standard error, and asterisks indicate significant differences from the untreated plants, as established by Student's test ($P<0.05$)

Taken together, results shown in Figure 1 demonstrate the existence of MKK7-dependent basal defenses that can affect DC3000 growth in *Arabidopsis*, and validate the use of this model pathosystem for the characterization of MKK7 potential interactors.

MKK7 participates in *Arabidopsis* ROS burst signaling and activates MAP kinase modules

One of the early events occurring during PTI activation is the production of Reactive Oxygen Species (ROS) (Felix et al., 1999). In *Arabidopsis*, transgenic expression of HopZ1a has been described to actively block the production of ROS, in a manner dependent on the integrity of HopZ1a catalytic site (Lewis et al., 2014). To determine if MKK7 participates in the signaling pathway leading to the production of ROS in response to flagellin, we performed a plate-based assay using flg22 peptide to induce PTI in leaf discs obtained from MKK7-DEX transgenic plants, measuring ROS production by luminol-dependent chemiluminiscence (Figure 2A). Overexpression of MKK7 in induced MKK7-DEX plants triggered a stronger ROS burst than that triggered in non-induced MKK7-DEX plants (Figure 2A). Results shown in Figure 2A indicate that MKK7 takes part in the signaling events leading to ROS production in response to flg22 treatment.

Plant receptor recognition of bacterial PAMPs can also lead to the activation of MAPK signaling cascades (Pitzschke et al., 2009; Macho and Zipfel, 2015)**.** Transgenic expression of HopZ1a in *Arabidopsis* has been described to suppress the MAP kinase activation triggered upon flg22 treatment, as indicated by the suppression of MPK3 and MPK6 phosphorylation (Lewis et al., 2014). To determine if MKK7 participates in the signaling pathway leading to the activation of MAP kinase cascades, we induced 2-

weeks old MKK7-DEX plants 24 hours prior to flg22 treatment. After treatment, we recovered samples at 0, 5, 10, and 15 minutes, and analyzed MPK activation by western blot. As shown in figure 2B, overexpression of MKK7 triggers a faster activation of MPK3, MPK6 and MPK4/11 in response to flg22.

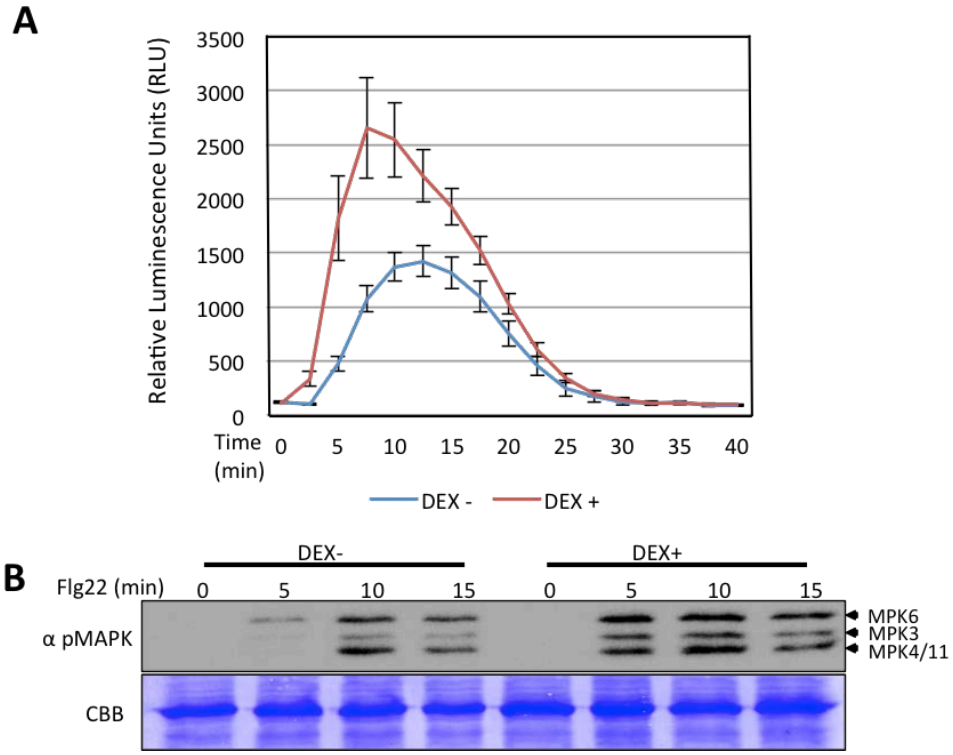

Figure 2. Overexpression of MKK7 enhances PTI response. (**A**) Reactive Oxygen Species (ROS) burst triggered by flg22. 3 weeks-old leaves discs were incubated with dexamethasone (DEX+) or water (DEX-) 24h prior to flg22 treatment. Immediately after flg22 treatment, luminescence was measured. Error bars represent standard error from 24 leaf discs per treatment. (**B**) MPKs activation in response to flg22 treatment. 2 weeks-old plants were overnight incubated with dexamethasone (DEX+) or water (DEX-). This solution was removed to apply flg22 treatment. 3 whole plants were frozen in liquid nitrogen at the indicated time point. Western blot analysis was carried out to detect activated MPKs. Coomassie blue staining is shown as loading control.

MKK7 participates in the ETI defense response triggered in *Arabidopsis* by heterologous expression of AvrRpt2

Expression of MKK7 is induced in *Arabidopsis* by inoculation of DC3000 expressing the heterologous effector AvrRpt2 (Zhang et al., 2007b). Expression of AvrRpt2 from DC3000 triggers the ETI defense response in *Arabidopsis* plants expressing the resistance protein RPS2, which in turn results in the growth attenuation of the DC3000 strain harboring the effector. Since the results of Zhang and collaborators (2007) suggested a role of MKK7 in ETI signaling, we set out to

investigate whether silencing of MKK7 would interfere with AvrRpt2-induced ETI in *Arabidopsis*, by measuring the effect of such silencing on the growth attenuation displayed by DC3000 expressing AvrRpt2. Since previous efforts to identify an MKK7 knockout mutant have been unsuccessful (Zhang et al. 2007) we used MKK7 antisense lines (hereafter, asMKK7 plants), expressing an antisense MKK7 transgene under the control of a 35S promoter, generated in the wild-type background by Dai et al. (2006). We performed competitive index (CI) assays by co-inoculating DC3000 and DC3000 expressing AvrRpt2, in both Col-0 and asMKK7 *Arabidopsis* plants (Figure 3). As previously described (Macho et al., 2007) in Col-0 plants, we detected clear growth attenuation for DC3000 expressing AvrRpt2 in comparison with co-inoculated DC3000 (CI=0,06±0,02). Interestingly, when the same CIs where performed in the asMKK7 background, DC3000 bacteria expressing AvrRpt2 displayed a considerably lower growth attenuation, multiplying to almost the same levels as the co-inoculated DC3000 strain (CI=0,58±0,10). The growth attenuation of DC3000 expressing HopZ1a in Col-0 (CI=0,02±0,007) was not altered on the asMKK7 background (CI=0,05±0,004) (Figure 3), indicating that MKK7 is essential for RPS2-triggered immunity, which is SA-dependent, but not for SA-independent ZAR1-mediated immunity

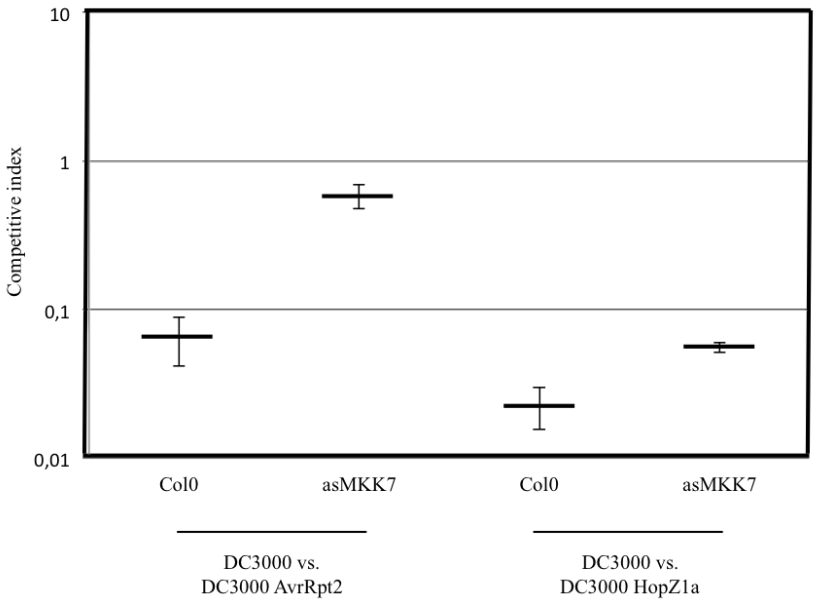

Figure 3. MKK7 is required for AvrRpt2-mediated ETI. Competitive indices (CI) resulting from mixed infections of DC3000 with derivatives expressing the effectors AvrRpt2 (left) or HopZ1a (right) in Arabidopsis Col-0 or asMKK7 plants. Index values shown correspond to the mean of three samples and error bars represent the standard error. Experiment was repeated three times with similar results.

HopZ1a suppresses MKK7-dependent defense signaling

Taken together, results presented previously validate MKK7 as a potential target for the virulence function of HopZ1a within the plant, since suppression of MKK7-dependent defense responses will account for all described HopZ1a-associated virulence phenotypes in the *Arabidopsis*-DC3000 pathosystem, *i.e.* suppression of plant defenses associated to PTI (Figures 1 and 2), ETI (Figure 3) and SAR (Zhang et al., 2007b). Therefore, we set out to analyze whether HopZ1a expression interfered specifically with MKK7-dependent defense signaling in *Arabidopsis*.

First, we analyzed whether HopZ1a was able to suppress MKK7-dependent PR1 accumulation (Figure 4A). Overexpression of MKK7 in the de-regulated *Arabidopsis* mutant *bud1* (Dai et al., 2006) has been shown to result in constitutive expression of the molecular marker genes for plant defense responses PR1, PR2, and PR5 (Zhang et al., 2007b). Furthermore, overexpression of MKK7 in induced MKK7-DEX plants has been described to induce PR1 gene expression (Liu et al., 2007). We induced MKK7 expression in MKK7-DEX plants by DEX treatment, 3 hours before inoculation by infiltration with *Pseudomonas fluorescens* strain Pf55 (hereafter Pf55), a non-pathogenic strain expressing a functional T3SS but only those effector genes purposely cloned and expressed from a plasmid, in this case the HopZ1a effector gene. We then monitored PR1 protein levels by Western blot in plant extracts taken at the inoculation site, 48 hours after bacterial inoculation (Figure 4A). As controls we included mock inoculated plants, and plants inoculated with a Pf55 strain not expressing the HopZ1a gene (Figure 4A). As expected, both control plants displayed local PR1 accumulation in the inoculated tissues as a consequence of transgenic MKK7 expression. PR1 accumulation was higher in Pf55-inoculated than in mock-inoculated plants, since in the former PR1 expression is also induced as a consequence of the mild basal defense triggered by the Pf55 strain. Local PR1 accumulation was almost completely abolished in plants inoculated with Pf55 expressing the HopZ1a effector protein, indicating that HopZ1a is capable of suppressing PR1 accumulation due to Pf55 defense elicitation, and more importantly, capable of suppressesing MKK7-dependent PR1 accumulation.

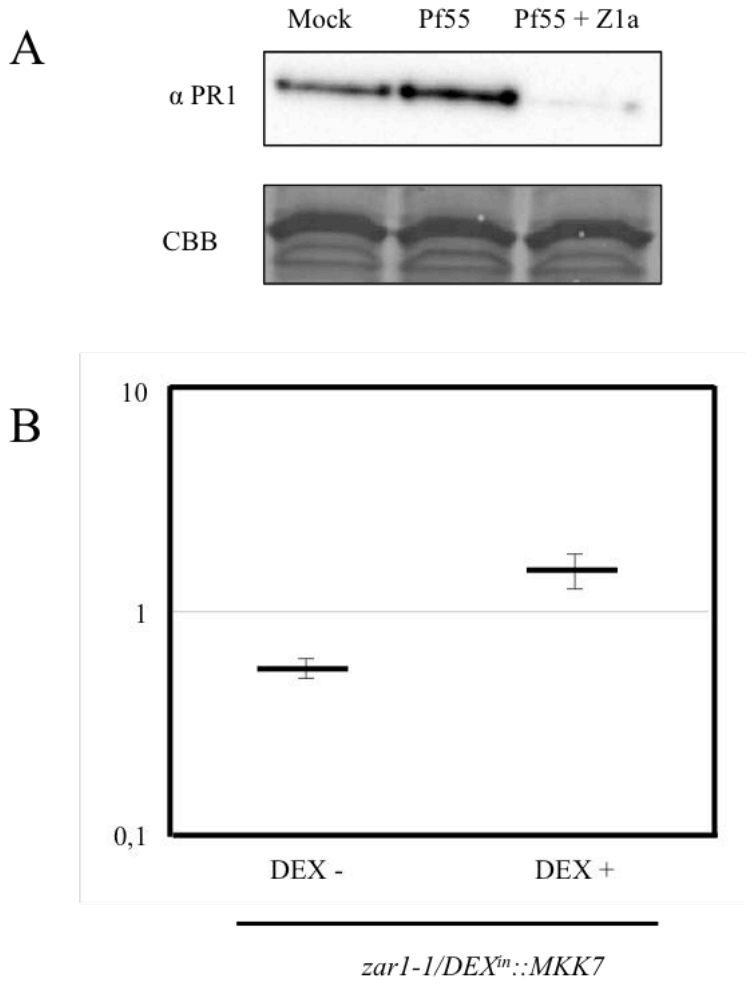

Figure 4. HopZ1a interferes in the MKK7 defense activation pathway. (**A**) Western blot showing PR-1 accumulation in DEX-MKK7 plants induced with dexamethasone. 3 hours after DEX treatment, plants were infiltrated with 10 mM $MgCl_2$ (Mock), or a $5x10^5$ cfu/ml bacterial suspension of Pf55 or Pf55 expressing HopZ1a. Samples were recovered at 48 hours. Ten micrograms of total protein were loaded per sample, and Coomassie staining is shown as loading control. Results presented are representative of two independent experiments. (**B**) Competitive indices (CI) resulting from mixed infections of DC3000 with DC3000 expressing the effector HopZ1a in *zar1-1/*DEX-MKK7 plants induced (DEX+) or un-induced (DEX-) with dexamethasone. Index values shown correspond to the mean of three samples and error bars represent the standard error. Experiment was repeated three times with similar results.

To investigate whether HopZ1a suppression of MKK7-dependent PR1 accumulation correlates with higher bacterial growth, we analyzed whether HopZ1a expression from DC3000 was able to abrogate the growth attenuation suffered by this strain in induced MKK7-DEX plants, as a consequence of MKK7 overexpression (Figure 4B). To analyze HopZ1a suppression ability in the absence of the ETI triggered by HopZ1a in *Arabidopsis* Col-0, we crossed DEX-MKK7 transgenic plants with *zar1-1* knockout plants, lacking the resistance gene *ZAR1* that is responsible of the HopZ1a-triggered immunity, and selected *zar1-1* / DEX-MKK7 homozygous lines. We used

these plants, either DEX-induced for MKK7 overexpression or non-induced, to perform CI analysis comparing the growth of DC3000 *versus* a co-inoculated DC3000 strain expressing HopZ1a (Figure 4B). As expected (Jiang et al., 2013; Rufian et al., 2015), in non-induced *zar1-1* plants growth of DC3000 expressing HopZ1a presents only a slight growth reduction compared with the co-inoculated DC3000 strain (CI=0,55±0,05). In contrast, in DEX-induced *zar1-1* plants overexpressing MKK7, DC3000 expressing HopZ1a displays a growth advantage *versus* DC3000 (CI=1,52±0,27), suggesting that HopZ1a can in fact suppress MKK7-dependent defense responses.

HopZ1a interacts with MKK7 *in vitro* and *in planta*

Data presented in Figure 4 demonstrates that HopZ1a suppresses MKK7-dependent defense signaling in *Arabidopsis*. To investigate whether such HopZ1a defense suppression ability is a consequence of its direct interference with MKK7 function, or rather an indirect effect due to its interaction with another component of the same signaling pathway, we analyzed *in planta* HopZ1a-MKK7 interaction using co-immunoprecipitation and BiFC assays.

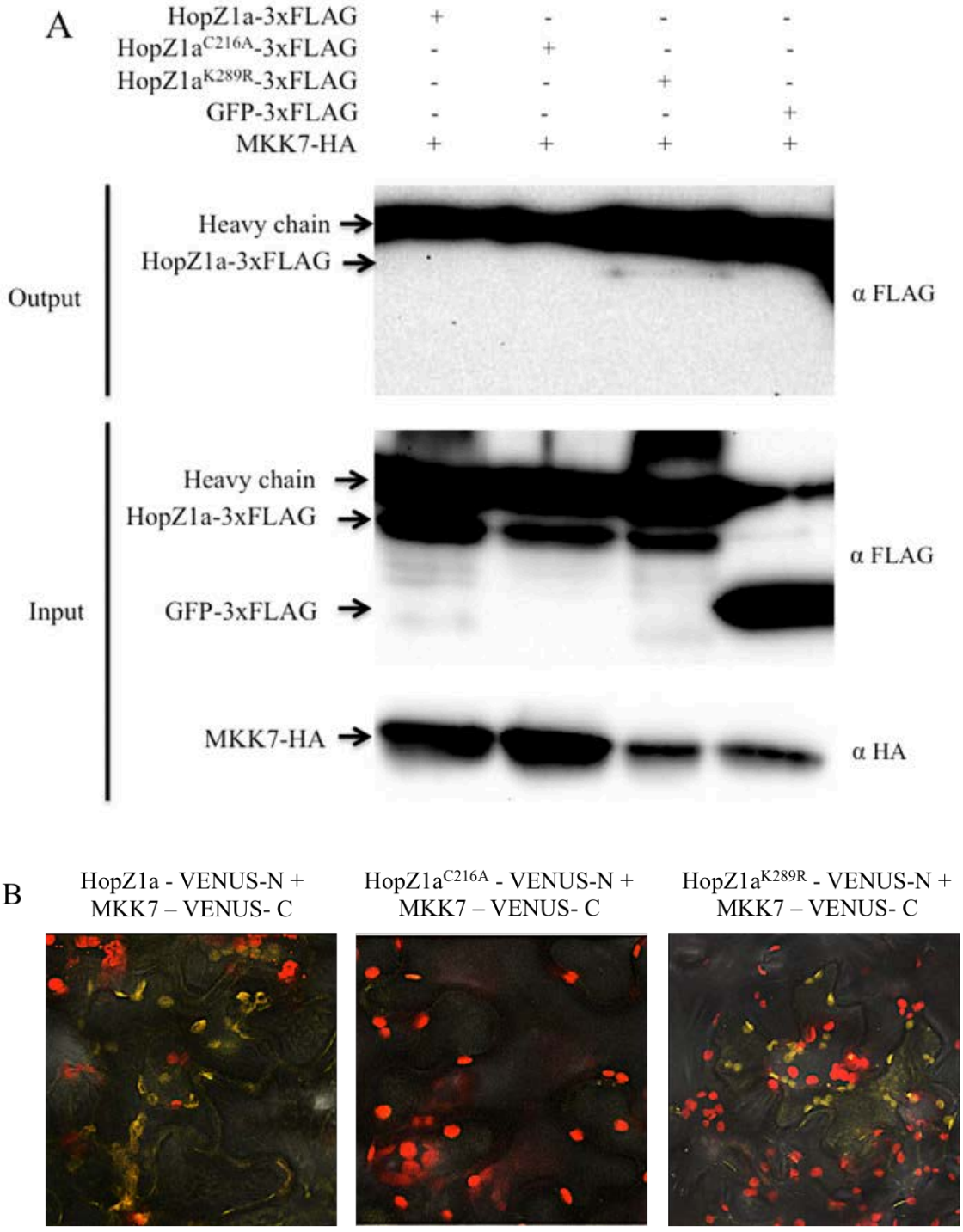

Figure 5. HopZ1a interacts with MKK7 *in planta*. (**A**) Coimmunoprecipitation assay using anti HA beads of MKK7-HA with HopZ1a and derivatives. *N. benthamiana* plants were agroinfiltrated with mixed inoculum containing the strains encoding MKK7-HA and each one of the 3xFLAG fusions. Protein extraction and immunoprecipitation was performed at 30 hours post inoculation. The output panel show the signal of the 3xFLAG fusion proteins in the elutions. The input panels show immunoblots of 10 ul of total proteins using anti FLAG or anti HA antibodies. (**B**) Bimolecular fluorocomplementation (BiFC) assay. The N-terminal of the fluorescent protein VENUS was fused to the C-terminal of HopZ1a, and the C-terminal of VENUS to the C-terminal of MKK7. Proteins were transiently expressed in *N. benthamiana* using Agrobacterium. Leaf sections were analyzed under the confocal 20 hours after inoculation.

For co-immunoprecipitation assays, we cloned MKK7 and HopZ1a in binary vectors in order to express C-terminal fusion proteins with either HA-tag or 3xFLAG-tag, respectively (Table 1). Since catalytically inactive enzymes have been sometimes found to exhibit stabilized interactions with substrates (Blanchetot et al., 2005), we also generated the corresponding plasmids to express the canonical HopZ1a catalytic mutant (HopZ1a^{C216A}-3xFLAG), and the leaky mutant in lysine K289 (HopZ1a^{K289R}-3xFLAG), which might be affected in the transacetylation of the target protein (Ma et al., 2015). Further, HopZ1a^{C216A} does not trigger HR when transiently expressed *in planta* (Jiang et al., 2013; Lewis et al., 2013) which might improve protein recovery.

We co-expressed MKK7-HA with, either HopZ1a-3xFLAG or each of its mutant derivatives HopZ1a^{C216A}-3xFLAG and HopZ1a^{K289R}-3xFLAG, in *N. benthamiana* leaves, under the control of a constitutive promoter, by using *Agrobacterium*-mediated transient expression. As a negative control, we used GFP-3xFLAG. We recovered the *Agrobacterium* infiltrated tissue at 24-30 hours after *Agrobacterium* inoculation, since transient expression of either MKK7 or HopZ1a, cause cell death in *N. benthamiana* at later time points (Ma et al., 2006; Lewis et al., 2008; Popescu et al., 2009). We then performed co-immunoprecipitation with protein extracts obtained from the recovered tissues using anti-HA beads, and the corresponding eluates were separated by SDS-PAGE and analyzed by western blot using anti-FLAG antibodies. We could not detect interaction of MKK7-HA with either HopZ1a-3xFLAG or the catalytic mutant HopZ1a^{C216A}-3xFLAG. Interestingly, we did detect a hybridization signal indicative of interaction between MKK7-HA and HopZ1a^{K289R}-3xFLAG (Figure 5A), demonstrating that both proteins are indeed interacting partners *in planta*.

To confirm the detected interaction, we performed a bimolecular complementation assay (BiFC). To this purpose, we generated binary plasmids expressing MKK7, HopZ1a, or the corresponding HopZ1a mutant derivatives, as fusions to either the N-terminal or the C-terminal domains of the fluorescent protein VENUS (Table 1). We expressed MKK7 as a fusion protein to the C-terminal domain of VENUS, and expressed HopZ1a and its mutant derivatives as fusion proteins to the N-terminal domain of VENUS. We then co-expressed MKK7-VENUS-C with each of the HopZ1a-VENUS-N fusion proteins in *N. benthamiana* by using *Agrobacterium*-mediated transient expression, and analyzed by microscopy the samples at 18-20 hours, a time point prior to the development of HR symptoms at the microscopic level. In this

assay, we detected fluorescence in those samples corresponding to the co-expression of MKK7-VENUS-C with either HopZ1a-VENUS-N or HopZ1a^{K289R}-VENUS-N (Figure 5B). Interestingly, fluorescence was not detectable in the sample corresponding to MKK7-VENUS-C co-expression with HopZ1a^{C216A}-VENUS-N (Figure 5B).

Taken together, our co-immunoprecipitation and BIFC results show that HopZ1a and MKK7 do interact *in planta*, and suggest that such interaction is transient, and may be locked-on in the HopZ1a^{K289R} mutant, but not in the catalytic mutant.

HopZ1a acetylates MKK7 *in vitro* on residue K167

HopZ1a has been described to function as an acetyltransferase *in vitro*, capable of strong autoacetylation, and also of transacetylation of tubulin and the *Arabidopsis* pseudokinase ZED1 (Lee et al., 2012; Lewis et al., 2013). To determine whether HopZ1a was able to acetylate MKK7, we performed a ^{14}C-labelled-acetyl-coenzyme A (acetyl-CoA) transferase reaction *in vitro*, in the presence of MKK7 and either HopZ1a, the catalytically inactive mutant HopZ1a^{C216A}, or mutant HopZ1a^{K289R}. As previously described, HopZ1a was strongly autoacetylated, while mutant HopZ1a^{C216A} was not (Figure 6). HopZ1a^{K289R} was acetylated to a similar level of the wild type version of the effector, in agreement with a recent report (Ma et al., 2015). Interestingly, MKK7 was acetylated in the presence of HopZ1a, but not in the presence of HopZ1a^{C216A} or HopZ1a^{K289R} (Figure 6), demonstrating that HopZ1a acetylates MKK7 *in vitro*.

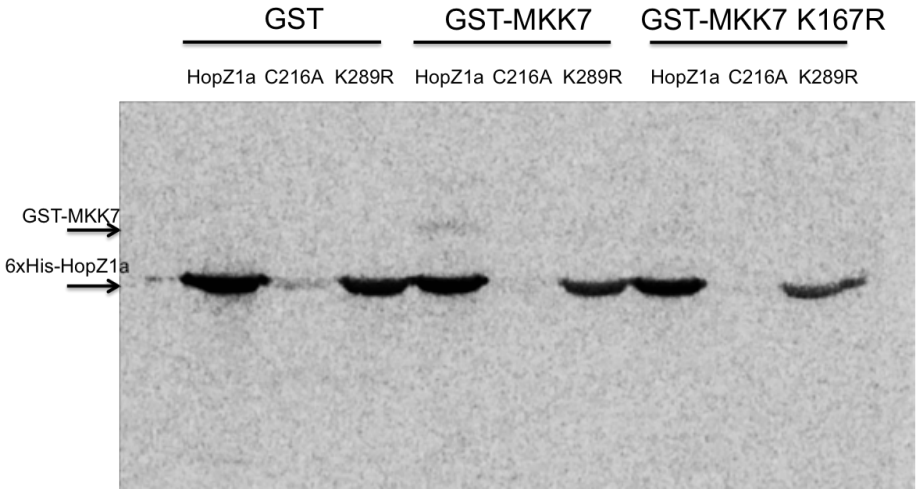

Figure 6. HopZ1a *in vitro* acetylates MKK7 in the lysine 167. Recombinant GST-MKK7, GST-MKK7^{K167R} or GST were incubated with 6xHis-HopZ1a, 6xHis-HopZ1a^{C216A} or 6xHis-HopZ1a^{K289R} in acetylation buffer containing ^{14}C-Acetyl CoA. Samples were separated in a SDS-PAGE and proteins were transferred to a PVDF membrane. The membrane was exposed to an imaging plate for one week.

We then set to determine which MKK7 residues were acetylated by HopZ1a, and to that purpose we examined the evidence available regarding HopZ1a acetylation of pseudokinase ZED1. HopZ1a acetylates the *Arabidopsis* pseudokinase ZED1 on threonine residues located in positions 125 and 177 of its amino acid sequence (Lewis et al., 2013). However, ZED1 pseudokinase is not considered a proper target of HopZ1a virulence activity, but rather believed to function as a decoy to trigger ZAR1-dependent ETI responses (Lewis et al., 2013). In fact, ZED1 is a non-functional kinase, since it lacks a critical proton accepting aspartate within its catalytic loop, a domain that also includes HopZ1a-acetylated threonine 177. Since decoys are expected to mimic the proteins targeted by pathogen effectors, we reasoned that HopZ1a acetylation on its *bona fide* target kinase was likely to happen on residues situated within the catalytic loop. MKK7 lacks threonine residues in this domain, but presents a lysine residue (K167).

We introduced a point mutation on MKK7 substituting the residue K167 with arginine, generating the mutant MKK7^{K167R}, and used it as substrate for HopZ1a acetylation *in vitro* (Figure 6). The MKK7^{K167R} mutant derivative was not acetylated (Figure 6). These results suggest that K167 is the only, or at least the main, MKK7 residue subject to HopZ1a acetylation.

Lysine residue K167 is essential for MKK7 activity *in vitro* and *in planta*

It has been previously shown that MKK7-dependent activation of the plant defense response requires MKK7 kinase activity (Zhang et al., 2007b). Recombinant MKK7 expressed in *E. coli* displays *in vitro* auto-phosphorylation activity, which is absent in the MKK7^{K74R} mutant version of the protein, in which a lysine in the ATP binding site was changed to an arginine (Dai et al., 2006). To determine whether the K167 residue is necessary for MKK7 kinase activity, we carried out *in vitro* GST-MKK7, GST-MKK7^{K74R}, and GST-MKK7^{K167R} autophosphorilation and *trans* phosphorylation assays using the generic substrate MBP (Myelin Basic Protein), (Figure 7A). Autophosphorylation of GST-MKK7 is abolished on the GST-MKK7^{K74R} mutant, as expected. Interestingly, the K167R mutation reduces autophosphorylation of MKK7 by an 82%, and completely abolished its *trans* phosphorylation activity on MBP (Figure 7A)

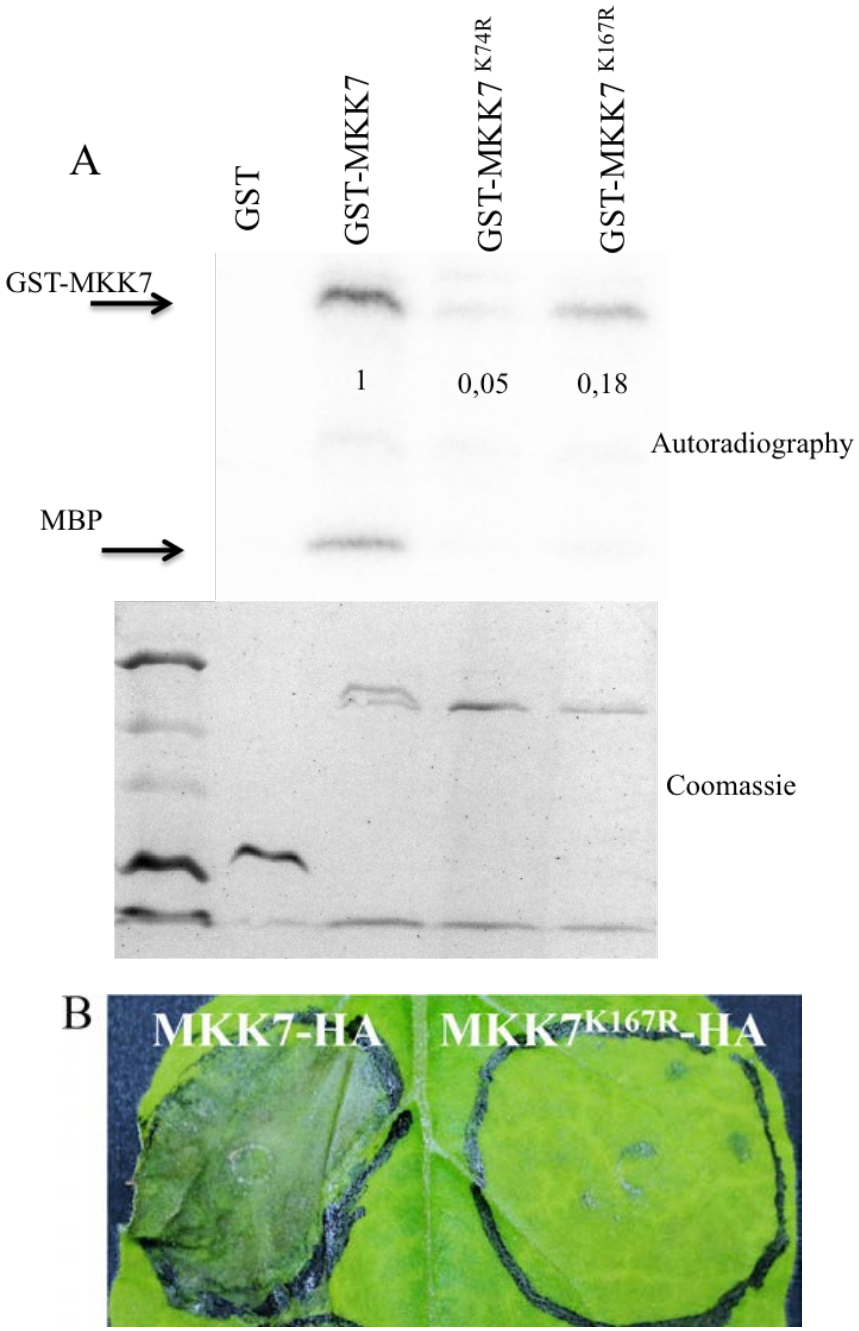

Figure 7. Lysine 167 is important for MKK7 activity. (**A**) Recombinant GST-MKK7, GST-MKK7^{K74R}, GST-MKK7^{K167}, or GST were incubated in kinase buffer containing ^{32}P-γ-ATP. Samples were separated in a SDS-PAGE and proteins were transferred to a PVDF membrane. The membrane was exposed to an imaging plate for one day. Coomassie staining is shown as loading control. (**B**) Agrobacterium transient expression in N. benthamiana of MKK7-HA and MKK7^{K167R}-HA. Pictures were taken two days post inoculation.

To confirm that residue K167 is also essential for MKK7 activity *in planta*, we expressed MKK7-HA and its mutant derivative MKK7^{K167R}-HA in *N. benthamiana* leaves, under the control of a constitutive promoter, by using *Agrobacterium*-mediated transient expression, and monitored cell death symptoms 40 hours after *Agrobacterium*

inoculation (Figure 7B). Transient overexpression of MKK7 resulted in the manifestation of macroscopic cell death in *N. benthamiana* tissues (Figure 7B), most likely as a result of its unregulated activation of the defense responses, as previously suggested by the failure to generate *Arabidopsis* transgenic plants expressing this kinase from a 35S promoter (Dai et al., 2006; Zhang et al., 2007b). Interestingly, MKK7^{K167R} expression did not elicited macroscopic HR (Figure 7B). These results indicate that the K167 residue, targeted for acetylation by HopZ1a, is essential for MKK7 activity *in planta*.

Acetylation of K167 by HopZ1a interferes with MKK7 kinase activity

Since we have demonstrated that HopZ1a acetylates MKK7 in a lysine residue that is essential for MKK7 kinase activity *in vitro*, and for HR induction *in planta*, we set out to analyze whether such acetylation indeed affected MKK7 function.. To this purpose, we performed an *in vitro* acetylation assay using HopZ1a as the means for MKK7 acetylation, followed by a kinase assay on the HopZ1a-modified MKK7 resulting from the previous experiment. We first incubated GST-MKK7 or GST-MKK7^{K167R} with either 6xHis-HopZ1a or 6xHis-HopZ1a^{C216A} in an acetylation buffer containing non-radioactive acetyl-CoA as acetyl group donor. After this incubation, we added the components needed for kinase reaction, including the artificial substrate MBP and ^{32}P-ATP to provide the necessary radioactive signal. The corresponding protein samples were separated by SDS-PAGE and transferred to a PVDF membrane, which was exposed to detect the autoradiographic signal. Data presented in Figure 8 indicates that the levels of phosphorylated MKK7 are reduced in those samples pre-treated with HopZ1a, when compared to those observed when MKK7 was pre-treated with the catalytic mutant HopZ1a^{C216A} (Figure 8). This suggests that acetylation of MKK7 by HopZ1a, which is dependent on the integrity of HopZ1a catalytic site, impairs to some degree the ability of the kinase to autophosphorylate. Furthermore, since the levels of phosphorylated MKK7^{K167R} remain unaffected, the inhibitory effect of HopZ1a seems to pivot on the modification of this particular MKK7 residue. More importantly, MKK7 trans-phosphorylation activity on MBP is completely abolished in those samples pre-treated with HopZ1a, but remains unaffected in those samples pre-treated with the catalytic mutant HopZ1a^{C216A}, suggesting that acetylation of MKK7 by HopZ1a, which is dependent on the integrity of HopZ1a catalytic site, completely abrogates the ability

of the kinase to phosphorylate proteins in trans, and therefore is likely to block MKK7-dependent signal transduction.

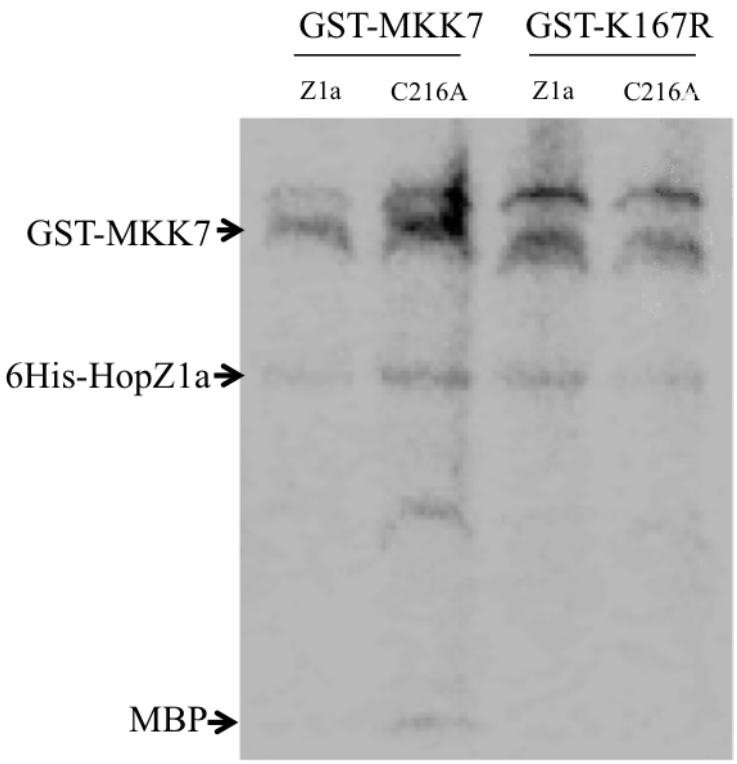

Figure 7. Acetylation of MKK7 by HopZ1a interferes with kinase activity. Recombinant GST-MKK7, or GST-MKK7^{K167}, were incubated in acetylation buffer with either HopZ1a or HopZ1aC216. After 1 hour, components of kinase buffer were added, including ^{32}P-γ-ATP. Samples were separated in a SDS-PAGE and proteins were transferred to a PVDF membrane. The membrane was exposed to an imaging plate for one day.

Discussion

MKK7 is a key regulator of plant immunity

The analysis of MKK7 interaction with HopZ1a, and the consequences of its modification by this effector, has allowed us to uncover a number of novel features to what seems to be an important regulator of plant defense. This work illustrates the application of bacterial effectors as tools to analyze the molecular mechanisms of their eukaryotic hosts.

Mitogen-activated protein kinase (MAPK) cascades play a central role on the activation of plant immunity pathways. In general, pathogen perception initiates the signaling by the activation of MAP kinase kinase kinases (MEKKs), which activate downstream MAP kinase kinases (MKKs) by phosphorylation of specific serine and threonine residues. In turn, MKKs phosphorylate MAP kinases (MPKs) in specific threonine and tyrosine residues, changing their localization and/or activating downstream substrates, including transcription factors, to activate the expression of defense genes (Mundy et al., 2012; Meng et al., 2013).

MKKs containing the consensus sequence S/TXDXXXS/T are autoactive and do not require upstream phosphorylation from MKKKs. MKK7 possesses tandem copies of this consensus sequence, with the second one being canonical. We demonstrate here that MKK7 is indeed autoactive, since purified MKK7 autophosphorylates *in vitro* in addition to *trans* phosphorylating the generic substrate MBP (Figure 7A), indicating that upstream phosphorylation by an MKKK is not required for MKK7 kinase activity. An exhaustive analysis of MKK7 phosphorylated residues by mass spectrometry will be required to determine which of the two predicted consensus sequences is functional in MKK7. In spite of its ability to autophosphorylate *in vitro*, our results show that overexpression of MKK7 is not enough to trigger PTI-related events in *Arabidopsis*, since transgenic plants expressing MKK7 after induction with dexamethasone do not accumulate callose deposits, nor activate downstream MPKs, in the absence of flg22-induction (Figures 1 and 2). These results suggest that MKK7 is not active by default, but requires PAMP perception to activate defenses. In this regard, a number of works have shown negative regulation of plant defense responses by protein phosphatase type 2C (PP2C), including the regulation of MAPK activity by dephosphorylation (Lee and

Ellis, 2007; Schweighofer et al., 2007; Anderson et al., 2011). Therefore it is conceivable that specific protein phosphatases may dephosphorylate MKK7 in the absence of PAMP perception, thus releasing MKK7 autoactivation and downstream signaling, and maintaining plant defenses down. Supporting this notion, transient overexpression of MKK7 in *N. benthamiana* induces a strong cell death phenotype, most likely associated to the unregulated activation of the defense responses (**Figure 7**). We can envision a situation in which resident protein phosphatases, unable to cope with the excess of MKK7 resulting from ectopic expression, cannot repress MKK7 autoactivation and downstream signaling. Interestingly, a number of *Arabidopsis* protein phosphatases, some of them described to have regulatory roles, are associated to MKK7 in the interaction database STRING (Jensen et al., 2009), all of them potential candidates to participate in the proposed negative regulation of MKK7 activity. Furthermore, there are a number of conserved residues in MKK7, apart from those serine and threonines included in the activation loop, which are potential targets of regulation by dephosphorylation. All these data opens a potential new line of research regarding MKK7 and plant defense signaling that should be continued.

Our results also show that overexpression of MKK7 enhances the ROS burst, but also MPK3/6 and 4/11 activation, and callose deposition (Figures 1 and 2). Interestingly two independent pathways upon PAMP perception have been described to regulate ROS burst and MPK activation (Ranf et al., 2011; Segonzac and Zipfel, 2011; Xu et al., 2013). Therefore, data presented here suggest that MKK7 might be part of a regulatory hub linking these independent basal defense pathways, in yet another novel feature of this MKK.

Flg22 perception induces phosphorylation of the RLCK BIK1, which becomes active and in turn phosphorylates the NADPH Oxidase RbohD to induce the ROS burst (Kadota et al., 2014; Li et al., 2014). Later on, other kinases such as the calcium-dependent kinase CPK5 further phosphorylate RbohD, amplifying the ROS burst in subsequent waves. RbohD regulates callose deposition, since *Arabidopsis rbohD* mutant plants exhibit decreased callose deposits after flg22 treatment compared with wild type plants (Zhang et al., 2007a). Interestingly, RbohD and ROS burst have been shown to be essential for systemic acquired resistance (SAR) (El-Shetehy et al., 2015), a defense mechanism that is also signaled by MKK7, in one of its most characteristic phenotypes (Zhang et al., 2007b). Since our results indicate that MKK7 participates in

the positive regulation of the ROS burst, we propose that such regulation could be achieved by direct or indirect phosphorylation of NADPH oxidases, therefore triggering the SAR response. Such molecular mechanism might be the one behind MKK7 role in SAR signaling (Liu et al., 2007). The putative phosphorylation of RbohD and/or related proteins by MKK7 should be further investigated.

In regards to MPK activation, two different MAPK modules activate MPKs in response to pathogen perception. The MEKK1 activates MKK1/2, which in turn phosphorylate MPK4, inducing expression of antimicrobial compounds and SA accumulation. The second module is comprised by MKK4/5, which activates MPK3 and MPK6, leading to the expression of several defense genes and ethylene induction (Meng and Zhang, 2013). In this work, we demonstrate that MKK7 overexpression produces a faster activation of both MAPK modules, resulting in faster activation of MPK3, MPK6 and MPK4. This role of MKK7 is remarkable, and somehow unexpected, since it has been suggested that the induction of ROS burst, as described above, and MAPK activation are independent signaling pathways (Ranf et al., 2011; Segonzac and Zipfel, 2011; Xu et al., 2013). However, protein microarray data have previously showed that MKK7 potentially activates six MPKs, including MPK3, MPK6 and MPK4 (Popescu et al., 2009). With our current data we cannot elucidate whether MKK7 activates these MPKs directly or indirectly, although the low intracellular levels of MKK7 (Zhang et al., 2007b), and its relative simplicity, makes us favor the latter.

We also demonstrate in this work a role for MKK7 in the signaling of AvrRpt2-dependent ETI (Figure 3). To date, such role has only been suggested by the induction of MKK7 expression as a result of expression of AvrRpt2 from infecting bacteria (Liu et al., 2007). In this sense, it is important to notice that the signaling pathway for AvrRpt2-triggered immunity, which is mediated by the NLR protein RPS2, is salicylic acid (SA)-dependent (Nawrath and Metraux, 1999), and that overexpression of MKK7 induces SA accumulation (Zhang et al., 2007b), indicating a role of MKK7 on activation of SA-dependent pathways. It is also relevant that MKK7 does not participate in HopZ1a-triggered ETI, mediated by ZAR1 and SA-independent (Figure 3).

HopZ1a targets MKK7

On the last years, a number of studies have shown that bacterial effectors can have multiple targets. An archetypal example of one such effector is the *P. syringae* effector HopF2. HopF2 ADP-ribosylates MKK5 to suppress PTI activation (Wang et al., 2010), while simultaneously acting upsteam of MKKs through its interaction with RLCK PBL1 and PRR co-receptor BAK1 (Zhou et al., 2014). Furthermore, HopF2 also inhibits AvrRpt2-triggered ETI by interacting with RIN4 (Wilton et al., 2010). Thus, the T3E HopF2 illustrates the fact that a single T3E can exert a single biochemical activity (kinase inhibition) on multiple host target proteins (MKK5, RIN4 and BAK1), thus interfering with different branches of defense signaling. HopF2 plant defense suppression abilities nicely shadow some of those described for HopZ1a, *i.e* interfering with PTI, a phenotype common to many T3Es, but also suppressing ETI, an interference not as often described for T3Es.

HopZ1a is also an example of T3E with multiple targets reported to date. HopZ1a interacts with, and weakly acetylates, tubulin inducing microtubule disruption (Lee et al., 2012). However, considering the weak acetylation of tubulin achieved by HopZ1a *in vitro*, the authors suggested the existence of an indirect mechanism for HopZ1a-mediated microtubule disruption, such as interaction with MKKs. In any case, chemical disruption by the microtubule inhibitor oryzalin slightly increases DC3000 growth but has no effect on the growth of a T3SS deficient mutant (Δ*hrcC*), indicating that microtubule disruption does not affect PTI (Lee et al., 2012). Another reported target for HopZ1a are the JAZ transcriptional repressors (Jiang et al., 2013). HopZ1a acetylates *Arabidopsis* JAZ6, directly or indirectly promoting its COI-dependent degradation, thus inducing the expression of JA and complementing the virulence function of DC3000 JA-mimic coronatine (Jiang et al., 2013). The inhibition of JAZ proteins proposed, while suggesting a mechanistic explanation for previously described HopZ1a triggered JA activation (Macho et al., 2010a), could only account for HopZ1a PTI suppression abilities assuming an absolutely antagonistic effect of JA and SA-dependent defenses, which remains a debatable topic. More relevantly, the pseudokinase ZED1 was recently described to act as a molecular decoy for HopZ1a action, since HopZ1a acetylation of ZED1 in specific threonines results in ZAR1-mediated activation of HopZ1a-triggered immunity. Since molecular decoys are supposed to mimic archetypal plant targets to detect the modifying action of different

T3Es, it makes more sense for the plant target of HopZ1a to be a kinase of some kind, rather than tubulin or the structurally unrelated JAZ proteins.. The finding of MKK7 as a target for HopZ1a nicely fits with the molecular decoy presented by the plant defense system to detect its action. Nonetheless, we cannot rule out that HopZ1a, as it is the case with HopF2, might have several targets including such as those already described (like JAZ regulators), or others pending to be identified such as previously discussed calcium-dependent kinases (CPKs) acting on RbohD. In any case, interference with MKK7 provides by itself a fully convincing explanation for the PTI, ETI and SAR suppression activities of HopZ1a (Macho et al., 2010a; Lewis et al., 2014). Since, as discussed above, MKK7 is a positive regulator of PTI, ETI and SAR, inactivation of this enzyme by acetylation would suppress all mentioned defense responses.

The acetyltransferase activity of HopZ1a, as occur in many other members of the YopJ superfamily, is essential for its function. Mass spectrometry analysis showed that acetylation of HopZ1a in two particular serine residues is required for the binding of its co-factor IP6 (Ma et al., 2015). However, these serine residues are not required for *trans* acetylation and acetylation of a lysine residue is important, although not essential, for its function (Ma et al., 2015; Rufian et al., 2015).

Acetylation on the serine residues of HopZ1a could perhaps affect the binding capability to its targets. We have shown that interaction between HopZ1a and MKK7 is enhanced by HopZ1a K289R mutation (**Figure 5**). Acetylation of MKK7 is expected to be a highly dynamic process, and the HopZ1a-MKK7 complex highly transient. Our results indicate that mutation K289R somehow prolongs the life of this complex. Interestingly, the catalytic mutant HopZ1a^{C216A} is unable to interact with MKK7. In this regard, Wang et al. (2010) showed that *in vivo*, the interaction between MKK5 and HopF2 was impaired by either R71A or D175A catalytic mutations. These results indicate that the interaction between HopZ1a and MKK7 is specific and requires acetylation of HopZ1a.

The lysine 167 is a novel-described residue targeted by an effector

Serine/threonine (S/T) kinases are enzymes that phosphorylates either serine or threonine residues. In contrast, tyrosine (Y) kinases phosphorylate tyrosines, whereas mixed function kinases phosphorylates both serine/threonine and tyrosine

simultaneously (Nelson, 2008). Based on the comparison of PKA (cAMP-dependent protein kinase) and IRK (Insulin Receptor protein-tyrosine Kinase) structures, Taylor et al. (Taylor et al., 1996) described three residues as critical to differentiate S/T kinases from Y kinases: a threonine at the end of the activation loop in S/T kinases (T203 in MKK7), replaced with a proline in Y kinases, a lysine in the catalytic loop of S/T kinases (K167 in MKK7) corresponding to an arginine in Y kinases, and a threonine in the phosphorylation site of the activation loop in S/T kinases, which corresponds to a tyrosine in Y kinases. We have found that lysine 167, which is conserved among all *Arabidopsis* MKKs, is important for MKK7 function (Figure 8). Substitution of this lysine by an arginine reduces MKK7 kinase activity by an 80%. Is important to notice that arginine is a positively charged residue, as is lysine, and that the named residue is present in this position on tyrosine kinases. Lost of function in the $MKK7^{K167R}$ could indicate a specific role of this lysine in S/T kinases. However, the specific role of lysine 167 in MKK7 function remains unclear. We can speculate two possible roles for this residue based on information available for orthologs S/T kinases. PKA K168 forms a hydrogen bond to, and neutralizes, the negative charge of the γ-phosphate of ATP, stabilizing this phosphate during the transfer (Cheek et al., 2005), and also H-bonds to the substrate, triggering the closure of the active site (Nelson, 2008). Also, interaction of PKA K168 with the aspartic acid residue D166 seems to be crucial for the correct placement of the substrate into the catalytic loop (Montenegro et al., 2012). Similarly, MKK7 K167 could stabilize the γ-phosphate of the ATP bound on K74, and interact with D165 to allow substrate positioning. HopZ1a acetylates the MKK7 lysine 167, removing its positive charge. This change on the electric state of this residue could abolish the attraction to the negative γ-phosphate of ATP and to the aspartic acid 165, affecting its kinase activity. *Vibrio parahemeolyticus* effector VopA, belonging to the YopJ / HopZ family, acetylates lysine 172 on human MKK6 (Trosky et al., 2007). However, lysine 172 does not correspond with the conserved lysine in the catalytic loop. Indeed, MKK6 K172 is located before the HRD characteristic motif, and is not conserved among S/T kinaes, while MKK7 K167 localizes two residues after HRD. The MKK6 K172 aligns with the lysine 160 on MKK7. A mutation changing the lysine 160 to an arginine has no effect on MKK7 kinase activity (data not shown), indicating a different role for each of these lysine residues.

Concluding remarks

The aim of this thesis was the study of different aspects of the plant-pathogen interaction using the model the bacterial pathogen *Pseudomonas syringae*. To address this point, we have used different experimental and methodological approaches, from cellular to molecular biology, from genetics to biochemistry. At the beginning of this work, the use of cellular biology techniques and fluorescent proteins allowed us to get new insights in the colonization and infection process of *P. syringae* within the plant. The phenotypic heterogeneity observed by confocal microscopy on the colonization and responses of plant tissues inoculated with a mixed inoculum of isogenic strains differing on their virulence, lead us to investigate the source of this variation within the bacterial population. Using transcriptional fusions to GFP as a reporter for the expression of different elements of the T3SS, and single-cell analysis techniques, we established that expression of HrpL, the transcriptional activator of the T3SS genes, and that of HopAB1, one of its effectors, is bistable within the plant. Although we cannot rule out additional sources of variation, these findings provide a plausible explanation for the phenotypic diversity observed within infected plant tissues. HopAB1 was the fist effector for which a virulence activity was demonstrated, postulated to be suppression of HopF1-triggered immunity (Jackson et al., 1999). Orthologs of HopAB1 in other *P. syringae* pathovars have been described to suppress and also trigger defense response in different plant species (Jackson et al., 2002; de Torres et al., 2006). For example, HopAB2 from *P. syringae* pv. tomato DC3000, acts as an E3 ubiquitin ligase activity that promotes degradation of the tomato Fen kinase and suppresses ETI responses (Rosebrock et al., 2007). Previous results from our laboratory have shown that constitutive expression of HopAB1 in Pph 1448a from a plasmid from either a strong (P*nptII*) or a medium-to-low promoter (P*lacZ*) does not complement the attenuation of growth within the plant caused by a Δ*hopAB1* mutation. In fact, expression of HopAB1 from these promoters attenuated bacterial growth within the plant to a larger degree that its mutation (Macho et al., 2012). However, plasmid expression of HopAB1 from its native promoter did not cause growth attenuation and complemented growth of a Δ*hopAB1* mutant. Constitutive expression of the effector could alter secretion hierarchy or promote unspecific activities of the effector within the plant cell, negatively affecting bacterial growth. However, since *Agrobacterium*-mediated transient expression of HopAB1 in the bean plants of the same cultivar elicits cell death (Vinatzer et al., 2006), its also possible that an excess of HopAB1 translocation within infected tissues could lead to defense activation and growth attenuation of wild type bacteria. Thus, bistability

on the expression and translocation of HopAB1 could be important to maintain the overall translocated protein levels below the threshold for ETI activation..

The second part of this thesis focuses on another effector that can also activate ETI, through indirect recognition by the NLR protein ZAR1, and suppresses ETI activated against other effectors. In this part of the work, we provide a mechanism for HopZ1a-mediated suppression of PTI, ETI and SAR, through the identification of MKK7 as a target for HopZ1a-mediated acetylation. Unpublished data from our laboratory indicate that *P. syringae* pv. syringae strain 7B40, which contains a *hopZ1a* gene, can suppress HopZ1a-triggered ETI response through an unknown mechanism (Rufian et al., *in preparation-b*). Taking into account that HopZ1a suppresses SAR, bistability of the T3SS genes in this strain could provide an interesting mechanism for colonization of distal tissue. Thus, it is tempting to speculate what would happen if bistability did indeed take place in this strain. If this were the case, a bacterium expressing the effector *hopZ1a* would be detected by the plant cell, which in response would trigger ETI, causing local cell death and activation of SAR that would, limit its proliferation. However, suppression of SAR by HopZ1a could pave the way for bacteria not-expressing the T3SS to colonize distal tissue, in a cooperative manner similar to that described for *Salmonella typhimurium* subpopulations generated through bistable expression of one of its T3SS the SPI-1. Interestingly, expression of the SPI-1 T3SS and expression of the flagellum is counter-regulated in *Salmonella*, also similar to the downregulation of motility reported HrpL (Ortiz-Martin et al., 2010a). Following this model, a bacteria subpopulation not expressing the T3SS could move to distal tissue and colonize distal tissues where activation of SAR would have been suppressed by the ON-population whose growth had been restricted through HopZ1a-triggered local defenses. In this case, the T3SS ON subpopulation would have an altruistic behavior since its virulence activity would not benefit itself but the OFF-population, as that demonstrated for the subpopulations of *Salmonella* generated through SPI1 bistability.

Finally, plant defense suppression has been extensively shown as an essential process for the pathogen to proliferate and colonize the plant tissue. Effectors alter a number of plant processes to carry out such suppression, and use a wide array of biochemical activities to do so. Thus, effectors are frequently used as molecular probes to deeper our understanding of the plant immune system, as well as to gain insight into how bacteria generate disease. And our results on the role of MKK7 in plant defense,

revealed during the characterization of HopZ1a activity, are proof of this notion. We have demonstrated the existence of phenotypic heterogeneity on the expression of bacterial virulence factors. However, we cannot rule out that the heterogeneity found in the response of the plant to *P. syringae* could also originate from phenotypic heterogeneity within neighboring plant cells. This heterogeneity would have a different origin, since plant cells are distributed in tissues, communicated and specialized. One example of phenotypic heterogeneity at this side of the interaction is found during callose deposition experiments. Is frequent to find strong differences on callose desposition triggered by the peptide flg22 within the same leaf. Indeed, the edges of the leaves present less callose deposition than the rest of the tissue (Zhou et al., 2012). Furthermore, the ER bodies, structures composed of cisternae derived from the endoplasmic reticulum, containing antimicrobial compounds, present a seemingly random distribution within the leaf (Nakano et al., 2014; Rufian et al., *in preparation-a*). Moreover, *Arabidopsis* has been shown to undergo epigenetic changes during *P. syringae* infection, and these changes have been shown to affect the activation of defenses, and do not take place in the plant cells of the infected tissue (Yu et al., 2013). Although highly speculative, clues provide a tantalizing scenario full of possibilities to study the presence of such heterogeneity, its origin and, most importantly, its implication in plant resistance.

Conclusions

1. The use of mixed infections of *P. syringae* strains differently labeled with fluorescent proteins allows following bacterial colonization of the plant apoplast, revealing information such as dynamics of colony establishment or development, or interaction and interferences between different strains, not accessible through the use of individual infections.
2. Close proximity to wild type bacteria is required to complement growth within the apoplast of a non-pathogenic derivative, lacking a functional type III secretion system.
3. The effector-triggered immunity induced by strain RW60, visualized under a confocal microscope as accumulation of autofluorescent phenolic compounds on the cell outline, can restrict growth of closely located wild type bacteria, but can also be suppressed by them, giving rise to a highly heterogeneous scenario.
4. The expression of *hrpL*, encoding the type III secretion system transcriptional activator,, as well as that of effector gene *hopAB1* is bistable both *in planta* and within inducing laboratory medium, providing a mechanistic explanation for the phenotypic heterogeneity observed by microscopy during bacterial colonization of the plant apoplast.
5. Bacteria sorted on the basis of differences on the expression of effector gene *hopAB1* displays differences in virulence.
6. The HrpV/HrpG double negative regulatory loop acts as a bistable switch required for turning the heterogeneous expression of the type III secretion genes into bistability, in a process that requires the transcriptional activator HrpL, and is enhanced through a positive feedback loop mediated by the pilus protein HrpA.
7. The autoacetylation of residue K289 is important but not essential for HopZ1a suppression of effector-triggered immunity and systemic acquired resistance.
8. The HopZ1a^{K289R} mutant induces a strong defense response in both *Arabidopsis* and *Nicotiana benthamiana* plants.
9. The plant MAP Kinase Kinase 7 (MKK7) is a positive regulator of the plant immune system, implicated in the activation of pattern-triggered immunity, effector-triggered immunity and systemic acquired resistance.
10. HopZ1a suppresses accumulation of PR1 and growth restriction triggered by the overexpression of MKK7.
11. HopZ1a interacts with MKK7 and acetylates its lysine 167, which is essential for MKK7 kinase activity *in vitro* and for defense response activation *in planta*.

Resumen

Durante la interacción planta-patógeno, se producen multitud de eventos moleculares que determinarán el resultado de la interacción a favor de la enfermedad o la resistencia de la planta. Una completa comprensión de los eventos de evasión, disparo y supresión de defensas implicados en esta interacción requieren de un estudio multidisciplinar enfocado desde diferentes puntos de vista, y ese es el objetivo general de esta tesis.

La presente tesis doctoral se estructura alrededor de dos objetivos centrales: (I) Conocer a nivel celular el comportamiento individual y poblacional de la bacteria patógena *Pseudomonas syringae* durante el proceso de colonización e interacción de con el húesped; (II) Caracterización molecular de la supresión de defensa mediada por el efector HopZ1a. Ambos objetivos se desarrollan en los cuatro capítulos que componen la tesis doctoral.

Introducción

Pseudomonas syringae es una bacteria patógena de plantas que ha sido ampliamente investigada desde 1980. Las estirpes de *P. syringae* han sido clasificadas como el patógeno bacteriano más importante tanto por su relevancia científica como modelo, como por su creciente relevancia económica (Mansfield et al., 2012). *P. syringae* es una bacteria Gram-negativa que coloniza la parte aérea de la planta, incluyendo hojas y frutos. Esta bacteria tiene un estilo de vida dual, con una fase inicial epifita en la superficie de la planta, y una fase endofítica en el interior de la planta, donde establece una población bacteriana con una interacción con el huésped de tipo hemibiotrofo. Este patógeno coloniza los espacios intercelulares o apoplasto, donde alcanza su población más alta y este proceso no requiere la muerte del tejido colonizado. Sin embargo, conforme el proceso infectivo avanza, bien debido a la acción de determinantes de virulencia del patógeno o la respuesta de defensa desencadenada frente a ellos en la planta, el tejido infectado acaba muriendo y dando lugar a manchas necróticas visibles. Este modo de patogénesis difiere de patógenos estrictamente biotrofos, que no producen la muerte de la célula huésped durante la infección, y de patógenos necrotrofos, que necesitan matar a la célula huésped para obtener nutrientes y colonizar.

P. syringae es un complejo de especies capaz de causar enfermedad conjuntamente en una amplia gama de huéspedes, incluidos cultivos económicamente importantes, plantas leñosas y malas hierbas, como la planta modelo *Arabidopsis thaliana*. No obstante, las

plantas son generalmente resistentes a la mayoría de las estirpes, y la capacidad de una estirpe dada a causar enfermedad en un huésped es la excepción. Este fenómeno se llama rango de huésped, y en base a ello, el complejo *P. syringae* se divide en más de 50 patovares (Young, 2010). Además, las estirpes que pertenecen al mismo patovar pueden a su vez diferir en capacidad de causar enfermendad en diferentes variedades o ecotipos. Sobre la base de estas diferencias, los patovares se pueden subdividir en razas. En los últimos años, la obtención y anotación de la secuencia completa de los genomas de las tres cepas modelo pertenecientes a diferentes patovares: pv. tomato DC3000 (Buell et al., 2003), pv. phaseolicola 1448A (Joardar et al., 2005), y pv. syringae B728a (Feil et al., 2005) ha proporcionado una gran cantidad de información y herramientas que ha representado un notable salto adelante en nuestro conocimiento de este campo.

P. syringae pv. tomato es el agente causal de la mancha bacteriana del tomate. En 1986, Cuppels generó la cepa DC3000, un derivado resistente a la rifampicina de una cepa silvestre, que fue utilizado para estudios de auxotrofía y patogenicidad. Algunos años más tarde, Whalen y colaboradores (1991) demostró la capacidad de DC3000 para causar enfermedad en la planta modelo *Arabidopsis thaliana*. La capacidad de DC3000 para infectar tanto tomate como plantas de *Arabidopsis* atrajo el interés de los científicos del campo por esta cepa para su uso como modelo de estudio en el campo de la interacción planta-patógenos, y su análisis ha generado conocimiento en el campo de la ptaogénesis y la defensa en plantas relevantes para todo tipo de patógenos, incluyendo virus, hongos y oomicetos.

DC3000 es una epífita débil (Boller, 2009), en comparación con cepas de otros patovares como B728a. Mientras B728a puede mantener niveles poblacionales altos en la superficie de la hoja durante días, la mayoría de la población de DC3000 muere en menos de 48h. Por lo tanto, DC3000 necesita entrar en el apoplasto para sobrevivir a más largo plazo y proliferar. Uno de los mecanismos de esta cepa para entrar en el tejido huésped es la coronatina, una toxina que imita la hormona vegetal metil-jasmonato (Weiler et al., 1994). Tras la detección de la entrada de bacterias al apoplasto, la planta induce el cierre de los estomas para frenar dicha entrada e impedir la colonización bacteriana. Sin embargo, la coronatina activa las vías celulares que dan lugar a la reapertura de los estomas, permitiendo así la entrada al apoplasto a un mayor número de bacterias, suficientes para causar enfermedad en un huésped sensible (Melotto et al., 2008).

P. syringae pv. phaseolicola es la bacteria responsable de la enfermedad de la grasa de la judía (*Phaseolus vulgaris*). Esta enfermedad se caracteriza por el desarrollo de lesiones acuosas en las hojas y vainas de judía, rodeadas de halos cloríticos (Burkholder, 1926), y esta muy extendida a nivel mundial. Puesto que este patógeno pueden colonizar y sobrevivir en las semillas secas, los campos infectados por *P. syringae* pv. phaseolicola suelen ser destruidos para evitar su dispersión. Una de las principales estrategias de control para evitar este tipo de plagas es la rotación de cultivares resistentes. Según el tipo de interacción de resistencia/ susceptibilidad que se produce entre ocho importantes cultivares de judía y 175 cepas representativas de *P. syringae* pv. phaseolicola, este patovar puede dividirse en nueve razas (Taylor et al., 1996). Las estirpes que pertenecen a la raza 6, incluyendo la estirpe modelo 1448A, son capaces de producir enfermedad en todos los cultivares analizados.

Pseudomonas syringae pv. syringae es el grupo más heterogéneo entre los patovares de *P. syringae*. Incluye estirpes que producen enfermedad en cultivos tan dispares como la lila, judía, peral, o mango, entre otros. Una de las características compartidas por muchas de las cepas de este grupo, incluyendo B728a, es la producción de la toxina siringolina A (Ramel et al, 2009). Esta toxina actúa en el interior de la célula vegetal como un inhibidor del proteasoma, lo que conlleva a la supresión de las respuestas de defensa de la planta, permitiendo así la proliferación bacteriana (Schellenberg et al, 2010;. Kolodziejel et al., 2011). Además, la siringolina A facilita el movimiento sistémico del patógeno desde el sitio de infección primario a través del xilema (Misas-Villamil et al., 2012).

Muchas estirpes de *P. syringae* poseen toxinas que contribuyen a su virulencia. Pero todas ellas necesitan un sistema de secreción tipo III (T3SS) para ser patogénica. El T3SS es una compleja nanomáquina que exporta proteínas bacterianas directamente al citosol de la célula huésped. Los componentes del T3SS se codifican por un grupo de genes llamado *hrp* (hypersensitive and pathogenesis) y están muy conservados entre bacterias Gram-negativas portadoras de este sistema. Los genes que codifican las proteínas conservadas entre patógenos de animales y plantas se renombraron como *hrc* (hrp conserved). Los genes *hrp/hrc* se agrupan en islas de patogenicidad ubicadas en el genoma. El T3SS no se expresa constitutivamente, sino que se induce bajo condiciones de estrés, tales como medio mínimo, o el apoplasto de la planta. El principal regulador del sistema es HrpL, un miembro de la familia ECF de factores sigma alternativos que

activa la expresión de genes con una secuencia consenso (*hrp* box) en sus promotores (Xiao y Hutcheson 1994; Fouts et al., 2002). El ensamblaje del T3SS es un proceso complejo regulado por retroalimentación positivos y negativos (Ortiz-Martin et al, 2010a;.. Ortiz Martin et al, 2010b) en el que incluso proteínas estructurales, como HrpA, puede participar, controlando directa o indirectamente la expresión de HrpL (Preston et al., 1998). Las proteínas estructurales forman una jeringuilla compuesta por un anillo interior a la membrana, un anillo de membrana externa y un pilus a traves del cual las proteínas son secretadas. Además de las proteínas reguladoras y estructurales, hay otras proteínas que se pueden considerar parte del sistema, incluyendo harpins, chaperonas y efectores. Los harpins son proteínas secretadas, pero no translocadas a la célula huésped. Estas proteínas tienen un papel auxiliar en la penetración del pilus en la pared celular de la planta y en la translocación de los efectores (Kvitko et al., 2007). Las chaperonas son pequeñas proteínas esenciales para el plegamiento apropiado de sus dianas, las proteínas translocadas o efectores. Las chaperonas se unen a los efectores en el interior del citoplasma bacteriano, protegiéndolos frente a la agregación y la degradación, y dirigiéndolos al complejo de la aguja. Finalmente, los efectores son las proteínas translocados al citoplasma de la célula de la planta, donde modifican diferentes procesos de la misma para favorecer la proliferación bacteriana.

Las plantas son organismos sésiles, y como tales, se encuentran expuestas a toda clase de estreses tanto bióticos como abióticos. Cuando un organismo patógeno entra en contacto con la planta, se produce un reconocimiento de patrones moleculares asociados al patógeno (PAMPs), que da lugar a una respuesta de defensa llamada PTI (Pattern-triggered immunity). Esta respuesta es suficiente para frenar el proceso de infección en la mayoría de los casos. Sin embargo, el patógeno puede llegar a superar esta respuesta de defensa mediante mecanismos de virulencia. En bacterias Gram-negativas, como *P. syringae*, el T3SS es el principal mecanismo de virulencia que permite a la bacteria suprimir la respuesta de defensa de la planta mediante la translocación de efectores tipo III (T3E). La planta, a su vez, es capaz de detectar a estos efectores, disparando una respuesta de defensa llamada ETI (effector-triggered immunity) que da lugar a una muerte celular programada conocida como respuesta hipersensible (HR). Sin embargo, la ETI también puede ser suprimida por efectores del patógeno, permitiendo el proceso de infección. Este proceso de activación/ supresión de defensas fue propuesto por Jones y Dangl (2006) y su resultante dará lugar a una interacción compatible (infección) o

incompatible (resistencia). Sin embargo, en la naturaleza la interacción planta-patógeno se vuelve más complicada, ya que las respuestas de defensa de la planta frente a diferentes patógenos puede llegar a ser antagónica. Esta situación se da con la activación de respuestas de defensa dependientes de ácido salicílico (SA), típica frente a organismos biotrofos o hemibiotrofos. La ruta de defensa dependiente de SA tiene una señalización antagónica en algunos puntos a la ruta disparada por ácido jasmónico (JA), esencial en la respuesta de defensa frente a patógenos necrotrofos y herbívoros. Además, el SA activa una respuesta sistémica adquirida en la planta (SAR) que restringe el crecimiento en tejidos distales. Bacterias asociadas a plantas, también pueden activar una respuesta sistémica independiente de SA, llamado resistencia sistémica inducida (ISR).

Incluso en el contexto de una infección simple de *P. syringae,* se producen cambios en el genoma que pueden dar lugar a variantes isogénicas dentro de la planta. Un ejemplo claro de este tipo de cambios se produce en la estirpe 1302A de *P. syringae* pv. phaseolicola. Esta estirpe dispara ETI dependiente del efector HopAR1 en plantas de judía resistentes. En estas condiciones, una subpoblación bacteriana escinde una isla genómica (PPHGI-1) en la que se encuentra *hopAR1,* apagando su expresión. Esta nueva subpoblación consigue así evitar el disparo de ETI de la planta (Godfrey et al., 2011).

Capítulo I: Las dinámicas de crecimiento de poblaciones heterogéneas de *P. syringae* en la planta revelan una diversidad de interacciones.

En el laboratorio, mediante el uso de infecciones mixtas, se ha comprobado que una estirpe patógena puede complementar el crecimiento de otra no patógena, mientras que la respuesta de defensa disparada por una estirpe produce un efecto dominante negativo sobre el crecimiento de otra (Klement and Lovrekovick, 1961; Omer and Wood, 1969). Sin embargo, estas interferencias entre estirpes pueden evitarse utilizando la dosis de inóculo y el método de inoculación adecuada en cada caso (Macho et al., 2007). En el primer capítulo de esta tesis, hemos marcado con distintas proteínas fluorescentes estirpes isogénicas con diferencias en la virulencia, para poder visualizarlas dentro de la planta mediante microscopía confocal en el contexto de infecciones mixtas. Tras comprobar la mejor combinación de proteínas fluorescentes para visualizar bacterias en el interior de la planta (eYFP y eCFP), y que dichas proteínas no tienen efecto en la

patogénesis bacteriana, hemos comprobado el impacto de la dosis de inoculación por infiltración en la formación de colonias mixtas. Altas dosis de inóculo ($5x10^7$ cfu/ml) permiten la formación de colonias mixtas desde el inicio de la infección. Inoculaciones con dosis más bajas permiten evitar la formación de estas colonias. Sin embargo, el crecimiento en tamaño de la micro-colonia puede hacer que dos micro-colonias que en origen eran independientes, puedan llegar a contactar. Este tipo de contacto también se puede evitar disminuyendo la dosis hasta $5x10^4$ cfu/ml). Para comprobar la interferencia por complementación de una estirpe silvestre sobre un mutante incapaz de expresar el sistema de secreción, inoculamos ambas estirpes a diferentes dosis. Mediante microscopía confocal, observamos que la estirpe deficiente en el sistema de secreción solo puede crecer cuando se encuentra pegada a la estirpe silvestre. Inoculaciones a altas dosis permiten la proliferación del mutante al mismo nivel que el silvestre, mientras que disminuyendo la dosis se evita por completo la complementación. Además, encontramos que la interferencia por complementación puede ayudar a una estirpe no patógena a colonizar tejido distal, acompañada por una estirpe silvestre.

Cuando inoculamos una estirpe que produce ETI en la planta (avirulenta), observamos un área de autofluorescencia en las células vegetales que rodean la micro-colonia bacteriana. Esta autofluorescencia es debida a la liberación de compuestos antimicrobianos como resultado de la respuesta de defensa. Al inocular una estirpe silvestre con una que dispara ETI, colonias correspondientes a la estirpe silvestre ven atenuado su crecimiento por la respuesta disparada por la otra estirpe. Estos datos concuerdan con los resultados de crecimiento publicados anteriormente (Macho et al., 2007). Sin embargo, también observamos situaciones en las que las colonias silvestres son capaces de suprimir la respuesta disparada por la estirpe avirulenta. Esto es debido a que la estirpe silvestre posee el efector capaz de suprimir esta respuesta de defensa. Además observamos colonias de la estirpe avirulenta que, sin tener ninguna colonia silvestre cerca, no disparan respuesta de defensa, y colonias silvestres con gran diferencia en sus tamaños. Esta heterogeneidad en la interacción puede ser explicada por diferencias en el estadio de la infección en el que se encuentre cada micro-colonia. Otra explicación posible es que existan diferencias de expresión entre bacterias en componentes esenciales para la patogénesis, como es el sistema de secreción.

Capítulo II: Heterogeneidad fenotípica y bistabilidad en el sistema de secreción tipo III de *P. syringae.*

Las poblaciones bacterianas han sido consideradas durante mucho tiempo clonales, y como tales, genética y fenotípicamente idénticas. Sin embargo, trabajos realizados durante las últimas décadas han demostrado que en condiciones de estrés, como las que se encuentra una bacteria fitopatógena en su hospedador, se pueden formar distintas subpoblaciones bacterianas, fenómeno conocido como bistabilidad. Estos cambios se han asociado en bacterias patógenas de animales a modificaciones epigenéticas que causan heterogeneidad fenotípica reversible sin alterar el genotipo (Casadesús y Low, 2013). *Pseudomonas syringae* es una bacteria fitopatógena, cuya virulencia es dependiente del T3SS. En el segundo capítulo de la tesis, se ha analizado la expresión de tres genes del T3SS: un gen que codifica para una proteína estructural (*hrcU*), un regulador general del sistema (*hrpL*) y un efector (*hopAB1*). Para llevar a cabo este análisis, hemos realizado fusiones transcripcionales a gfp en el genoma de P. syringae pv. phaseolicola 1448A bajo el control de los promotores previamente mencionados. Posteriormente, hemos analizado la expresión de GFP mediante microscopía de fluorescencia y citomentría de flujo. Hemos demostrado que la expresión de los tres genes es heterogénea cuando la bacteria crece en medio mínimo (HIM), y esta heterogeneidad se convierte en bistabilidad para el caso del efector *hopAB1* durante la fase de crecimiento exponencial. Además, demostramos que la bistabilidad es un proceso reversible, ya las poblaciones aparecen y desaparecen dependiendo de las fases de crecimiento del cultivo. Esta diferencia en los niveles de expresión tiene un impacto en la planta, ya que la separación de poblaciones bacterianas basada en la expresión de *hopAB1* y la posterior inoculación en planta demuestra que dichas diferencias en expresión tienen un efecto en la virulencia de la bacteria. En el interior de la planta, la bistabilidad de *hopAB1* se intensifica, y la expresión del regulador *hrpL* se vuelve bistable.

Capítulo III: La auto-acetilación del residuo K289 no es esencial para la supresión de defensas mediada por HopZ1a.

La importancia de los efectores durante la interacción planta-patógeno hizo que nos interesáramos por la caracterización de la actividad de HopZ1a, un efector perteneciente a la superfamilia YopJ, conservados en muchas especies de bacterias Gram-negativas.

En nuestro laboratorio, describimos la supresión de defensas ETI y SAR (Macho et al., 2010), y más recientemente, se ha descrito que dicho efector también suprime PTI (Lewis et al., 2014). HopZ1a presenta actividad acetiltransferasa (Lee et a., 2012), dependiente de la autoacetilación en su lisina 289. En el tercer capítulo, realizamos un análisis fenotípico de cómo una mutación puntual que afecte a la autoacetilación del efector, puede afectar a su virulencia. En primer lugar, realizamos un mutante puntual K289R en un plásmido que expresa constitutivamente el efector. La expresión de la versión silvestre de HopZ1a desde *P. syringae pv. tomato* DC3000 suprime la acumulación local de PR1 (Pathogeneis-related 1), un marcador de defensas dependientes de SA. Cuando expresamos desde DC3000 la versión mutante K289R del efector, observamos una disminución en la supresión de acumulación de PR1, indicando que el residuo 289 es importante para la actividad del efector. Sin embargo, esta supresión no se pierde por completo, como sí ocurre en el mutante catalítico C216A. Posteriormente, para analizar el impacto de la autoacetilación en la lisina 289 sobre la actividad de supresión de ETI de HopZ1a, realizamos ensayos de COI (Cancelled-Out Index) en inoculaciones mixtas con HopZ1a y sus respectivos mutantes, junto con el efector AvrRpt2. Como resultado, vemos que mientras que tanto HopZ1a como el mutante K289R pueden suprimir la ETI disparada por AvrRpt2, si bien la supresión de defensa es más efectiva en la versión silvestre del efector. En el caso de la actividad de HopZ1a en la supresión de la activación de respuestas sistémicas, la mutación K289R no presenta ningún efecto en los experimentos realizados. Además de analizar el impacto de la autoacetilación en la actividad de virulencia del efector, decidimos estudiar el efecto de la mutación K289R en la actividad de avirulencia del efector (el disparo de defensa en la planta). Para ello, hicimos ensayos de producción de HR en *Arabidopsis*, observando que tanto la versión silvestre de HopZ1a como el mutante K289R producen HR. Esta respuesta de defensa es cuantificable por crecimiento bacteriano mediante ensayos de índice de competitividad (CI), y también ocurre en la planta modelo *Nicotiana benthamiana* cuando el efector es expresado transitoriamente. Una de las características de la respuesta de defensa ETI es la capacidad de frenar los síntomas de la infección bacteriana. DC3000 produce amarilleo y necrosis en las hojas, y afecta al tamaño de la planta cuando es inoculado por spray. Sin embargo, cuando DC3000 expresa HopZ1a, la respuesta de defensa frente al efector protege a la planta de la bacteria, y evita la producción de síntomas. En las estas condiciones, el mutante afectado en la lisina 289 presenta la misma capacidad de disparar que la versión

silvestre, evitando la aparición de los síntomas típicos de DC3000. Por tanto, concluimos que la lisina 289 es importante pero no esencial para la actividad de HopZ1a. Para comprobar si hay sitios alternativos de acetilación en HopZ1a, realizamos un ensayo de acetilación in vitro seguido de un western blot usando un anticuerpo anti lisinas acetiladas. Como resultado, observamos que en ausencia de la lisina 289, aun se produce autoacetilación en el efector, lo que podría explicar los fenotipos intermedios observados.

Capítulo IV: El efector bacteriano HopZ1a acetila MKK7 para suprimir respuestas de defensa de la planta.

El hecho de que HopZ1a suprima respuestas de defensa a distintos niveles (PTI, ETI y SAR), hace que el efector resulte atractivo como herramienta para el estudio de los sistemas de defensa de la planta. Hasta la fecha, se han encontrado cuatro dianas moleculares para HopZ1a (Zhou et al., 2010; Lee at al., 2012; Jiang et al., 2013 y Lewis et al., 2013), pero ninguna de ellas es un enlace directo con la actividad de supresión de defensas del efector. Una de estas dianas, ZED1, es una pseudoquinasa cuya única función es la detección de la actividad de HopZ1a para activar una respuesta de defensa (Lewis et al., 2013), lo que nos hizo pensar que el efector puede estar actuando sobre proteínas quinasas con efecto en defensa. Además, otros efectores de la familia YopJ/HopZ acetilan MAPK quinasas en sus hospedadores. En *Arabidopsis* existen 10 MAPK quinasas, una de las cuales, MKK7, está implicada en la activación de defensas basales y SAR (Zhang et al., 2007). Este fenotipo nos llevó a proponer a MKK7 como candidata a diana molecular mediante la cual HopZ1a suprime defensas. Hemos demostrado que la sobreexpresión de MKK7 tiene un efecto sobre la activación de defensas frente a DC3000, inhibiendo el crecimiento bacteriano. Además, el tratamiento con flagelina (flg22) en plantas que sobreexpresan MKK7 incrementa el disparo de especies reactivas de oxígeno (ROS), la activación de MPK, y la deposición de calosa. Estos resultados indican que MKK7 es un regulador positivo de PTI. Además, hemos comprobado que en plantas en las que MKK7 se encuentra silenciada, la respuesta ETI frente a AvrRpt2 se ve comprometida. Curiosamente, en estas mismas plantas, la respuesta frente a HopZ1a es igual que en plantas silvestres. Esto indica que MKK7 es esencial para la ruta de defensa disparada por AvrRpt2, pero no para la de HopZ1a. Ensayos de *pull-down in vitro*, o co-inmunoprecipitación y BiFC *in planta*, demuestran

que HopZ1a y MKK7 interaccionan. Para comprobar si HopZ1a acetila a MKK7, realizamos un ensayo de acetilación in vitro usando como donador de grupo acetilo ^{14}C-Acetil-CoA. Tras el revelado, observamos una leve banda en MKK7 cuando se encuentra con HopZ1a, pero no cuando se encuentra con el mutante catalítico C216A. Para identificar los posibles residuos acetilados por HopZ1a, tomamos como referencia la secuencia de ZED1, donde HopZ1a acetila una treonina. En el alineamiento de los sitios activos de ZED1 y MKK7, la treonina acetilada por HopZ1a en ZED1 coincide con una lisina en MKK7, la 167. Un mutante K167R ya no es acetilado en presencia de HopZ1a, por lo que la lisina 167 es el residuo acetilado por el efector. Para comprobar la importancia de este residuo en la actividad de la proteína, llevamos a cabo un ensayo de fosforilación in vitro usando como donador de grupos fosfato ^{32}P-ATP. MKK7 se autofosforila y es capaz de trans-fosforilar al sustrato genérico MBP (Myelin Basic Protein). Sin embargo, el mutante K167R presenta hasta un 80% menos de autofosforilación y pierde por completo la capacidad de trans-fosforilar MBP. Con el objetivo de comprobar el efecto de la mutación K167R en la planta, expresamos transitoriamente MKK7 y MKK7 K167R en *Nicotiana benthamiana*. Mientras que la expresión transitoria de la proteína silvestre da lugar a la aparición de muerte celular debido a la activación de defensas, la expresión de MKK7 K167R no produce ningún fenotipo. Por último, para comprobar si la acetilación en el residuo K167 tiene el mismo efecto que la mutación, llevamos a cabo un experimento acoplado de acetilación in vitro, seguido de fosforilación. Observamos que en presencia de HopZ1a, la acetilación de MKK7 disminuye, comparada con la acetilación que presenta en la mezcla con el mutante catalítico C216A. Por tanto, concluimos que MKK7 es un componente esencial en la respuesta de defensa, es la diana molecular de HopZ1a, y que su acetilación altera su función.

References

References

Alfano, J.R., and Collmer, A. (1997). The type III (Hrp) secretion pathway of plant pathogenic bacteria: trafficking harpins, Avr proteins, and death. *J. Bacteriol.* 179**,** 5655-5662.

Anderson, J.C., Bartels, S., Gonzalez Besteiro, M.A., Shahollari, B., Ulm, R., and Peck, S.C. (2011). Arabidopsis MAP Kinase Phosphatase 1 (AtMKP1) negatively regulates MPK6-mediated PAMP responses and resistance against bacteria. *Plant J* 67**,** 258-268. doi: 10.1111/j.1365-313X.2011.04588.x.

Arnoldini, M., Vizcarra, I.A., Pena-Miller, R., Stocker, N., Diard, M., Vogel, V., Beardmore, R.E., Hardt, W.D., and Ackermann, M. (2014). Bistable expression of virulence genes in salmonella leads to the formation of an antibiotic-tolerant subpopulation. *PLoS Biol* 12**,** e1001928. doi: 10.1371/journal.pbio.1001928.

Averre, C.W., and Kelman, A. (1964). Severity of bacterial wilt as influenced by ratio of virulent to avirulent cells of *Pseudomonas solanacearum* in inoculum. *Phytopathology* 54**,** 779-783.

Axtell, M.J., and Staskawicz, B.J. (2003). Initiation of RPS2-specified disease resistance in Arabidopsis is coupled to the AvrRpt2-directed elimination of RIN4. *Cell* 112**,** 369-377. doi: S0092867403000369 [pii].

Baltrus, D.A., Nishimura, M.T., Romanchuk, A., Chang, J.H., Mukhtar, M.S., Cherkis, K., Roach, J., Grant, S.R., Jones, C.D., and Dangl, J.L. (2011). Dynamic evolution of pathogenicity revealed by sequencing and comparative genomics of 19 Pseudomonas syringae isolates. *PLoS Pathog* 7**,** e1002132. doi: 10.1371/journal.ppat.1002132
PPATHOGENS-D-11-00602 [pii].

Bao, Y., Lies, D.P., Fu, H., and Roberts, G.P. (1991). An improved Tn7-based system for the single-copy insertion of cloned genes into chromosomes of gram-negative bacteria. *Gene* 109**,** 167-168.

Barrett, L.G., Bell, T., Dwyer, G., and Bergelson, J. (2011). Cheating, trade-offs and the evolution of aggressiveness in a natural pathogen population. *Ecol Lett* 14**,** 1149-1157. doi: 10.1111/j.1461-0248.2011.01687.x.

Baumler, A.J., Winter, S.E., Thiennimitr, P., and Casadesus, J. (2011). Intestinal and chronic infections: Salmonella lifestyles in hostile environments. *Environ Microbiol Rep* 3**,** 508-517. doi: 10.1111/j.1758-2229.2011.00242.x.

Bennett, M., Gallagher, M., Fagg, J., Bestwick, C., Paul, T., Beale, M., and Mansfield, J. (1996). The hypersensitive reaction, membrane damage and accumulation of autofluorescent phenolics in lettuce cells challenged by Bremia lactucae. *The Plant Journal* 9**,** 851-865. doi: 10.1046/j.1365-313X.1996.9060851.x.

Beuzón, C.R., and Holden, D.W. (2001). Use of mixed infections with *Salmonella* strains to study virulence genes and their interactions *in vivo*. *Microbes Infect.* 3**,** 1345-1352.

Bigger, J. (1944). Treatment of Staphylococcal infections with penicillin by intermittent sterilisation. *Lancet* 244**,** 497-500.

Blanchetot, C., Chagnon, M., Dube, N., Halle, M., and Tremblay, M.L. (2005). Substrate-trapping techniques in the identification of cellular PTP targets. *Methods* 35**,** 44-53. doi: 10.1016/j.ymeth.2004.07.007.

Block, A., and Alfano, J.R. (2011). Plant targets for Pseudomonas syringae type III effectors: virulence targets or guarded decoys? *Curr Opin Microbiol* 14**,** 39-46. doi: 10.1016/j.mib.2010.12.011.

Boller, T., and Felix, G. (2009). A renaissance of elicitors: perception of microbe-associated molecular patterns and danger signals by pattern-recognition receptors. *Annu Rev Plant Biol* 60**,** 379-406. doi: 10.1146/annurev.arplant.57.032905.105346.

Buell, C.R., Joardar, V., Lindeberg, M., Selengut, J., Paulsen, I.T., Gwinn, M.L., Dodson, R.J., Deboy, R.T., Durkin, A.S., Kolonay, J.F., Madupu, R., Daugherty, S., Brinkac, L., Beanan, M.J., Haft, D.H., Nelson, W.C., Davidsen, T., Zafar, N., Zhou, L., Liu, J., Yuan, Q., Khouri, H., Fedorova, N., Tran, B., Russell, D., Berry, K., Utterback, T., Van Aken, S.E., Feldblyum, T.V., D'ascenzo, M., Deng, W.L., Ramos, A.R., Alfano, J.R., Cartinhour, S., Chatterjee, A.K., Delaney, T.P., Lazarowitz, S.G., Martin, G.B., Schneider, D.J., Tang, X., Bender, C.L., White, O., Fraser, C.M., and Collmer, A. (2003). The complete genome sequence of the *Arabidopsis* and tomato pathogen *Pseudomonas syringae* pv. *tomato* DC3000. *Proc. Natl. Acad. Sci.* 100**,** 10181-10186.

Cameron, R.K., Dixon, R.A., and Lamb, C.J. (1994). Biologically induced systemic acquired resistance in *Arabidopsis thaliana*. *Plant J* 5**,** 715-725.

Campbell-Valois, F.X., Schnupf, P., Nigro, G., Sachse, M., Sansonetti, P.J., and Parsot, C. (2014). A fluorescent reporter reveals on/off regulation of the Shigella type III secretion apparatus during entry and cell-to-cell spread. *Cell Host Microbe* 15**,** 177-189. doi: 10.1016/j.chom.2014.01.005.

Cecchini, N.M., Steffes, K., Schlappi, M.R., Gifford, A.N., and Greenberg, J.T. (2015). Arabidopsis AZI1 family proteins mediate signal mobilization for systemic defence priming. *Nat Commun* 6**,** 7658. doi: 10.1038/ncomms8658.

Chai, Y., Chu, F., Kolter, R., and Losick, R. (2008). Bistability and biofilm formation in Bacillus subtilis. *Mol Microbiol* 67**,** 254-263. doi: 10.1111/j.1365-2958.2007.06040.x.

Charkowski, A.O., Huang, H.C., and Collmer, A. (1997). Altered localization of HrpZ in *Pseudomonas syringae* pv. *syringae* hrp mutants suggests that different components of the type III secretion pathway control protein translocation across the inner and outer membranes of gram-negative bacteria. *J. Bacteriol.* 179**,** 3866-3874.

Cheek, S., Ginalski, K., Zhang, H., and Grishin, N.V. (2005). A comprehensive update of the sequence and structure classification of kinases. *BMC Struct Biol* 5**,** 6. doi: 10.1186/1472-6807-5-6.

Cheng, W., Munkvold, K.R., Gao, H., Mathieu, J., Schwizer, S., Wang, S., Yan, Y.B., Wang, J., Martin, G.B., and Chai, J. (2011). Structural analysis of Pseudomonas syringae AvrPtoB bound to host BAK1 reveals two similar kinase-interacting domains in a type III Effector. *Cell host & microbe* 10**,** 616-626. doi: 10.1016/j.chom.2011.10.013.

Cheong, M.S., Kirik, A., Kim, J.G., Frame, K., Kirik, V., and Mudgett, M.B. (2014). AvrBsT acetylates Arabidopsis ACIP1, a protein that associates with microtubules and is required for immunity. *PLoS pathogens* 10**,** e1003952. doi: 10.1371/journal.ppat.1003952.

Chisholm, S.T., Coaker, G., Day, B., and Staskawicz, B.J. (2006). Host-microbe interactions: shaping the evolution of the plant immune response. *Cell* 124**,** 803-814. doi: S0092-8674(06)00183-8 [pii]
10.1016/j.cell.2006.02.008.

Claudi, B., Sprote, P., Chirkova, A., Personnic, N., Zankl, J., Schurmann, N., Schmidt, A., and Bumann, D. (2014). Phenotypic variation of Salmonella in host tissues delays eradication by antimicrobial chemotherapy. *Cell* 158**,** 722-733. doi: 10.1016/j.cell.2014.06.045.

Cornelis, G.R., and Van Gijsegem, F. (2000). Assembly and function of type III secretory systems. *Annu. Rev. Microbiol.* 54**,** 735-774.

Cummings, L.A., Wilkerson, W.D., Bergsbaken, T., and Cookson, B.T. (2006). In vivo, fliC expression by Salmonella enterica serovar Typhimurium is heterogeneous, regulated by ClpX, and anatomically restricted. *Mol Microbiol* 61**,** 795-809. doi: 10.1111/j.1365-2958.2006.05271.x.

Cunnac, S., Boucher, C., and Genin, S. (2004). Characterization of the cis-acting regulatory element controlling HrpB-mediated activation of the type III secretion system and effector genes in *Ralstonia solanacearum*. *J Bacteriol* 186**,** 2309-2318.

Cuppels, D.A. (1986). Generation and Characterization of Tn*5* Insertion Mutations in *Pseudomonas syringae* pv. *tomato*. *Appl. Environ. Microbiol.* 51**,** 323-327.

Dai, Y., Wang, H., Li, B., Huang, J., Liu, X., Zhou, Y., Mou, Z., and Li, J. (2006). Increased expression of MAP KINASE KINASE7 causes deficiency in polar auxin transport and leads to plant architectural abnormality in Arabidopsis. *Plant Cell* 18**,** 308-320. doi: 10.1105/tpc.105.037846.

Davidson, C.J., and Surette, M.G. (2008). Individuality in bacteria. *Annu Rev Genet* 42**,** 253-268. doi: 10.1146/annurev.genet.42.110807.091601.

Davidsson, P.R., Kariola, T., Niemi, O., and Palva, E.T. (2013). Pathogenicity of and plant immunity to soft rot pectobacteria. *Front Plant Sci* 4**,** 191. doi: 10.3389/fpls.2013.00191.

Davis, K.M., Mohammadi, S., and Isberg, R.R. (2015). Community behavior and spatial regulation within a bacterial microcolony in deep tissue sites serves to protect against host attack. *Cell Host Microbe* 17**,** 21-31. doi: 10.1016/j.chom.2014.11.008.

De Torres, M., Mansfield, J.W., Grabov, N., Brown, I.R., Ammouneh, H., Tsiamis, G., Forsyth, A., Robatzek, S., Grant, M., and Boch, J. (2006). *Pseudomonas syringae* effector AvrPtoB suppresses basal defence in *Arabidopsis*. *Plant J.* 47**,** 368-382.

Deblaere, R., Bytebier, B., De Greve, H., Deboeck, F., Schell, J., Van Montagu, M., and Leemans, J. (1985). Efficient octopine Ti plasmid-derived vectors for Agrobacterium-mediated gene transfer to plants. *Nucleic Acids Res* 13**,** 4777-4788.

Deng, W.L., Rehm, A.H., Charkowski, A.O., Rojas, C.M., and Collmer, A. (2003). *Pseudomonas syringae* exchangeable effector loci: sequence diversity in representative pathovars and virulence function in *P*. s*yringae* pv. *syringae* B728a. *J. Bacteriol.* 185**,** 2592-25602.

Diard, M., Garcia, V., Maier, L., Remus-Emsermann, M.N., Regoes, R.R., Ackermann, M., and Hardt, W.D. (2013). Stabilization of cooperative virulence by the expression of an avirulent phenotype. *Nature* 494**,** 353-356. doi: 10.1038/nature11913.

Diard, M., Sellin, M.E., Dolowschiak, T., Arnoldini, M., Ackermann, M., and Hardt, W.D. (2014). Antibiotic treatment selects for cooperative virulence of Salmonella typhimurium. *Curr Biol* 24**,** 2000-2005. doi: 10.1016/j.cub.2014.07.028.

Ding, Z., Wang, H., Liang, X., Morris, E.R., Gallazzi, F., Pandit, S., Skolnick, J., Walker, J.C., and Van Doren, S.R. (2007). Phosphoprotein and phosphopeptide interactions with the FHA domain from Arabidopsis kinase-associated protein phosphatase. *Biochemistry* 46**,** 2684-2696. doi: 10.1021/bi061763n.

Doczi, R., Brader, G., Pettko-Szandtner, A., Rajh, I., Djamei, A., Pitzschke, A., Teige, M., and Hirt, H. (2007). The Arabidopsis mitogen-activated protein kinase kinase MKK3 is upstream of group C mitogen-activated protein kinases and participates in pathogen signaling. *Plant Cell* 19**,** 3266-3279. doi: 10.1105/tpc.106.050039.

Dodds, P.N., and Rathjen, J.P. (2010). Plant immunity: towards an integrated view of plant-pathogen interactions. *Nat Rev Genet* 11**,** 539-548. doi: nrg2812 [pii]
10.1038/nrg2812.

El-Shetehy, M., Wang, C., Shine, M.B., Yu, K., Kachroo, A., and Kachroo, P. (2015). Nitric oxide and reactive oxygen species are required for systemic acquired resistance in plants. *Plant Signal Behav* 10**,** e998544. doi: 10.1080/15592324.2014.998544.

Feil, H., Feil, W.S., Chain, P., Larimer, F., Dibartolo, G., Copeland, A., Lykidis, A., Trong, S., Nolan, M., Goltsman, E., Thiel, J., Malfatti, S., Loper, J.E., Lapidus, A., Detter, J.C., Land, M., Richardson, P.M., Kyrpides, N.C., Ivanova, N., and Lindow, S.E. (2005). Comparison of the complete genome sequences of *Pseudomonas syringae* pv. *syringae* B728a and pv. *tomato* DC3000. *Proc. Natl. Acad. Sci.* 102**,** 11064-11069.

Felix, G., Duran, J.D., Volko, S., and Boller, T. (1999). Plants have a sensitive perception system for the most conserved domain of bacterial flagellin. *The Plant journal : for cell and molecular biology* 18**,** 265-276.

Feng, F., Yang, F., Rong, W., Wu, X., Zhang, J., Chen, S., He, C., and Zhou, J.M. (2012). A Xanthomonas uridine 5'-monophosphate transferase inhibits plant immune kinases. *Nature* 485**,** 114-118. doi: 10.1038/nature10962.

Feng, F., and Zhou, J.M. (2012). Plant-bacterial pathogen interactions mediated by type III effectors. *Curr Opin Plant Biol* 15**,** 469-476. doi: S1369-5266(12)00039-8 [pii]
10.1016/j.pbi.2012.03.004.

Ferreira, A.O., Myers, C.R., Gordon, J.S., Martin, G.B., Vencato, M., Collmer, A., Wehling, M.D., Alfano, J.R., Moreno-Hagelsieb, G., Lamboy, W.F., Declerck, G., Schneider, D.J., and Cartinhour, S.W. (2006). Whole-genome expression profiling defines the HrpL regulon of *Pseudomonas syringae* pv. *tomato* DC3000, allows de novo reconstruction of the Hrp cis clement, and

identifies novel coregulated genes. *Mol Plant Microbe Interact* 19**,** 1167-1179.

Fouts, D.E., Abramovitch, R.B., Alfano, J.R., Baldo, A.M., Buell, C.R., Cartinhour, S., Chatterjee, A.K., D'ascenzo, M., Gwinn, M.L., Lazarowitz, S.G., Lin, N.C., Martin, G.B., Rehm, A.H., Schneider, D.J., Van Dijk, K., Tang, X., and Collmer, A. (2002). Genomewide identification of *Pseudomonas syringae* pv. tomato DC3000 promoters controlled by the HrpL alternative sigma factor. *Proc. Natl. Acad. Sci.* 99**,** 2275-2280.

Freeman, B.C., and Beattie, G.A. (2009). Bacterial growth restriction during host resistance to Pseudomonas syringae is associated with leaf water loss and localized cessation of vascular activity in Arabidopsis thaliana. *Mol Plant Microbe Interact* 22**,** 857-867. doi: 10.1094/MPMI-22-7-0857.

Freter, R., Allweiss, B., O'brien, P.C., Halstead, S.A., and Macsai, M.S. (1981). Role of chemotaxis in the association of motile bacteria with intestinal mucosa: *in vitro* studies. *Infect. Immun.* 34**,** 241-249.

Gehl, C., Waadt, R., Kudla, J., Mendel, R.R., and Hansch, R. (2009). New GATEWAY vectors for high throughput analyses of protein-protein interactions by bimolecular fluorescence complementation. *Mol Plant* 2**,** 1051-1058. doi: 10.1093/mp/ssp040.

Glazebrook, J. (2005). Contrasting mechanisms of defense against biotrophic and necrotrophic pathogens. *Annu Rev Phytopathol* 43**,** 205-227. doi: 10.1146/annurev.phyto.43.040204.135923.

Godfrey, S.A., Lovell, H.C., Mansfield, J.W., Corry, D.S., Jackson, R.W., and Arnold, D.L. (2011). The stealth episome: suppression of gene expression on the excised genomic island PPHGI-1 from Pseudomonas syringae pv. phaseolicola. *PLoS Pathog* 7**,** e1002010. doi: 10.1371/journal.ppat.1002010.

Godfrey, S.A., Mansfield, J.W., Corry, D.S., Lovell, H.C., Jackson, R.W., and Arnold, D.L. (2010). Confocal imaging of Pseudomonas syringae pv. phaseolicola colony development in bean reveals reduced multiplication of strains containing the genomic island PPHGI-1. *Mol Plant Microbe Interact* 23**,** 1294-1302. doi: 10.1094/MPMI-05-10-0114.

Gohre, V., and Robatzek, S. (2008). Breaking the barriers: microbial effector molecules subvert plant immunity. *Annu Rev Phytopathol* 46**,** 189-215. doi: 10.1146/annurev.phyto.46.120407.110050.

Gohre, V., Spallek, T., Haweker, H., Mersmann, S., Mentzel, T., Boller, T., De Torres, M., Mansfield, J.W., and Robatzek, S. (2008). Plant pattern-recognition receptor FLS2 is directed for degradation by the bacterial ubiquitin ligase AvrPtoB. *Curr Biol* 18**,** 1824-1832. doi: S0960-9822(08)01489-9 [pii]

10.1016/j.cub.2008.10.063.

Gómez-Gómez, L., and Boller, T. (2000). FLS2: an LRR receptor-like kinase involved in the perception of the bacterial elicitor flagellin in Arabidopsis. *Molecular Cell* 5**,** 1003-1011.

Gómez-Gómez, L., Felix, G., and Boller, T. (1999). A single locus determines sensitivity to bacterial flagellin in Arabidopsis thaliana. *The Plant journal : for cell and molecular biology* 18**,** 277-284.

Green, S., Studholme, D.J., Laue, B.E., Dorati, F., Lovell, H., Arnold, D., Cottrell, J.E., Bridgett, S., Blaxter, M., Huitema, E., Thwaites, R., Sharp, P.M., Jackson, R.W., and Kamoun, S. (2010). Comparative genome analysis provides insights into the evolution and adaptation of Pseudomonas syringae pv. aesculi on Aesculus hippocastanum. *PLoS One* 5**,** e10224. doi: 10.1371/journal.pone.0010224.

Guy, E., Lautier, M., Chabannes, M., Roux, B., Lauber, E., Arlat, M., and Noel, L.D. (2013). xopAC-triggered immunity against Xanthomonas depends on Arabidopsis receptor-like cytoplasmic kinase genes PBL2 and RIPK. *PloS one* 8**,** e73469. doi: 10.1371/journal.pone.0073469.

Haefele, D.M., and Lindow, S.E. (1987). Flagellar Motility Confers Epiphytic Fitness Advantages upon Pseudomonas syringae. *Appl Environ Microbiol* 53**,** 2528-2533.

Hanahan, D. (1983). Studies of transformation of *Escherichia coli* with plasmids. *J. Mol. Biol.* 166**,** 557-580.

Hao, Y.H., Wang, Y., Burdette, D., Mukherjee, S., Keitany, G., Goldsmith, E., and Orth, K. (2008). Structural requirements for Yersinia YopJ inhibition of MAP kinase pathways. *PLoS One* 3**,** e1375. doi: 10.1371/journal.pone.0001375.

Hatterman D.R., R.S.M. (1989). Motility of Pseudomonas syringae pv. glycinea and its role in infection. *Phytopathology* 79.

Hautefort, I., Thompson, A., Eriksson-Ygberg, S., Parker, M.L., Lucchini, S., Danino, V., Bongaerts, R.J., Ahmad, N., Rhen, M., and Hinton, J.C. (2008). During infection of epithelial cells Salmonella enterica serovar Typhimurium undergoes a time-dependent transcriptional adaptation that results in simultaneous expression of three type 3 secretion systems. *Cell Microbiol* 10**,** 958-984. doi: 10.1111/j.1462-5822.2007.01099.x.

Helaine, S., and Holden, D.W. (2013). Heterogeneity of intracellular replication of bacterial pathogens. *Curr Opin Microbiol* 16**,** 184-191. doi: 10.1016/j.mib.2012.12.004.

Henry, E., Yadeta, K.A., and Coaker, G. (2013). Recognition of bacterial plant pathogens: local, systemic and transgenerational immunity. *New Phytol* 199**,** 908-915. doi: 10.1111/nph.12214.

Hernandez, S.B., Cota, I., Ducret, A., Aussel, L., and Casadesus, J. (2012). Adaptation and preadaptation of Salmonella enterica to Bile. *PLoS Genet* 8**,** e1002459. doi: 10.1371/journal.pgen.1002459.

Hotson, A., and Mudgett, M.B. (2004). Cysteine proteases in phytopathogenic bacteria: identification of plant targets and activation of innate immunity. *Curr Opin Plant Biol* 7**,** 384-390. doi: 10.1016/j.pbi.2004.05.003.

Hugouvieux, V., Barber, C.E., and Daniels, M.J. (1998). Entry of Xanthomonas campestris pv. campestris into hydathodes of Arabidopsis thaliana leaves: a system for studying early infection events in bacterial pathogenesis. *Mol Plant Microbe Interact* 11**,** 537-543. doi: 10.1094/MPMI.1998.11.6.537.

Huynh, T.V., Dahlbeck, D., and Staskawicz, B.J. (1989). Bacterial blight of soybean: regulation of a pathogen gene determining host cultivar specificity. *Science* 245**,** 1374-1377.

Jackson, R.W., Athanassopoulos, E., Tsiamis, G., Mansfield, J.W., Sesma, A., Arnold, D.L., Gibbon, M.J., Murillo, J., Taylor, J.D., and Vivian, A. (1999). Identification of a pathogenicity island, which contains genes for virulence and avirulence, on a large native plasmid in the bean pathogen *Pseudomonas syringae* pathovar *phaseolicola*. *Proc. Natl. Acad. Sci.* 96**,** 10875-10880.

Jackson, R.W., Mansfield, J.W., Ammouneh, H., Dutton, L.C., Wharton, B., Ortiz-Barredo, A., Arnold, D.L., Tsiamis, G., Sesma, A., Butcher, D., Boch, J., Young, J.K., Martin, G.B., Tegli, S., Murillo, J., and Vivian, A. (2002). Location and activity of members of a family of *virPphA* homologues in pathovars of *Pseudomonas syringae* and *P. savastanoi*. *Molecular Plant Pathology* 3**,** 205-216.

Jackson, R.W., Mansfield, J.W., Arnold, D.L., Sesma, A., Paynter, C.D., Murillo, J., Taylor, J.D., and Vivian, A. (2000). Excision from tRNA genes of a large chromosomal region, carrying *avrPphB*, associated with race change in the bean pathogen, *Pseudomonas syringae* pv. *phaseolicola*. *Mol. Microbiol.* 38**,** 186-197.

Jambunathan, N., Siani, J.M., and Mcnellis, T.W. (2001). A humidity-sensitive Arabidopsis copine mutant exhibits precocious cell death and increased disease resistance. *Plant Cell* 13**,** 2225-2240.

Jensen, L.J., Kuhn, M., Stark, M., Chaffron, S., Creevey, C., Muller, J., Doerks, T., Julien, P., Roth, A., Simonovic, M., Bork, P., and Von Mering, C. (2009). STRING 8--a

global view on proteins and their functional interactions in 630 organisms. *Nucleic Acids Res* 37**,** D412-416. doi: 10.1093/nar/gkn760.

Jiang, S., Yao, J., Ma, K.W., Zhou, H., Song, J., He, S.Y., and Ma, W. (2013). Bacterial effector activates jasmonate signaling by directly targeting JAZ transcriptional repressors. *PLoS Pathog* 9**,** e1003715. doi: 10.1371/journal.ppat.1003715.

Joardar, V., Lindeberg, M., Jackson, R.W., Selengut, J., Dodson, R., Brinkac, L.M., Daugherty, S.C., Deboy, R., Durkin, A.S., Giglio, M.G., Madupu, R., Nelson, W.C., Rosovitz, M.J., Sullivan, S., Crabtree, J., Creasy, T., Davidsen, T., Haft, D.H., Zafar, N., Zhou, L., Halpin, R., Holley, T., Khouri, H., Feldblyum, T., White, O., Fraser, C.M., Chatterjee, A.K., Cartinhour, S., Schneider, D.J., Mansfield, J., Collmer, A., and Buell, C.R. (2005). Whole-genome sequence analysis of *Pseudomonas syringae* pv. *phaseolicola* 1448A reveals divergence among pathovars in genes involved in virulence and transposition. *J Bacteriol* 187**,** 6488-6498.

Jones, J.D., and Dangl, J.L. (2006). The plant immune system. *Nature* 444**,** 323-329.

Jones, R.M., Wu, H., Wentworth, C., Luo, L., Collier-Hyams, L., and Neish, A.S. (2008). Salmonella AvrA Coordinates Suppression of Host Immune and Apoptotic Defenses via JNK Pathway Blockade. *Cell Host Microbe* 3**,** 233-244. doi: 10.1016/j.chom.2008.02.016.

Josenhans, C., and Suerbaum, S. (2002). The role of motility as a virulence factor in bacteria. *Int J Med Microbiol* 291**,** 605-614. doi: 10.1078/1438-4221-00173.

Kadota, Y., Sklenar, J., Derbyshire, P., Stransfeld, L., Asai, S., Ntoukakis, V., Jones, J.D., Shirasu, K., Menke, F., Jones, A., and Zipfel, C. (2014). Direct regulation of the NADPH oxidase RBOHD by the PRR-associated kinase BIK1 during plant immunity. *Molecular cell* 54**,** 43-55. doi: 10.1016/j.molcel.2014.02.021.

Kaiser, P., Diard, M., Stecher, B., and Hardt, W.D. (2012). The streptomycin mouse model for Salmonella diarrhea: functional analysis of the microbiota, the pathogen's virulence factors, and the host's mucosal immune response. *Immunol Rev* 245**,** 56-83. doi: 10.1111/j.1600-065X.2011.01070.x.

Kim, J.G., Stork, W., and Mudgett, M.B. (2013). Xanthomonas type III effector XopD desumoylates tomato transcription factor SlERF4 to suppress ethylene responses and promote pathogen growth. *Cell Host Microbe* 13**,** 143-154. doi: 10.1016/j.chom.2013.01.006.

Kim, M.G., Da Cunha, L., Mcfall, A.J., Belkhadir, Y., Debroy, S., Dangl, J.L., and Mackey, D. (2005). Two *Pseudomonas syringae* type III effectors inhibit RIN4-regulated basal defense in *Arabidopsis*. *Cell* 121**,** 749-759.

Kim, N.H., Choi, H.W., and Hwang, B.K. (2010). Xanthomonas campestris pv. vesicatoria effector AvrBsT induces cell death in pepper, but suppresses defense responses in tomato. *Mol Plant Microbe Interact* 23**,** 1069-1082. doi: 10.1094/MPMI-23-8-1069.

Kinkel, L.L., Wilson, M., and Lindow, S.E. (2000). Plant species and plant incubation conditions influence variability in epiphytic bacterial population size. *Microb. Ecol.* 39**,** 1-11.

Klement, Z., and Lovrekovich, L. (1961). Defense reactions induced by phytopathogenic bacteria in bean pods. *Phytopathology* 41**,** 217-227.

Kohler, T., Buckling, A., and Van Delden, C. (2009). Cooperation and virulence of clinical Pseudomonas aeruginosa populations. *Proc Natl Acad Sci U S A* 106**,** 6339-6344. doi: 10.1073/pnas.0811741106.

Kussell, E., Kishony, R., Balaban, N.Q., and Leibler, S. (2005). Bacterial persistence: a model of survival in changing environments. *Genetics* 169**,** 1807-1814. doi: 10.1534/genetics.104.035352.

Kussell, E., and Leibler, S. (2005). Phenotypic diversity, population growth, and information in fluctuating environments. *Science* 309**,** 2075-2078. doi: 10.1126/science.1114383.

Kvitko, B.H., Ramos, A.R., Morello, J.E., Oh, H.S., and Collmer, A. (2007). Identification of harpins in *Pseudomonas syringae* pv. *tomato* DC3000, which are functionally similar to HrpK1 in promoting translocation of type III secretion system effectors. *J. Bacteriol.* 189**,** 8059-8072.

Lam, H.N., Chakravarthy, S., Wei, H.L., Buinguyen, H., Stodghill, P.V., Collmer, A., Swingle, B.M., and Cartinhour, S.W. (2014). Global analysis of the HrpL regulon in the plant pathogen Pseudomonas syringae pv. tomato DC3000 reveals new regulon members with diverse functions. *PLoS One* 9**,** e106115. doi: 10.1371/journal.pone.0106115.

Lambertsen, L., Sternberg, C., and Molin, S. (2004). Mini-Tn7 transposons for site-specific tagging of bacteria with fluorescent proteins. *Environ Microbiol* 6**,** 726-732. doi: 10.1111/j.1462-2920.2004.00605.x
EMI605 [pii].

Lee, A.H., Hurley, B., Felsensteiner, C., Yea, C., Ckurshumova, W., Bartetzko, V., Wang, P.W., Quach, V., Lewis, J.D., Liu, Y.C., Bornke, F., Angers, S., Wilde, A., Guttman, D.S., and Desveaux, D. (2012). A bacterial acetyltransferase destroys plant microtubule networks and blocks secretion. *PLoS Pathog* 8**,** e1002523. doi: 10.1371/journal.ppat.1002523.

Lee, D.J., Bingle, L.E., Heurlier, K., Pallen, M.J., Penn, C.W., Busby, S.J., and Hobman, J.L. (2009). Gene doctoring: a method for recombineering in laboratory and pathogenic Escherichia coli strains. *BMC Microbiol* 9**,** 252. doi: 10.1186/1471-2180-9-252.

Lee, J.S., and Ellis, B.E. (2007). Arabidopsis MAPK phosphatase 2 (MKP2) positively regulates oxidative stress tolerance and inactivates the MPK3 and MPK6 MAPKs. *J Biol Chem* 282**,** 25020-25029. doi: 10.1074/jbc.M701888200.

Lennox, E.S. (1955). Transduction of linked genetic characters of the host by bacteriophage P1. *Virology* 1**,** 190-206.

Lewis, J.D., Abada, W., Ma, W., Guttman, D.S., and Desveaux, D. (2008). The HopZ family of *Pseudomonas syringae* type III effectors require myristoylation for virulence and avirulence functions in *Arabidopsis thaliana*. *J. Bacteriol.* 190**,** 2880-2891.

Lewis, J.D., Lee, A.H., Hassan, J.A., Wan, J., Hurley, B., Jhingree, J.R., Wang, P.W., Lo, T., Youn, J.Y., Guttman, D.S., and Desveaux, D. (2013). The Arabidopsis ZED1 pseudokinase is required for ZAR1-mediated immunity induced by the Pseudomonas syringae type III effector HopZ1a. *Proceedings of the National Academy of Sciences of the United States of America* 110**,** 18722-18727. doi: 10.1073/pnas.1315520110.

Lewis, J.D., Wilton, M., Mott, G.A., Lu, W., Hassan, J.A., Guttman, D.S., and Desveaux, D. (2014). Immunomodulation by the Pseudomonas syringae HopZ type III effector family in Arabidopsis. *PLoS One* 9**,** e116152. doi: 10.1371/journal.pone.0116152.

Lewis, J.D., Wu, R., Guttman, D.S., and Desveaux, D. (2010). Allele-specific virulence attenuation of the Pseudomonas syringae HopZ1a type III effector via the Arabidopsis ZAR1 resistance protein. *PLoS Genet* 6**,** e1000894. doi: 10.1371/journal.pgen.1000894.

Li, G., Froehlich, J.E., Elowsky, C., Msanne, J., Ostosh, A.C., Zhang, C., Awada, T., and Alfano, J.R. (2014). Distinct Pseudomonas type-III effectors use a cleavable transit peptide to target chloroplasts. *The Plant journal : for cell and molecular biology* 77**,** 310-321. doi: 10.1111/tpj.12396.

Lindeberg, M., Stavrinides, J., Chang, J.H., Alfano, J.R., Collmer, A., Dangl, J.L., Greenberg, J.T., Mansfield, J.W., and Guttman, D.S. (2005). Proposed guidelines for a unified nomenclature and phylogenetic analysis of type III Hop effector proteins in the plant pathogen *Pseudomonas syringae*. *Mol. Plant-Microbe Interact.* 18**,** 275-282.

Lindow, S.E., and Brandl, M.T. (2003). Microbiology of the phyllosphere. *Appl Environ Microbiol* 69**,** 1875-1883.

Liu, Y., Ren, D., Pike, S., Pallardy, S., Gassmann, W., and Zhang, S. (2007). Chloroplast-generated reactive oxygen species are involved in hypersensitive response-like cell death mediated by a mitogen-activated protein kinase cascade. *The Plant journal : for cell and molecular biology* 51**,** 941-954. doi: 10.1111/j.1365-313X.2007.03191.x.

Liu, Z., Wu, Y., Yang, F., Zhang, Y., Chen, S., Xie, Q., Tian, X., and Zhou, J.M. (2013). BIK1 interacts with PEPRs to mediate ethylene-induced immunity. *Proceedings of the National Academy of Sciences of the United States of America* 110**,** 6205-6210. doi: 10.1073/pnas.1215543110.

Lovell, H.C., Jackson, R.W., Mansfield, J.W., Godfrey, S.A., Hancock, J.T., Desikan, R., and Arnold, D.L. (2011). In planta conditions induce genomic changes in Pseudomonas syringae pv. phaseolicola. *Mol Plant Pathol* 12**,** 167-176. doi: 10.1111/j.1364-3703.2010.00658.x.

Ma, K.W., Jiang, S., Hawara, E., Lee, D., Pan, S., Coaker, G., Song, J., and Ma, W. (2015). Two serine residues in Pseudomonas syringae effector HopZ1a are required for acetyltransferase activity and association with the host co-factor. *New Phytol* 208**,** 1157-1168. doi: 10.1111/nph.13528.

Ma, W., Dong, F.F., Stavrinides, J., and Guttman, D.S. (2006). Type III effector diversification via both pathoadaptation and horizontal transfer in response to a coevolutionary arms race. *PLoS Genet* 2**,** e209. doi: 10.1371/journal.pgen.0020209.

Macho, A.P. (2015). Subversion of plant cellular functions by bacterial type-III effectors: beyond suppression of immunity. *New Phytol*. doi: 10.1111/nph.13605.

Macho, A.P., Guevara, C.M., Tornero, P., Ruiz-Albert, J., and Beuzon, C.R. (2010a). The Pseudomonas syringae effector protein HopZ1a suppresses effector-triggered immunity. *New Phytol* 187**,** 1018-1033. doi: NPH3381 [pii]
10.1111/j.1469-8137.2010.03381.x.

Macho, A.P., Guidot, A., Barberis, P., Beuzon, C.R., and Genin, S. (2010b). A competitive index assay identifies several Ralstonia solanacearum type III effector mutant strains with reduced fitness in host plants. *Mol Plant Microbe Interact* 23**,** 1197-1205. doi: 10.1094/MPMI-23-9-1197.

Macho, A.P., Rufian, J.S., Ruiz-Albert, J., and Beuzon, C.R. (2016). Competitive Index: Mixed Infection-Based Virulence Assays for Genetic Analysis in Pseudomonas syringae-Plant Interactions. *Methods Mol Biol* 1363**,** 209-217. doi: 10.1007/978-1-4939-3115-6_17.

Macho, A.P., Ruiz-Albert, J., Tornero, P., and Beuzón, C.R. (2009). Identification of new type III effectors and analysis of the plant response by competitive index. *Mol Plant Pathol* 10**,** 69-80.

Macho, A.P., Schwessinger, B., Ntoukakis, V., Brutus, A., Segonzac, C., Roy, S., Kadota, Y., Oh, M.H., Sklenar, J., Derbyshire, P., Lozano-Duran, R., Malinovsky, F.G., Monaghan, J., Menke, F.L., Huber, S.C., He, S.Y., and Zipfel, C. (2014). A bacterial tyrosine phosphatase inhibits plant pattern recognition receptor activation. *Science* 343**,** 1509-1512. doi: 10.1126/science.1248849.

Macho, A.P., and Zipfel, C. (2015). Targeting of plant pattern recognition receptor-triggered immunity by bacterial type-III secretion system effectors. *Curr Opin Microbiol* 23**,** 14-22. doi: 10.1016/j.mib.2014.10.009.

Macho, A.P., Zumaquero, A., Gonzalez-Plaza, J.J., Ortiz-Martin, I., Rufian, J.S., and Beuzon, C.R. (2012). Genetic analysis of the individual contribution to virulence of the type III effector inventory of Pseudomonas syringae pv. phaseolicola. *PLoS One* 7**,** e35871. doi: 10.1371/journal.pone.0035871.

Macho, A.P., Zumaquero, A., Ortiz-Martín, I., and Beuzón, C.R. (2007). Competitive index in mixed infections: a sensitive and accurate assay for the genetic analysis of *Pseudomonas syringae*-plant interactions. *Molecular Plant Pathology* 8**,** 437-450.

Macnab, R.M. (1996). "Flagella and motility," in *Escherichia coli and Salmonella: Cellular and Molecular Biology,* ed. R.C.I. F. C. Neidhardt, J. L. Ingraham, E. C. C. Lin, K. B. Low, B. Magasanik, W. S. Reznikoff, M. Riley, M. Schaechter, and H. E. Umbarger 2ed (Washington, D.C.: ASM Press), 123-145.

Manina, G., Dhar, N., and Mckinney, J.D. (2015). Stress and host immunity amplify Mycobacterium tuberculosis phenotypic heterogeneity and induce nongrowing metabolically active forms. *Cell Host Microbe* 17**,** 32-46. doi: 10.1016/j.chom.2014.11.016.

Mansfield, J., Genin, S., Magori, S., Citovsky, V., Sriariyanum, M., Ronald, P., Dow, M., Verdier, V., Beer, S.V., Machado, M.A., Toth, I., Salmond, G., and Foster, G.D. (2012). Top 10 plant pathogenic bacteria in molecular plant pathology. *Mol Plant Pathol* 13**,** 614-629. doi: 10.1111/j.1364-3703.2012.00804.x.

Mansfield, J.W. (2009). From bacterial avirulence genes to effector functions via the hrp delivery system: an overview of 25 years of progress in our understanding of plant innate immunity. *Mol Plant Pathol* 10**,** 721-734. doi: MPP576 [pii]
10.1111/j.1364-3703.2009.00576.x.

Matas, I.M., Castaneda-Ojeda, M.P., Aragon, I.M., Antunez-Lamas, M., Murillo, J., Rodriguez-Palenzuela, P., Lopez-Solanilla, E., and Ramos, C. (2014).

Translocation and functional analysis of Pseudomonas savastanoi pv. savastanoi NCPPB 3335 type III secretion system effectors reveals two novel effector families of the Pseudomonas syringae complex. *Mol Plant Microbe Interact* 27**,** 424-436. doi: 10.1094/MPMI-07-13-0206-R.

Meinzer, U., Barreau, F., Esmiol-Welterlin, S., Jung, C., Villard, C., Leger, T., Ben-Mkaddem, S., Berrebi, D., Dussaillant, M., Alnabhani, Z., Roy, M., Bonacorsi, S., Wolf-Watz, H., Perroy, J., Ollendorff, V., and Hugot, J.P. (2012). Yersinia pseudotuberculosis effector YopJ subverts the Nod2/RICK/TAK1 pathway and activates caspase-1 to induce intestinal barrier dysfunction. *Cell Host Microbe* 11**,** 337-351. doi: 10.1016/j.chom.2012.02.009.

Melotto, M., Underwood, W., and He, S.Y. (2008). Role of stomata in plant innate immunity and foliar bacterial diseases. *Annu Rev Phytopathol* 46**,** 101-122. doi: 10.1146/annurev.phyto.121107.104959.

Melotto, M., Underwood, W., Koczan, J., Nomura, K., and He, S.Y. (2006). Plant stomata function in innate immunity against bacterial invasion. *Cell* 126**,** 969-980. doi: S0092-8674(06)01015-4 [pii]
10.1016/j.cell.2006.06.054.

Mesa, S., Reutimann, L., Fischer, H.-M., and Hennecke, H. (2009). Posttranslational control of transcription factor FixK2, a key regulator for the Bradyrhizobium japonicum-soybean symbiosis. *Proc Natl Acad Sci USA* 106**,** 21860-21865. doi: 10.1073/pnas.0908097106.

Misas-Villamil, J.C., Kolodziejek, I., and Van Der Hoorn, R.A. (2011). Pseudomonas syringae colonizes distant tissues in Nicotiana benthamiana through xylem vessels. *Plant J* 67**,** 774-782. doi: 10.1111/j.1365-313X.2011.04632.x.

Mitchell, K., Brown, I., Knox, P., and Mansfield, J. (2015). The role of cell wall-based defences in the early restriction of non-pathogenic hrp mutant bacteria in Arabidopsis. *Phytochemistry* 112**,** 139-150. doi: 10.1016/j.phytochem.2014.07.015.

Mittal, R., Peak-Chew, S.Y., and Mcmahon, H.T. (2006). Acetylation of MEK2 and I kappa B kinase (IKK) activation loop residues by YopJ inhibits signaling. *Proc Natl Acad Sci U S A* 103**,** 18574-18579. doi: 10.1073/pnas.0608995103.

Mittal, R., Peak-Chew, S.Y., Sade, R.S., Vallis, Y., and Mcmahon, H.T. (2010). The acetyltransferase activity of the bacterial toxin YopJ of Yersinia is activated by eukaryotic host cell inositol hexakisphosphate. *J Biol Chem* 285**,** 19927-19934. doi: 10.1074/jbc.M110.126581.

Montenegro, M., Masgrau, L., Gonzalez-Lafont, A., Lluch, J.M., and Garcia-Viloca, M. (2012). Influence of the enzyme phosphorylation state and the substrate on

PKA enzyme dynamics. *Biophys Chem* 161**,** 17-28. doi: 10.1016/j.bpc.2011.11.001.

Morris, C.E., Sands, D.C., Vinatzer, B.A., Glaux, C., Guilbaud, C., Buffiere, A., Yan, S., Dominguez, H., and Thompson, B.M. (2008). The life history of the plant pathogen Pseudomonas syringae is linked to the water cycle. *ISME J* 2**,** 321-334. doi: 10.1038/ismej.2007.113.

Mucyn, T.S., Yourstone, S., Lind, A.L., Biswas, S., Nishimura, M.T., Baltrus, D.A., Cumbie, J.S., Chang, J.H., Jones, C.D., Dangl, J.L., and Grant, S.R. (2014). Variable suites of non-effector genes are co-regulated in the type III secretion virulence regulon across the Pseudomonas syringae phylogeny. *PLoS Pathog* 10**,** e1003807. doi: 10.1371/journal.ppat.1003807.

Mukherjee, S., Hao, Y.H., and Orth, K. (2007). A newly discovered post-translational modification--the acetylation of serine and threonine residues. *Trends Biochem Sci* 32**,** 210-216. doi: 10.1016/j.tibs.2007.03.007.

Mukherjee, S., Keitany, G., Li, Y., Wang, Y., Ball, H.L., Goldsmith, E.J., and Orth, K. (2006). Yersinia YopJ acetylates and inhibits kinase activation by blocking phosphorylation. *Science* 312**,** 1211-1214. doi: 10.1126/science.1126867.

Murillo, J., Shen, H., Gerhold, D., Sharma, A., Cooksey, D.A., and Keen, N.T. (1994). Characterization of pPT23B, the plasmid involved in syringolide production by *Pseudomonas syringae* pv. *tomato* PT23. *Plasmid* 31**,** 275-287.

Nakano, R.T., Yamada, K., Bednarek, P., Nishimura, M., and Hara-Nishimura, I. (2014). ER bodies in plants of the Brassicales order: biogenesis and association with innate immunity. *Front Plant Sci* 5**,** 73. doi: 10.3389/fpls.2014.00073.

Nawrath, C., and Metraux, J.P. (1999). Salicylic acid induction-deficient mutants of Arabidopsis express PR-2 and PR-5 and accumulate high levels of camalexin after pathogen inoculation. *Plant Cell* 11**,** 1393-1404.

Nelson, J. (2008). *Structure and Function in Cell Signalling.*

Nielsen, A.T., Dolganov, N.A., Rasmussen, T., Otto, G., Miller, M.C., Felt, S.A., Torreilles, S., and Schoolnik, G.K. (2010). A bistable switch and anatomical site control Vibrio cholerae virulence gene expression in the intestine. *PLoS Pathog* 6**,** e1001102. doi: 10.1371/journal.ppat.1001102.

Nikos Alexandratos, and Bruinsma, J. (2012). World agriculture towards 2030/2050: the 2012 revision. *FAO, Food and Agriculture Organization of the United Nations*.

Novick, A., and Weiner, M. (1957). Enzyme Induction as an All-or-None Phenomenon. *Proc Natl Acad Sci U S A* 43**,** 553-566.

Oh, H.S., and Collmer, A. (2005). Basal resistance against bacteria in Nicotiana benthamiana leaves is accompanied by reduced vascular staining and suppressed by multiple Pseudomonas syringae type III secretion system effector proteins. *The Plant journal : for cell and molecular biology* 44**,** 348-359. doi: 10.1111/j.1365-313X.2005.02529.x.

Omer, M.E.H., and Wood, R.K.S. (1969). Growth of *Pseudomonas phaseolicola* in susceptible and resistant bean plants. *Ann. Appl. Biol.* 63**,** 103-116.

Orth, K., Xu, Z., Mudgett, M.B., Bao, Z.Q., Palmer, L.E., Bliska, J.B., Mangel, W.F., Staskawicz, B., and Dixon, J.E. (2000). Disruption of signaling by Yersinia effector YopJ, a ubiquitin-like protein protease. *Science* 290**,** 1594-1597.

Ortiz-Martin, I., Thwaites, R., Macho, A.P., Mansfield, J.W., and Beuzon, C.R. (2010a). Positive regulation of the Hrp type III secretion system in Pseudomonas syringae pv. phaseolicola. *Mol Plant Microbe Interact* 23**,** 665-681. doi: 10.1094/MPMI-23-5-0665.

Ortiz-Martin, I., Thwaites, R., Mansfield, J.W., and Beuzon, C.R. (2010b). Negative regulation of the Hrp type III secretion system in Pseudomonas syringae pv. phaseolicola. *Mol Plant Microbe Interact* 23**,** 682-701. doi: 10.1094/MPMI-23-5-0682.

Paquette, N., Conlon, J., Sweet, C., Rus, F., Wilson, L., Pereira, A., Rosadini, C.V., Goutagny, N., Weber, A.N., Lane, W.S., Shaffer, S.A., Maniatis, S., Fitzgerald, K.A., Stuart, L., and Silverman, N. (2012). Serine/threonine acetylation of TGFbeta-activated kinase (TAK1) by Yersinia pestis YopJ inhibits innate immune signaling. *Proc Natl Acad Sci U S A* 109**,** 12710-12715. doi: 10.1073/pnas.1008203109.

Pitman, A.R., Jackson, R.W., Mansfield, J.W., Kaitell, V., Thwaites, R., and Arnold, D.L. (2005). Exposure to host resistance mechanisms drives evolution of bacterial virulence in plants. *Curr Biol* 15**,** 2230-2235. doi: 10.1016/j.cub.2005.10.074.

Pitzschke, A., Schikora, A., and Hirt, H. (2009). MAPK cascade signalling networks in plant defence. *Curr Opin Plant Biol* 12**,** 421-426. doi: 10.1016/j.pbi.2009.06.008.

Popescu, S.C., Popescu, G.V., Bachan, S., Zhang, Z., Gerstein, M., Snyder, M., and Dinesh-Kumar, S.P. (2009). MAPK target networks in Arabidopsis thaliana revealed using functional protein microarrays. *Genes Dev* 23**,** 80-92. doi: 10.1101/gad.1740009.

Preston, G., Deng, W.L., Huang, H.C., and Collmer, A. (1998). Negative regulation of *hrp* genes in *Pseudomonas syringae* by HrpV. *J. Bacteriol.* 180**,** 4532-4537.

Rahme, L.G., Mindrinos, M.N., and Panopoulos, N.J. (1991). Genetic and transcriptional organization of the hrp cluster of *Pseudomonas syringae* pv. *phaseolicola*. *J. Bacteriol.* 173**,** 575-586.

Ramel, C., Tobler, M., Meyer, M., Bigler, L., Ebert, M.O., Schellenberg, B., and Dudler, R. (2009). Biosynthesis of the proteasome inhibitor syringolin A: the ureido group joining two amino acids originates from bicarbonate. *BMC Biochem* 10**,** 26. doi: 10.1186/1471-2091-10-26.

Ranf, S., Eschen-Lippold, L., Pecher, P., Lee, J., and Scheel, D. (2011). Interplay between calcium signalling and early signalling elements during defence responses to microbe- or damage-associated molecular patterns. *The Plant Journal* 68**,** 100-113. doi: 10.1111/j.1365-313X.2011.04671.x.

Rico, A., and Preston, G.M. (2008). Pseudomonas syringae pv. tomato DC3000 uses constitutive and apoplast-induced nutrient assimilation pathways to catabolize nutrients that are abundant in the tomato apoplast. *Mol Plant Microbe Interact* 21**,** 269-282. doi: 10.1094/MPMI-21-2-0269.

Rohmer, L., Guttman, D.S., and Dangl, J.L. (2004). Diverse evolutionary mechanisms shape the type III effector virulence factor repertoire in the plant pathogen *Pseudomonas syringae*. *Genetics* 167**,** 1341-1360.

Roine, E., Wei, W., Yuan, J., Nurmiaho-Lassila, E.L., Kalkkinen, N., Romantschuk, M., and He, S.Y. (1997). Hrp pilus: an *hrp*-dependent bacterial surface appendage produced by *Pseudomonas syringae* pv. *tomato* DC3000. *Proc. Natl. Acad. Sci.* 94**,** 3459-3464.

Rosebrock, T.R., Zeng, L., Brady, J.J., Abramovitch, R.B., Xiao, F., and Martin, G.B. (2007). A bacterial E3 ubiquitin ligase targets a host protein kinase to disrupt plant immunity. *Nature* 448**,** 370-374. doi: nature05966 [pii]
10.1038/nature05966.

Rufian, J.S., Elmore, J.M., Bejarano, E.R., Beuzón, C.R., and Coaker, G. (*in preparation-a*). Role of the ER bodies in the plant immune system.

Rufian, J.S., Lucía, A., Guevara, C.M., Macho, A.P., Zumaquero, A., Beuzón, C.R., and Ruíz-Albert, J. (*in preparation-b*). Suppression of HopZ-effector triggered defence responses. *Manuscript in preparation for Molecular Plant Pathology*.

Rufian, J.S., Lucía, A., Macho, A.P., Orozco-Navarrete, B., Arroyo-Mateos, M.A., Bejarano, E.R., Beuzón, C.R., and Ruiz-Albert, J. (2015). Auto-acetylation on

K289 is not essential for HopZ1a-mediated plant defense suppression. *Frontiers in Microbiology* 6. doi: 10.3389/fmicb.2015.00684.

Saini, S., Ellermeier, J.R., Slauch, J.M., and Rao, C.V. (2010a). The role of coupled positive feedback in the expression of the SPI1 type three secretion system in Salmonella. *PLoS Pathog* 6**,** e1001025. doi: 10.1371/journal.ppat.1001025.

Saini, S., Koirala, S., Floess, E., Mears, P.J., Chemla, Y.R., Golding, I., Aldridge, C., Aldridge, P.D., and Rao, C.V. (2010b). FliZ induces a kinetic switch in flagellar gene expression. *J Bacteriol* 192**,** 6477-6481. doi: 10.1128/JB.00751-10.

Sanchez-Duran, M.A., Dallas, M.B., Ascencio-Ibanez, J.T., Reyes, M.I., Arroyo-Mateos, M., Ruiz-Albert, J., Hanley-Bowdoin, L., and Bejarano, E.R. (2011). Interaction between geminivirus replication protein and the SUMO-conjugating enzyme is required for viral infection. *J Virol* 85**,** 9789-9800. doi: 10.1128/JVI.02566-10.

Sanchez-Romero, M.A., and Casadesus, J. (2014). Contribution of phenotypic heterogeneity to adaptive antibiotic resistance. *Proc Natl Acad Sci U S A* 111**,** 355-360. doi: 10.1073/pnas.1316084111.

Sarkar, S.F., Gordon, J.S., Martin, G.B., and Guttman, D.S. (2006). Comparative genomics of host-specific virulence in Pseudomonas syringae. *Genetics* 174**,** 1041-1056. doi: 10.1534/genetics.106.060996.

Saucet, S.B., Ma, Y., Sarris, P.F., Furzer, O.J., Sohn, K.H., and Jones, J.D. (2015). Two linked pairs of Arabidopsis TNL resistance genes independently confer recognition of bacterial effector AvrRps4. *Nat Commun* 6**,** 6338. doi: 10.1038/ncomms7338.

Schellenberg, B., Ramel, C., and Dudler, R. (2010). Pseudomonas syringae virulence factor syringolin A counteracts stomatal immunity by proteasome inhibition. *Mol Plant Microbe Interact* 23**,** 1287-1293. doi: 10.1094/MPMI-04-10-0094.

Schroth, N.J.P.a.M.N. (1974). Role of Flagellar Motility in the Invasion of Bean Leaves by Pseudomonas phaseolicola. *Phytopathology* 64**,** 1389-1397.

Schweighofer, A., Kazanaviciute, V., Scheikl, E., Teige, M., Doczi, R., Hirt, H., Schwanninger, M., Kant, M., Schuurink, R., Mauch, F., Buchala, A., Cardinale, F., and Meskiene, I. (2007). The PP2C-type phosphatase AP2C1, which negatively regulates MPK4 and MPK6, modulates innate immunity, jasmonic acid, and ethylene levels in Arabidopsis. *Plant Cell* 19**,** 2213-2224. doi: 10.1105/tpc.106.049585.

Segonzac, C., and Zipfel, C. (2011). Activation of plant pattern-recognition receptors by bacteria. *Curr Opin Microbiol* 14**,** 54-61. doi: 10.1016/j.mib.2010.12.005.

Shan, L., He, P., Li, J., Heese, A., Peck, S.C., Nurnberger, T., Martin, G.B., and Sheen, J. (2008). Bacterial effectors target the common signaling partner BAK1 to disrupt multiple MAMP receptor-signaling complexes and impede plant immunity. *Cell Host Microbe* 4**,** 17-27.

Shang, Y., Li, X., Cui, H., He, P., Thilmony, R., Chintamanani, S., Zwiesler-Vollick, J., Gopalan, S., Tang, X., and Zhou, J.M. (2006). RAR1, a central player in plant immunity, is targeted by Pseudomonas syringae effector AvrB. *Proc Natl Acad Sci U S A* 103**,** 19200-19205. doi: 0607279103 [pii]
10.1073/pnas.0607279103.

Shao, F., Golstein, C., Ade, J., Stoutemyer, M., Dixon, J.E., and Innes, R.W. (2003). Cleavage of Arabidopsis PBS1 by a bacterial type III effector. *Science* 301**,** 1230-1233. doi: 10.1126/science.1085671.

Shenge, K.C., Mabagala, R.B., Mortensen, C.N., Stephan, D. And Wydra, K (2007). First report of bacterial speck of tomato caused by Pseudomonas syringae pv. tomatoin Tanzania. *Plant Disease* 91**,** 462.

Spoel, S.H., and Dong, X. (2012). How do plants achieve immunity? Defence without specialized immune cells. *Nat Rev Immunol* 12**,** 89-100. doi: 10.1038/nri3141.

Srikhanta, Y.N., Fox, K.L., and Jennings, M.P. (2010). The phasevarion: phase variation of type III DNA methyltransferases controls coordinated switching in multiple genes. *Nat Rev Microbiol* 8**,** 196-206. doi: 10.1038/nrmicro2283.

Stecher, B., Barthel, M., Schlumberger, M.C., Haberli, L., Rabsch, W., Kremer, M., and Hardt, W.D. (2008). Motility allows S. Typhimurium to benefit from the mucosal defence. *Cell Microbiol* 10**,** 1166-1180. doi: 10.1111/j.1462-5822.2008.01118.x.

Stecher, B., Hapfelmeier, S., Muller, C., Kremer, M., Stallmach, T., and Hardt, W.D. (2004). Flagella and chemotaxis are required for efficient induction of Salmonella enterica serovar Typhimurium colitis in streptomycin-pretreated mice. *Infect Immun* 72**,** 4138-4150. doi: 10.1128/IAI.72.7.4138-4150.2004.

Stewart, M.K., and Cookson, B.T. (2012). Non-genetic diversity shapes infectious capacity and host resistance. *Trends Microbiol* 20**,** 461-466. doi: 10.1016/j.tim.2012.07.003.

Sweet, C.R., Conlon, J., Golenbock, D.T., Goguen, J., and Silverman, N. (2007). YopJ targets TRAF proteins to inhibit TLR-mediated NF-kappaB, MAPK and IRF3 signal transduction. *Cell Microbiol* 9**,** 2700-2715. doi: 10.1111/j.1462-5822.2007.00990.x.

Szczesny, R., Buttner, D., Escolar, L., Schulze, S., Seiferth, A., and Bonas, U. (2010). Suppression of the AvrBs1-specific hypersensitive response by the YopJ effector homolog AvrBsT from Xanthomonas depends on a SNF1-related kinase. *New Phytol* 187**,** 1058-1074. doi: 10.1111/j.1469-8137.2010.03346.x.

Tai, T.H., Dahlbeck, D., Clark, E.T., Gajiwala, P., Pasion, R., Whalen, M.C., Stall, R.E., and Staskawicz, B.J. (1999). Expression of the Bs2 pepper gene confers resistance to bacterial spot disease in tomato. *Proc Natl Acad Sci U S A* 96**,** 14153-14158.

Tasset, C., Bernoux, M., Jauneau, A., Pouzet, C., Briere, C., Kieffer-Jacquinod, S., Rivas, S., Marco, Y., and Deslandes, L. (2010). Autoacetylation of the Ralstonia solanacearum effector PopP2 targets a lysine residue essential for RRS1-R-mediated immunity in Arabidopsis. *PLoS Pathog* 6**,** e1001202. doi: 10.1371/journal.ppat.1001202.

Taylor, J.D., Teverson, D.M., Allen, D.J., and Pastor-Corrales, M.A. (1996). Identification and origin of races od *Pseudomonas syringae* pv. *phaseolicola* from Africa and other bean growing area. *Plant Pathol.* 45**,** 469-478.

Taylor, R.K., Miller, V.L., Furlong, D.B., and Mekalanos, J.J. (1987). Use of *phoA* gene fusions to identify a pilus colonization factor coordinately regulated with cholera toxin. *Proc. Natl. Acad. Sci* 84**,** 2833-2837.

Teverson, D.M. (1991). *Genetics of pathogenicity and resistance in the halo-blight disease of beans in Africa. PhD Thesis.*, University of Birmingham.

Thomma, B.P., Nurnberger, T., and Joosten, M.H. (2011). Of PAMPs and effectors: the blurred PTI-ETI dichotomy. *Plant Cell* 23**,** 4-15. doi: 10.1105/tpc.110.082602.

Thwaites, R., Spanu, P.D., Panopoulos, N.J., Stevens, C., and Mansfield, J.W. (2004). Transcriptional regulation of components of the type III secretion system and effectors in *Pseudomonas syringae* pv *phaseolicola*. *Mol. Plant Microbe Interact.* 17**,** 1250-1258.

Trosky, J.E., Li, Y., Mukherjee, S., Keitany, G., Ball, H., and Orth, K. (2007). VopA inhibits ATP binding by acetylating the catalytic loop of MAPK kinases. *J Biol Chem* 282**,** 34299-34305. doi: 10.1074/jbc.M706970200.

Trosky, J.E., Mukherjee, S., Burdette, D.L., Roberts, M., Mccarter, L., Siegel, R.M., and Orth, K. (2004). Inhibition of MAPK signaling pathways by VopA from Vibrio parahaemolyticus. *J Biol Chem* 279**,** 51953-51957. doi: 10.1074/jbc.M407001200.

Tsiamis, G., Mansfield, J.W., Hockenhull, R., Jackson, R.W., Sesma, A., Athanassopoulos, E., Bennett, M.A., Stevens, C., Vivian, A., Taylor, J.D., and Murillo, J. (2000). Cultivar-specific avirulence and virulence functions assigned to *avrPphF* in *Pseudomonas syringae* pv. *phaseolicola*, the cause of bean halo-blight disease. *EMBO J.* 19**,** 3204-3214.

Van Der Woude, M.W. (2011). Phase variation: how to create and coordinate population diversity. *Curr Opin Microbiol* 14**,** 205-211. doi: 10.1016/j.mib.2011.01.002.

Van Loon, L.C., Bakker, P.A., and Pieterse, C.M. (1998). Systemic resistance induced by rhizosphere bacteria. *Annu Rev Phytopathol* 36**,** 453-483. doi: 10.1146/annurev.phyto.36.1.453.

Van Vliet, S., and Ackermann, M. (2015). Bacterial Ventures into Multicellularity: Collectivism through Individuality. *PLoS Biol* 13**,** e1002162. doi: 10.1371/journal.pbio.1002162.

Veening, J.W., Smits, W.K., and Kuipers, O.P. (2008). Bistability, epigenetics, and bet-hedging in bacteria. *Annu Rev Microbiol* 62**,** 193-210. doi: 10.1146/annurev.micro.62.081307.163002.

Vinatzer, B.A., Teitzel, G.M., Lee, M.W., Jelenska, J., Hotton, S., Fairfax, K., Jenrette, J., and Greenberg, J.T. (2006). The type III effector repertoire of *Pseudomonas syringae* pv. *syringae* B728a and its role in survival and disease on host and non-host plants. *Mol. Microbiol.* 62**,** 26-44.

W.H., B. (1926). A new bacterial disease of the bean. *Phytopathology* 16**,** 915-927.

Wang, G., Roux, B., Feng, F., Guy, E., Li, L., Li, N., Zhang, X., Lautier, M., Jardinaud, M.F., Chabannes, M., Arlat, M., Chen, S., He, C., Noel, L.D., and Zhou, J.M. (2015). The Decoy Substrate of a Pathogen Effector and a Pseudokinase Specify Pathogen-Induced Modified-Self Recognition and Immunity in Plants. *Cell Host Microbe* 18**,** 285-295. doi: 10.1016/j.chom.2015.08.004.

Wang, Y., Li, J., Hou, S., Wang, X., Li, Y., Ren, D., Chen, S., Tang, X., and Zhou, J.M. (2010). A Pseudomonas syringae ADP-ribosyltransferase inhibits Arabidopsis mitogen-activated protein kinase kinases. *The Plant cell* 22**,** 2033-2044. doi: 10.1105/tpc.110.075697.

Wei, C.F., Deng, W.L., and Huang, H.C. (2005). A chaperone-like HrpG protein acts as a suppressor of HrpV in regulation of the *Pseudomonas syringae* pv. *syringae* type III secretion system. *Mol. Microbiol.* 57**,** 520-536.

Wei, W., Plovanich-Jones, A., Deng, W.L., Jin, Q.L., Collmer, A., Huang, H.C., and He, S.Y. (2000). The gene coding for the Hrp pilus structural protein is required for type III secretion of Hrp and Avr proteins in *Pseudomonas syringae* pv. *tomato*. *Proc. Natl. Acad. Sci.* 97**,** 2247-2252.

Weiler, E.W., Kutchan, T.M., Gorba, T., Brodschelm, W., Niesel, U., and Bublitz, F. (1994). The Pseudomonas phytotoxin coronatine mimics octadecanoid signalling molecules of higher plants. *FEBS Lett* 345**,** 9-13.

Whalen, M.C., Innes, R.W., Bent, A.F., and Staskawicz, B.J. (1991). Identification of *Pseudomonas syringae* pathogens of *Arabidopsis* and a bacterial locus determining avirulence on both *Arabidopsis* and soybean. *Plant Cell* 3**,** 49-59.

Wiley, D.J., Rosqvist, R., and Schesser, K. (2007). Induction of the Yersinia type 3 secretion system as an all-or-none phenomenon. *J Mol Biol* 373**,** 27-37. doi: 10.1016/j.jmb.2007.07.077.

Willmann, R., Lajunen, H.M., Erbs, G., Newman, M.-A., Kolb, D., Tsuda, K., Katagiri, F., Fliegmann, J., Bono, J.-J., Cullimore, J.V., Jehle, A.K., Götz, F., Kulik, A., Molinaro, A., Lipka, V., Gust, A.A., and Nürnberger, T. (2011). Arabidopsis lysin-motif proteins LYM1 LYM3 CERK1 mediate bacterial peptidoglycan sensing and immunity to bacterial infection. *Proceedings of the National Academy of Sciences* 108**,** 19824-19829. doi: 10.1073/pnas.1112862108.

Wilton, M., Subramaniam, R., Elmore, J., Felsensteiner, C., Coaker, G., and Desveaux, D. (2010). The type III effector HopF2 Pto targets Arabidopsis RIN4 protein to promote Pseudomonas syringae virulence. *Proc Natl Acad Sci U S A* 107**,** 2349-2354. doi: 0904739107 [pii]
10.1073/pnas.0904739107.

Wright, C.A., and Beattie, G.A. (2004). Pseudomonas syringae pv. tomato cells encounter inhibitory levels of water stress during the hypersensitive response of Arabidopsis thaliana. *Proc Natl Acad Sci U S A* 101**,** 3269-3274. doi: 10.1073/pnas.0400461101
0400461101 [pii].

Wu, S., Lu, D., Kabbage, M., Wei, H.L., Swingle, B., Records, A.R., Dickman, M., He, P., and Shan, L. (2011). Bacterial effector HopF2 suppresses arabidopsis innate immunity at the plasma membrane. *Molecular plant-microbe interactions : MPMI* 24**,** 585-593. doi: 10.1094/MPMI-07-10-0150.

Xavier, J.B., Kim, W., and Foster, K.R. (2011). A molecular mechanism that stabilizes cooperative secretions in Pseudomonas aeruginosa. *Mol Microbiol* 79**,** 166-179. doi: 10.1111/j.1365-2958.2010.07436.x.

Xiang, T., Zong, N., Zhang, J., Chen, J., Chen, M., and Zhou, J.M. (2011). BAK1 is not a target of the Pseudomonas syringae effector AvrPto. *Molecular plant-microbe interactions : MPMI* 24**,** 100-107. doi: 10.1094/MPMI-04-10-0096.

Xiang, T., Zong, N., Zou, Y., Wu, Y., Zhang, J., Xing, W., Li, Y., Tang, X., Zhu, L., Chai, J., and Zhou, J.M. (2008). *Pseudomonas syringae* effector AvrPto blocks innate immunity by targeting receptor kinases. *Curr Biol* 18**,** 74-80.

Xiao, Y., Heu, S., Yi, J., Lu, Y., and Hutcheson, S.W. (1994). Identification of a putative alternate sigma factor and characterization of a multicomponent regulatory cascade controlling the expression of *Pseudomonas syringae* pv. syringae Pss61 *hrp* and *hrmA* genes. *J. Bacteriol.* 176**,** 1025-1036.

Xiao, Y., and Hutcheson, S.W. (1994). A single promoter sequence recognized by a newly identified alternate sigma factor directs expression of pathogenicity and host range determinants in *Pseudomonas syringae*. *J. Bacteriol.* 176**,** 3089-3091.

Xu, J., Li, Y., Wang, Y., Liu, H., Lei, L., Yang, H., Liu, G., and Ren, D. (2008). Activation of MAPK kinase 9 induces ethylene and camalexin biosynthesis and enhances sensitivity to salt stress in Arabidopsis. *J Biol Chem* 283**,** 26996-27006. doi: 10.1074/jbc.M801392200.

Xu, J., Xie, J., Yan, C., Zou, X., Ren, D., and Zhang, S. (2013). A chemical genetic approach demonstrates that MPK3/MPK6 activation and NADPH oxidase-mediated oxidative burst are two independent signaling events in plant immunity. *The Plant journal : for cell and molecular biology*. doi: 10.1111/tpj.12382.

Yoon, S., Liu, Z., Eyobo, Y., and Orth, K. (2003). Yersinia effector YopJ inhibits yeast MAPK signaling pathways by an evolutionarily conserved mechanism. *J Biol Chem* 278**,** 2131-2135. doi: 10.1074/jbc.M209905200.

Young, J.M. (1974). Development of bacterial populations *in vivo* in relation to plant pathogenicity. *N. Z. J. Agric. Res.* 17**,** 105-113.

Young, J.M. (2010). Taxonomy of *Pseudomonas syringae. Journal of Plant Pathology* 92**,** S1.5-S1.14.

Yu, A., Lepere, G., Jay, F., Wang, J., Bapaume, L., Wang, Y., Abraham, A.L., Penterman, J., Fischer, R.L., Voinnet, O., and Navarro, L. (2013). Dynamics and biological

relevance of DNA demethylation in Arabidopsis antibacterial defense. *Proc Natl Acad Sci U S A* 110**,** 2389-2394. doi: 10.1073/pnas.1211757110.

Yu, I.C., Parker, J., and Bent, A.F. (1998). Gene-for-gene disease resistance without the hypersensitive response in Arabidopsis dnd1 mutant. *Proc Natl Acad Sci U S A* 95**,** 7819-7824.

Zeng, L., Velasquez, A.C., Munkvold, K.R., Zhang, J., and Martin, G.B. (2012a). A tomato LysM receptor-like kinase promotes immunity and its kinase activity is inhibited by AvrPtoB. *The Plant journal : for cell and molecular biology* 69**,** 92-103. doi: 10.1111/j.1365-313X.2011.04773.x.

Zeng, Q., Laiosa, M.D., Steeber, D.A., Biddle, E.M., Peng, Q., and Yang, C.H. (2012b). Cell individuality: the bistable gene expression of the type III secretion system in Dickeya dadantii 3937. *Mol Plant Microbe Interact* 25**,** 37-47. doi: 10.1094/MPMI-05-11-0105.

Zhang, J., Li, W., Xiang, T., Liu, Z., Laluk, K., Ding, X., Zou, Y., Gao, M., Zhang, X., Chen, S., Mengiste, T., Zhang, Y., and Zhou, J.-M. (2010). Receptor-like cytoplasmic kinases integrate signaling from multiple plant immune receptors and are targeted by a Pseudomonas syringae effector. *Cell Host and Microbe* 7**,** 290-301. doi: 10.1016/j.chom.2010.03.007.

Zhang, J., Shao, F., Li, Y., Cui, H., Chen, L., Li, H., Zou, Y., Long, C., Lan, L., Chai, J., Chen, S., Tang, X., and Zhou, J.-M. (2007a). A Pseudomonas syringae Effector Inactivates MAPKs to Suppress PAMP-Induced Immunity in Plants. *Cell Host and Microbe* 1**,** 175-185. doi: 10.1016/j.chom.2007.03.006.

Zhang, X., Dai, Y., Xiong, Y., Defraia, C., Li, J., Dong, X., and Mou, Z. (2007b). Overexpression of Arabidopsis MAP kinase kinase 7 leads to activation of plant basal and systemic acquired resistance. *Plant J* 52**,** 1066-1079. doi: 10.1111/j.1365-313X.2007.03294.x.

Zhang, X., Xiong, Y., Defraia, C., Schmelz, E., and Mou, Z. (2008). The Arabidopsis MAP kinase kinase 7: A crosstalk point between auxin signaling and defense responses? *Plant Signal Behav* 3**,** 272-274.

Zhang, Z., Wu, Y., Gao, M., Zhang, J., Kong, Q., Liu, Y., Ba, H., Zhou, J., and Zhang, Y. (2012). Disruption of PAMP-induced MAP kinase cascade by a Pseudomonas syringae effector activates plant immunity mediated by the NB-LRR protein SUMM2. *Cell Host and Microbe* 11**,** 253-263. doi: 10.1016/j.chom.2012.01.015.

Zhou, H., Lin, J., Johnson, A., Morgan, R.L., Zhong, W., and Ma, W. (2011). Pseudomonas syringae type III effector HopZ1 targets a host enzyme to suppress isoflavone biosynthesis and promote infection in soybean. *Cell Host Microbe* 9**,** 177-186. doi: 10.1016/j.chom.2011.02.007.

Zhou, H., Monack, D.M., Kayagaki, N., Wertz, I., Yin, J., Wolf, B., and Dixit, V.M. (2005). Yersinia virulence factor YopJ acts as a deubiquitinase to inhibit NF-kappa B activation. *J Exp Med* 202**,** 1327-1332. doi: 10.1084/jem.20051194.

Zhou, J., Spallek, T., Faulkner, C., and Robatzek, S. (2012). CalloseMeasurer: a novel software solution to measure callose deposition and recognise spreading callose patterns. *Plant Methods* 8**,** 49. doi: 10.1186/1746-4811-8-49.

Zhou, J., Wu, S., Chen, X., Liu, C., Sheen, J., Shan, L., and He, P. (2014). The Pseudomonas syringae effector HopF2 suppresses Arabidopsis immunity by targeting BAK1. *The Plant journal : for cell and molecular biology* 77**,** 235-245. doi: 10.1111/tpj.12381.

Zipfel, C., Robatzek, S., Navarro, L., Oakeley, E.J., Jones, J.D., Felix, G., and Boller, T. (2004). Bacterial disease resistance in *Arabidopsis* through flagellin perception. *Nature* 428**,** 764-767.

Zumaquero, A., Macho, A.P., Rufian, J.S., and Beuzon, C.R. (2010). Analysis of the role of the type III effector inventory of Pseudomonas syringae pv. phaseolicola 1448a in interaction with the plant. *J Bacteriol* 192**,** 4474-4488. doi: JB.00260-10 [pii]
10.1128/JB.00260-10.

Appendix: Published work, not included in this thesis, with collaborations from the author